Master's thesis

NTNU
Norwegian University of Science and Technology
Faculty of Engineering
Department of Geoscience and Petroleum

Berit Berbusmel

Ore-forming processes in volcano-sedimentary hosted massive sulphide deposits in the Mofjell group, Nordland, Norway

Supervisor: Rune Berg-Edland Larsen

Co-supervisors: Terje Bjerkgård and Bjørn Eske Sørensen

Master's thesis in Bedrock and Resource Geology

May 2020

NTNU
Norwegian University of Science and Technology

SOTKAMO SILVER

Abstract

The Mofjell group in the Rödningsfjäll nappe complex host several ore deposits, and some of them have been mined. In this thesis two of the deposits that has not been mined, the Hesjelia zone and the Hellerfjellet zone, will be studied in the field, chemically, and microscopically. The deposits are defined as volcanic massive sulphide (VMS) deposits with large economical potential for Zn, Cu, Pb, Co, Ag and Au (Bjerkgård *et al.*, 2013a). Extensive deformation and metamorphism have affected the area after deposition and has made it difficult to unravel and predict how and if the deposits continue below the surface. The host rock of the deposits is a muscovite gneiss/ schist that is thought to have formed from alteration of grey gneiss and amphibolite by hydrothermal ore-forming fluids (Bjerkgård *et al.*, 2013a).

The aim of this thesis is to study the geological setting, ore-genetic zonation patterns if present and to compare and decide if the two deposits are connected or not. The results from this thesis together with Gundersen (2020 in prep.) thesis will hopefully make it easier to decide the best drilling targets. Field work with extensive mapping and sampling has been done to get an overview of the areas with their variations and similarities. One drill core (BH4508) from Hellerfjellet has been logged and analysed with a portable XRF to see if any zonation patterns could be unravelled. Whole rock litogeochemistry of the field samples has been obtained with various ICP (Inductively Couple Plasma) analyses to be able to understand the origin of the host rock and the mineralisation. These results were also used to unravel the differences and similarities between the Hellerfjellet and Hesjelia ore-zones. Thin sections of field samples and from the drill core has been characterised microscopically and some with Scanning Electron Microscope (SEM) to find textural and chemical differences in the minerals between the two zones. Zonation patterns in selected minerals was also searched for in the drill core samples.

The main conclusion is that the Hellerfjellet and the Hesjelia zone most likely are formed in two different ore-forming events in the same system of island arc and associated back-arc basin. Hellerfjellet zone with more sedimentary input compared to the Hesjelia zone is most likely deposited in or close to the back-arc basin, whereas Hesjelia zone is deposited closer to the volcanic arc. The massive ore in the Hellerfjellet zone has an average of 2.9% Zn, 1.4% Pb, 0.17% Cu and 41 g/t Ag, and in Hesjelia zone there is an average of 5.5% Zn, 0.05% Pb, 0.4% Cu and 5 g/t Ag. No clear zonation was found in the drill core when approaching the ore zone with the portable XRF, but the biotite and garnet changes compositions when approaching the ore and may be used as a guide for the proximity to the ore-zone.

Sammendrag

Mofjellgruppen i Rödningsfjäll skyvedekkekompleks er vert for flere malmforekomster, hvor noen av dem har vært utvunnet. I denne avhandlingen skal to av forekomstene som ikke har vært utvunnet før, Hesjelia sonen og Hellerfjellet sonen, bli studert i felt, kjemisk og mikroskopisk. Forekomstene er definert som en vulkansk massiv sulfid (VMS) forekomst med stort økonomisk potensiale for Zn, Cu, Pb, Co, Ag og Au (Bjerkgård *et al.*, 2013a). Omfattende deformasjon og metamorfose har påvirket området etter avsetning og har gjort det vanskelig å finne ut og forutsi om og hvis forekomstene fortsetter under bakken. Vertsbergarten til forekomsten er muskovittgneis/ skifer som trolig er dannet fra alterering av grå gneis og amfibolitt av hydrotermale malmdannende fluider (Bjerkgård *et al.*, 2013a).

Målet med denne avhandlingen er å studere den geologiske settingen, soneringsmønstre assosiert med malmdannelsen og å sammenligne og avgjøre om de to forekomstene er sammenkoblet eller ikke. Resultatet fra denne avhandlingen og Gundersen (2020 in prep.) avhandling vil forhåpentligvis gjøre det lettere å avgjøre den beste plassen for boring. Feltarbeid med grundig kartlegging og prøvetaking har blitt gjort for å få et overblikk over områdene med deres variasjoner og likheter. En borekjerne (BH4508) fra Hellerfjellet har blitt logget og analysert med bærbar XRF for å se om soneringsmønstre kunne bli avslørt. Helbergarts litogeokjemi av feltprøvene har blitt tatt med forskjellige ICP (Inductively Couple Plasma) analyser for å kunne forstå opprinnelsen til vertsbergartene og mineraliseringen. Disse resultatene ble også brukt til å avsløre forskjellene og likhetene mellom Hellerfjellet og Hesjelia malmsoner. Tynnslip av feltprøver og fra borekjernen har blitt karakterisert med mikroskop og noen også med Scanning Electron Microscope (SEM) for å finne tekstuelle og kjemiske forskjeller i mineralene mellom de to sonene. Soneringsmønster i utvalgte mineraler ble analysert for i borekjerneprøver.

Hovedkonklusjonen er at Hellerfjellet og Hesjelia sonene mest sannsynlig er dannet i to forskjellige malmdannende hendelser i det samme, øybue og assosierte bakbue basseng, systemet. Hellerfjellet sonen med mer sedimentært innhold, sammenlignet med Hesjelia sonen, er mest sannsynlig avsatt i eller nært bakbuebassenget, mens Hesjelia soner er avsatt i selve øybuen. Den massive malmen i Hellerfjellet sonen har et gjennomsnitt på 2.9% Zn, 1.4% Pb, 0.17% Cu og 41 g/t Ag, og i Hesjelia sonen er det i gjennomsnitt 5.5% Zn, 0.05% Pb, 0.4% Cu og 5 g/t Ag. Ingen klare soneringer ble funnet i borekjernen når man kommer nærmere malmen med den bærbare XRF'en, men biotitt og granat endre komposisjon når man nærmer seg malmen og kan muligens bli brukt som en ledetråd for at man er i nærigheten av malmsonen.

Preface

My biggest thanks are to my supervisors Rune Berg-Edland Larsen, and co-supervisors Terje Bjerkgård and Bjørn Eske Sørensen for the guidance and help through all the thesis, all the way from fieldwork to analyses and reading my manuscript. They have been helping me to understand what this actually is about. My field partner, Simon, also deserves a big thanks for the cooperation and discussions we have had through the period.

Sotkamo Silves OY has finalised the thesis, both the field work and the analyses, and also provided summer job that has given me valuable experience of how it is to work as a geologist. Thank you very much.

My boyfriend, Ludvig, deserves a medal for keeping up with me during the last months. It has been like a roller coaster of emotions.

My good friends I have shared "office" with through the last year has been a great support. It was a place where all of us could share our ups and downs, frustrations, and accomplishments through this process. Some of them will probably be my colleague in one of our future jobs, and I am really looking forward to cooperating with them. One of my friends has a saying that has helped me very much the last weeks of writing:

> "You will never get done with a master thesis; you say you're done".

Table of Contents

List of Figures

List of Tables

List of Abbreviations

NTNU	The Norwegian University of Science and Technology
NGU	Norges Geologiske Undersøkelser / Geological Survey of Norway
i.e.	Id est – that is - example
HAM	Hammertjønna
HES and HS	Hesjelia
HF	Hellerfjellet
RNC	Rödningdfjäll Nappe Complex
VMS	Volcanic Massive Sulphide

<u>Minerals</u>

Amp	Amphibole
Ap	Apatite
Brt	Barite
Bt	Biotite
Cal	Calcite
Chl	Chlorite
Cls	Celcian
Cpy	Chalcopyrite
Ep	Epidote
Fb	Freibergite
Flp	Feldspar
Ga	Galena
Grt	Garnet
Gr	Graphite
Hbl	Hornblende
Ilm	Ilmenite
Ky	Kyanite
Ms	Muscovite
Plg	Plagioclase
Po	Pyrrhotite
Py	Pyrite
Qz	Quartz
Ser	Sericite
Sp	Sphalerite
Zo	Zoisite

<u>Methods and various words</u>

PPL	Plane Polarized Light
XPL	Crossed polarized light
SEM	Scanning electron microscope
EDS	Electron dispersive spectrometry
WDS	Wavelength dispersive spectrometry
XRF	Meters below the surface
Mbs.	X-ray fluorescence

$f O_2$	Oxygen fugacity
m	Meter
g/t	Gram per ton

1 Introduction

This thesis is due to a collaboration between the Finnish mining company Sotkamo Silver OY (a daughter company of Sotkamo Silver AB in Sweden), the Geological Survey of Norway (NGU) and NTNU. The company has exploration permits in the Mofjellet district to the east of Mo i Rana in the county of Nordland in Norway. The thesis addresses two of the areas claimed by Sotkamo Silver OY (see Figure 1-1); the Hesjelia zone and the Hellerfjellet zone.

The deposits is by Bjerkgård *et al.* (2013a) suggested to be volcanogenic massive sulphide (VMS) deposits with large economical potential for Zn, Cu, Pb, Co, Ag and Au. All deposits have previously been explored, especially the Hesjelia zone, but because of a complex deformation history, it is challenging to model the sub-surface continuation of the orebodies. This thesis, and the study by Simon F Gundersen (2020), aims at clarifying the structure and architecture of the deposits, which may be crucial for further exploration of the areas of the deposits.

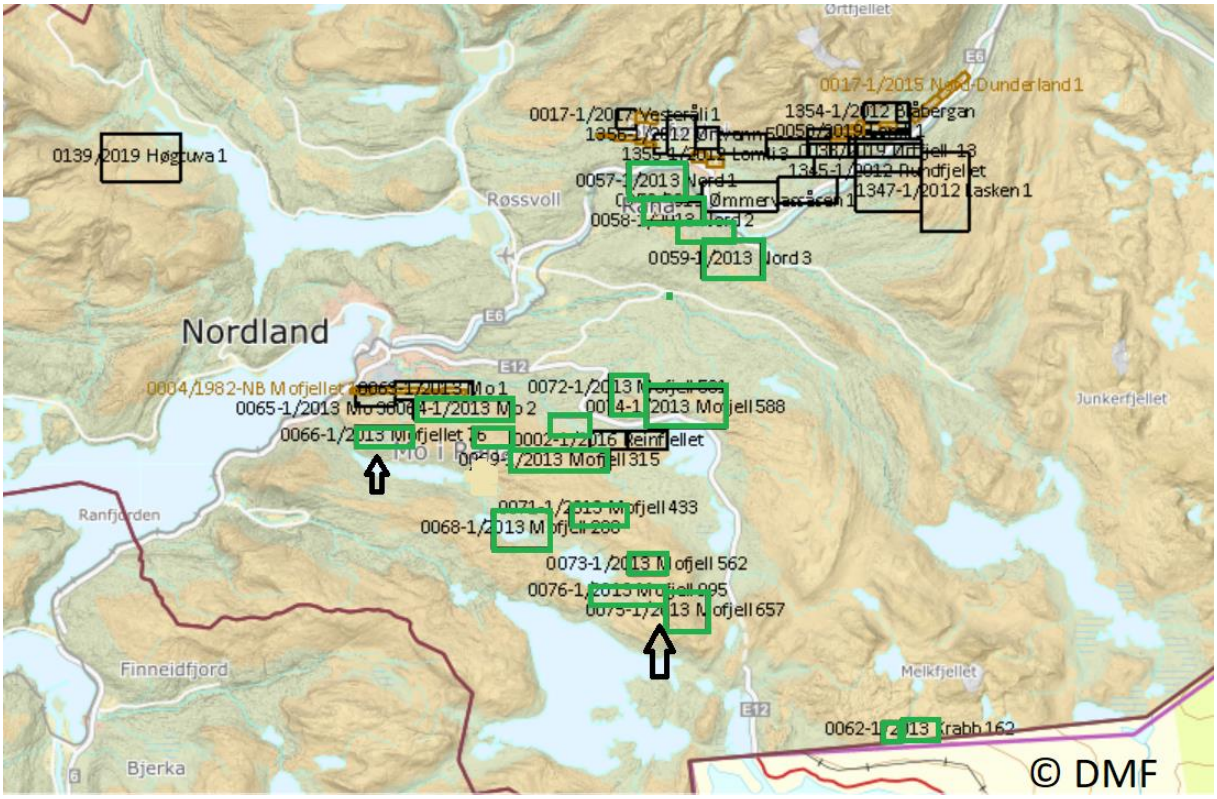

Figure 1-1 Map of the claimed areas by Sotkamo Silver OY in the Mo i Rana district (green squares). The arrows represent the areas studied in this work. Left arrow is the Hesjelia zone and the right arrow is the Hellerfjellet zone. Black and brown squares are permits by other companies. Map from DirektoratetForMineralforvaltning (n.d.); Kartverket (n.d.).

1.1 Goal of the study

The aim of this project is to study the geological setting, ore-genetic zonation patterns if present and to characterize the paragenesis associated with the sulphide mineralisations in the Hesjelia and Hellerfjellet zones. Another goal is to explore if there is continuity between the different outcropping mineralisations, e.g. if they are at the same structural/stratigraphic level, and to define differences and similarities between the various outcrops. Also, any mineralogical and chemical zonation patterns akin to the mineralizing processes will be unravelled. The surrounding wall rocks and especially the alteration zone will be mapped out in details. I will also compare the deposits with other deposits in the area and around the world. The goal of this and Gundersen, Simon F. (2020) projects is to find out the best target for drilling.

1.2 Previous studies

The Rana district was early mentioned as an interesting area for mining of iron and copper (Vogt, 1890). Hesjelia and Hellerfjellet are not noted here, but Dunderlandsdalen and Langvatn in the same nappe complex is described.

Several deposits in the area have been mined, and some are mined now. There are few reports on the deposits that have been mined before the second world war, but in the Geological Survey of Norway (n.d.)map-database; "mineralressurser" the current information about the deposits are stored. Some information is found in Bjerkgård *et al.* (2013a). A few examples will follow, see Figure 1-2 for locations of the examples;

The first deposit that was mined nearby the Hesjelia zone is Sølvberg grube, the main ore minerals is pyrrhotite and pyrite, with sphalerite and chalcopyrite as secondary minerals. The deposit was mined in 1861-1863, followed by exploration efforts.

In 1910-1911 the Heramb and Bertelberget were test mined on pyrrhotite, pyrite, chalcopyrite and sphalerite. The area comprises alternating layers of muscovite gneiss, biotite gneiss and amphibolite incorporated with thicker units of grey gneiss.

Mos mine was mined from 1911 to 1920 and 52 000 tons of pyrite was mined from a massive pyrite mineralisation.

The well-known Mofjellet deposit, near Hesjelia, also belongs to the Mofjell Group. Mofjellet Gruber was mined between 1928 and 1987 on base metals, the main commodities were Zn and Cu. The deposit produced 4.35 Mt of ore. The deposit is in three lenses situated on top of each other and are stratigraphically connected by a tight fold structure. The host rocks are mafic and felsic vulcanite's and meta-sediments that formed in an arc/back-arc setting.

The Bleikvassli deposit south of Mo i Rana is a volcano-sedimentary-hosted Zn-Pb(-Cu) deposit. It was mined from 1950 to 1997. The ore comprises semi-massive and disseminated sulphides in discontinuous layers. The metals that was mined were Cu, Zn, Pb, Ag and Au. In total the deposit produced about 5 Mt of ore.

Rana Gruber AS in the Dunderlandsdalen iron district is the only metal mine that is remains active in the Rana area, with the Ørtfjell deposit currently in production. During 2019 c. 100 Mt of iron ore was recovered. The host rock comprises various types of mica schist. (Bjerkgård and Hallberg, 2012)

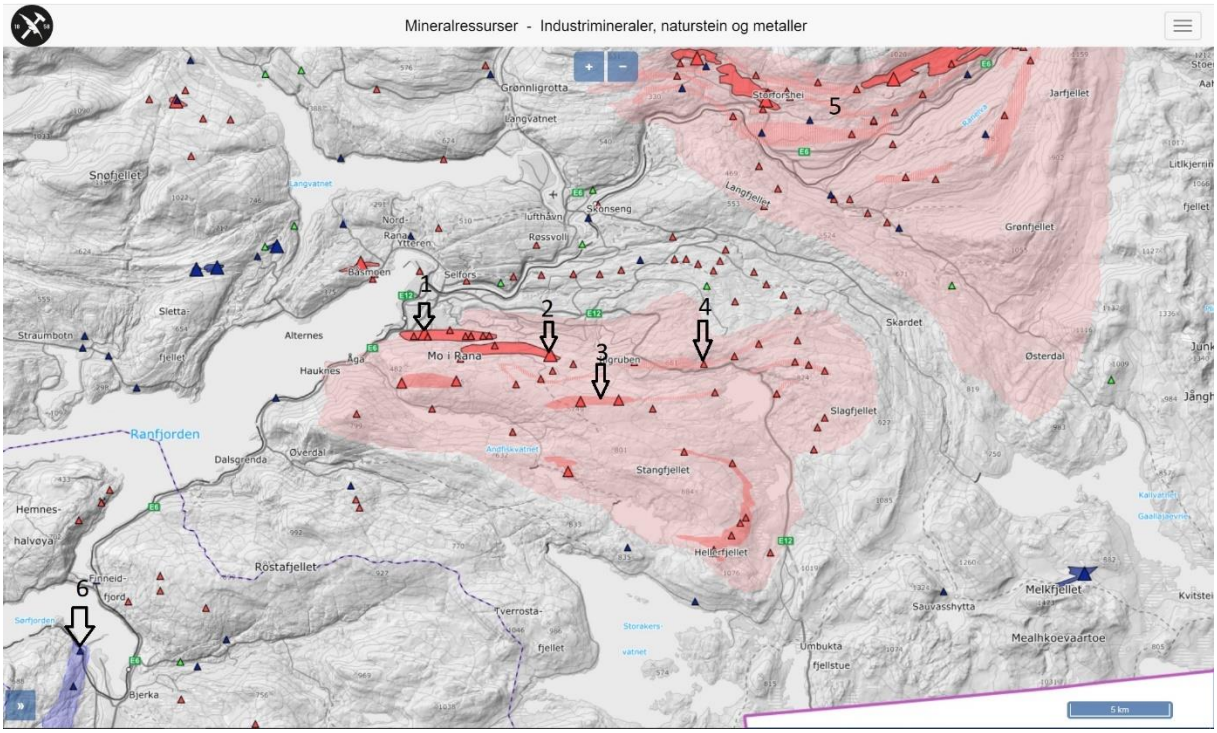

Figure 1-2 Map from the mineral resource map-database to NGU. The arrows are pointed to the examples mentioned in the text. 1: Mofjell grube. 2: Sølvberget grube. 3: Heramb and Bertelberget. 4: Mos Grube. 5: Rana gruber. 6: Bleikvassli. Modified from Geological Survey of Norway (n.d.)

The earliest report describing the Hesjelia and Hammertjønna deposits in the Hesjelia zone is from 1953, and was produced by Bergverkselskapet Nord-Norge A/S (BNN) during their mapping of the Mofjellet west area (BNN, 1953). A report by BNN from 1980 (Kruse, 1980) summarizes the activities in the Hesjelia area until 1980: In 1959 the company accomplished a drilling program, in 1976/77 structural and lithological mapping was done by M. Marker (at 1:5000 scale), whereas geophysical measurements were done in 1977. In the drilling program 10 holes were drilled, with a total yield of 559 meters. Based on drilling and mapping, the zone was estimated to have c. 1, 25 M ton (150 m north, 3000 m east and 3 m thickness). In the Ph.D. thesis by Mogens Marker (1983), the lithologies and the structures were mapped in detail. The main purpose of the mapping was to solve the complicated structures controlling the Mofjell Gruber orebody. Marker found that the rock units were subjected to four different fold phases.

Little is known about the exploration of the Hellerfjellet deposit. From old reports in the NGU Bergarkiv archives at BNN (Kleine-Hering and Schulze, 1969; Kruse, 1964; Spross, 1956) and a PhD (Saager, 1966) we know that the deposit was sampled in 1935, drilled with two Calyx holes in 1936 and that additional sampling and geological investigations were carried out in 1963. Most deposits in the larger Mofjellet area, including Hellerfjellet, Hesjelia and Hammartjønna, were sampled and investigated by NGU for the national ore database in the 1990s. These samples were used by Larsen et al. (1995a) to compare the deposits in the Mofjellet Group with the Plurdalen Group. One of the conclusions was that Plurdalen group was richer in Cu than the Mofjellet group but had lower concentrations of Au and Ag.

The most recent studies in this area have mostly been done by The Geological Survey of Norway in cooperation with others. Hesjelia and Hammertjønna has been explored more than Hellerfjellet and is mapped out in more detail.

The last fieldwork was done in 2009 and was published in 2013 by Bjerkgård et al. (2013a) based on reports from 2008 and 2009 (Bjerkgård *et al.*, 2008; Bjerkgård *et al.*, 2009). This was in cooperation with GEXCO who had exploration permits in most parts of Mofjellet at the time. Their results and claims were sold to the Sotkamo Silver OY in 2010. The main purpose of this work was to decide the lithotectonic setting of the Mofjellet Group and assess the potential for economic deposits. One hole was drilled between Hesjelia and Hammertjønna deposit, and this intersected the ore at the expected stratigraphic level hence supported a possible connection between the two mineralisations. The sulphide ores are associated with bimodal felsic and mafic igneous volcanic rocks and sediments that formed in an island-arc to back-arc setting (Bjerkgård et al., 2013). Nine main ore zones were identified, all on different structural levels. Some of the ore zones may be connected, but strong deformation complicates firm conclusions. The assessment concluded that the Hesjelia-Hammertjønna deposits and Hellerfjellet deposits were among the economically most interesting ore deposits and follow-up work was recommended.

1.3 Regional Geology and Geological setting

The Scandinavian Caledonides is the northernmost part of the Caledonian-Appalachian orogenic belt. This belt stretches from Alabama to northern Norway and was partially shaped as a result of episodes of opening and closure, respectively, of the Laurentian and Eurasian/Baltican continental cratons from Neoproterozoic to Devonian time. Continental break up (about 700 Ma ago) of the Proterozoic mega-continent Rodinia formed (amongst many other content) Laurentia (North America) and Baltica (north-western Eurasia). This was followed by ocean-floor spreading with the formation of the Iapetus ocean that later converged and culminated with continent-continent collision under the formation of the Scandinavian Caledonides. Extensional collapse gradually degraded the Scandinavian Caledonides during Mesozoic time before continental rifting eventually lead into renewed ocean-floor spreading and the formation of the proto-north Atlantic ocean. (Grenne *et al.*, 1999)

During the formation of the Scandinavian Caledonides, segments of Laurentia and Baltica were obducted in several allochthonous nappe complexes. The allochthonous main units are the Lower, Middle, Upper and Uppermost Allochthon, which is based on differences in lithologies, structures, metamorphism as well as ages. The allochthons are further divided into nappe complexes. (Roberts and Gee, 1985)

According to Roberts and Gee (1985) the uppermost allochthon generally is dominated by various gneisses and partly migmatite. Also, a large amount of schists and sandstones, some conglomerates, dolomite, calcite marbles and subordinate sedimentary iron ore deposits, variable amounts of amphibolite, greenstone, and serpentinite. Dating suggests that large parts of this allochthon has a pre-Caledonian tectonic history. Stephens et al.(1985) suggests that the rocks are from intra-oceanic environment emplaced upon a continental margin. Either from the eastern edge of Laurentia or a western micro-continent. The uppermost allochthon comprises the Helgeland nappe complex and the Rödingsfjëll nappe complex in the central Caledonides.

Rödingsfjället nappe Complex (RNC) lies below Helgeland nappe complex and above Seve-Köli nappe complex. It consists of amphibolite facies mica gneisses, marbles and amphibolite's and has a distinct metamorphic and tectonic contact against Seve-Köli nappe complex below. The contact is marked by a thick zone of blastomylonitic and phyllonitic rocks (Gustavson, 1978; Stephens *et al.*, 1985). RNC is divided in 8 nappes;

Beiarn, Dalselv, Slagfjell, Plurdal, Ramnåli, Straumbotn, Tjørnrast and, finally, the Snøfjell nappe (Søvegjarto *et al.*, 1988).

Slagfjell nappe is in the maps by Marker et al. and Søvegjarto et al.(2012; 1988) divided in three Groups; Hauknesting, Mofjell and Rostafjell Groups. The Slagfjell nappe comprises metamorphic rocks assumed to be of late Proterozoic to Cambro-Ordovician ages.

The Hellerfjellet and Hesjelia ore zones are situated in the Mofjellet Group, which belongs to the Slagfjell Nappe in the Rödingsfjället Nappe Complex (RNC). RNC is situated between the Seve-Köli Nappe Complex in the Upper Allochthon, and the Helgeland Nappe complex in the Uppermost Allochthon. (Bjerkgård *et al.*, 2012; Bjerkgård *et al.*, 1995; Stephens *et al.*, 1985). Figure 1-3 and Figure 1-4 are the bedrock maps of the areas studied in this thesis.

Mogens Marker(1983) described four different folding events in this area, all probably from different events in the Caledonian Orogen; F_1 with shallow plunging tight to isoclinal folds, F_2 is refolding F_1. F_2 is a large northward facing recumbent fold. F_3 refolded F_1 and F_2 into a gentle to open fold with flat-lying fold axes, all of them where probably trending roughly east west. The F_4 phase form gentle to open structures with a fold axis running parallel to the main trend of the Caledonian Orogeny.
Bjerkgård et al.(1995) describes the same events, but conclude that F_1 comprises two phases of isoclinal folding. They call them deformation events instead of fold episodes. So D_1 and D_2 is the same as F_1, D_3 as F_2, D_4 as F_3 and D_5 as F_4. D_1 and D_2 is hard to distinguish in the field.

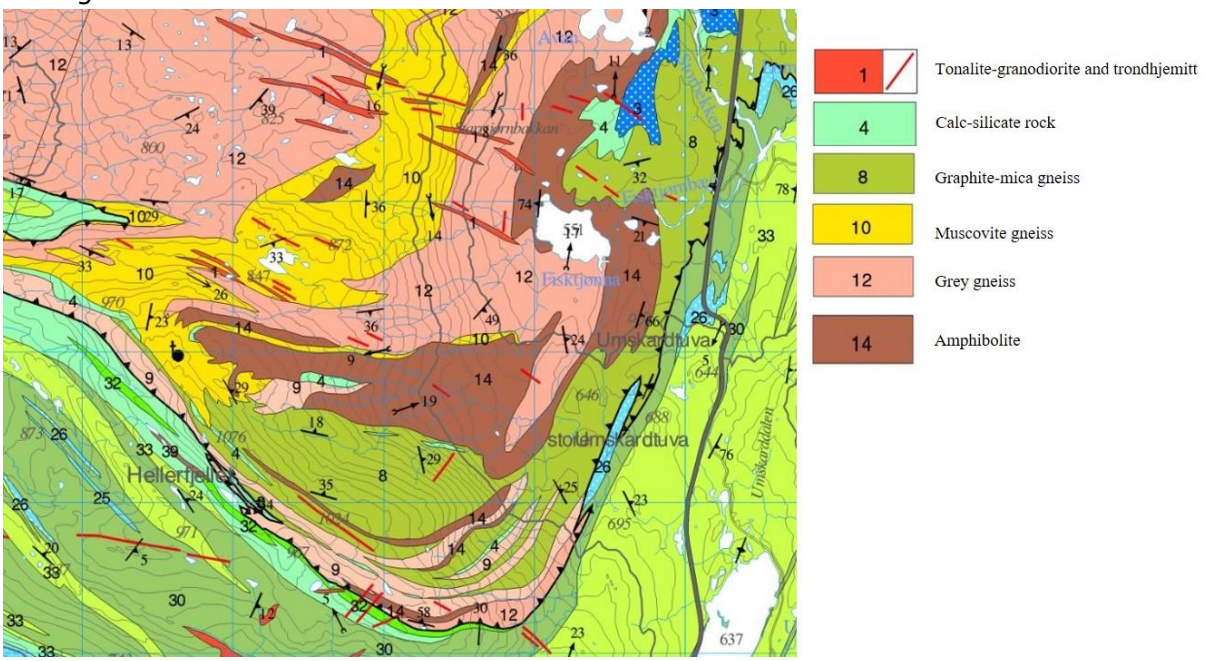

Figure 1-3 Bedrock map of Hellerfjellet with the lithology of the rocks relevant for this thesis (Modified from the 1:50 000 bedrock map Storakersvatnet, Marker et al. (2012))

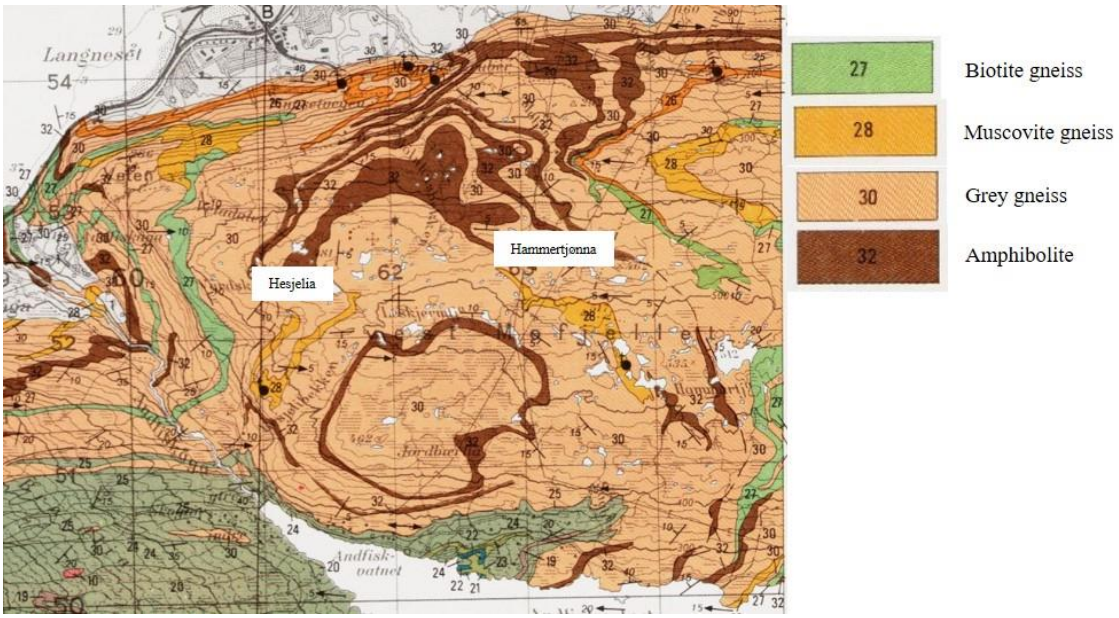

Figure 1-4 Bedrock map of Hesjelia and Hammertjønna with the lithology of the rocks relevant for this thesis. (Modified from the 1:50 000 bedrock map Mo i Rana, Søvegjarto et al. (1988))

2 The origin of the deposits

The deposits in the Mofjell group have been claimed to be both sediment hosted massive sulphide deposit (earlier SEDEX) and volcano massive sulphide (VMS) deposits. Because of extensive deformation and metamorphism, it is challenging to interpret the origin of the deposits. Grenne et al. and Larsen et al. (1999; 1995a) described them as sediment hosted type deposits, and also other deposits in the nappes were likewise classified, i.e. Bleikvassli (Larsen *et al.*, 1995b). Vokes (1976) and Bjerkgård et al.(2013b; 1976) lean on VMS-deposits as the preferred model. The chemical analyses from the most recent studies (Bjerkgård *et al.*, 2013a) document VMS signature and conclude that the deposits form in an extensional back-arc regime, partially based on the new classification scheme by Franklin *et al.* (2005). Accordingly, in this thesis it will be assumed that deposits classify as VMS deposit because the host rock is dominated by bimodal felsic and mafic igneous lithologies.

2.1 Sedimentary hosted versus volcanic massive sulphide deposit

Both sedimentary hosted massive sulphide deposit and VMS-deposits are made by precipitation of metals near or at the ocean floor from hydrothermal fluids. It may be difficult to separate them, but generally they are made in different tectonic settings and at different time and events during the earth's history. VMS deposits are made from hydrothermal fluids circulating through volcanic rocks and leaching it for metals in submarine environments. Often through black smokers by the mid-ocean ridges, island arcs, back-arc basins, and fore arc. Sedimentary hosted is a result of hydrothermal fluid circulating through sediments with little or no direct interaction with volcanic rocks, typically in interoceanic rift basins. The biggest sediment hosted massive sulphides is from Paleo- to Mesoproterozoic time. (Robb, 2005)

2.2 VMS deposits

Volcanogenic massive sulphide deposits (VMS) are "exhalative" deposit that forms near, or at the seafloor in submarine volcanic environments trough a focused discharge of hot metal-rich fluids. This is a process of formation which also takes place at the modern seafloor today. VMS deposits are major sources for Zn, Cu, Pb, Ag and Au, and Co. About 1100 VMS deposits are known worldwide, with estimated resource of about 10 billion tons. The classic model is a deposit which forms lenses of massive sulphides precipitated from metal-enriched fluids, related to sub-seafloor hydrothermal convection. The shape (Figure 2-1) of a VMS-deposit is typically a mound- to tabular-shaped stratabound body. It is composed of at least 40% massive sulphides, together with quartz, phyllosilicates, iron oxides and altered silicate wall rock. Below the massive ore deposit there is a discordant to semi-discordant stockwork of veins with disseminated sulphides surrounded by alteration zones. (Galley *et al.*, 2007)

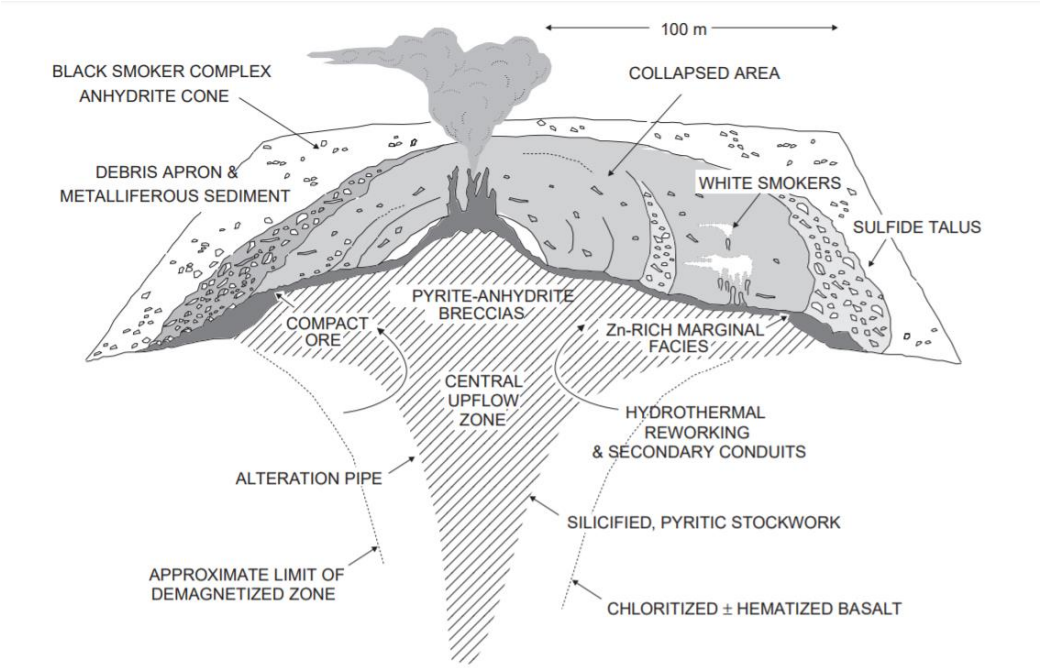

Figure 2-1 A cross section of the modern VMS-deposit formed at the mid-ocean ridge today. It is a semi-massive to massive sulphide lens with a stockwork vein system and alteration halo below (Hannington et al., 1998).

The size of the deposit is most importantly controlled by permeability of the host-rock stratigraphic succession and how long the heat source is available. The presence of cataclastic or siliciclastic (sedimentary rock made from breakage of existing rocks) components in the host stratigraphic succession is more favourable for large VMS-deposits than just volcanic. For a deposit to get large, it requires a fault plane accommodating the hydrothermal fluids. (Barrie and Hannington, 1999)

2.2.1 Classification of VMS-deposits

VMS-deposits have been classified in different ways trough time. Cox and Singer (1986) divided the deposits in three different groups: Cyprus subtype associated with marine mafic rocks, Besshi subtype associated with clastic terrigenous sediment and marine mafic volcanic rocks, and Kuroko subtype associated with clastic terrigenous sediments and marine felsic volcanic rocks. Another classification scheme is based on the ratio of the three major base metals Cu, Zn and Pb, and distinguish between Cu-Zn, Zn-Pb-Cu and Pb-Zn type deposit based upon ternary diagrams (Figure 2-2Figure 2-2) (Large, 1992). The problem with this classification scheme is that the deposit, and the setting is not described, and this makes it difficult to compare the deposits (Franklin *et al.*, 2005).

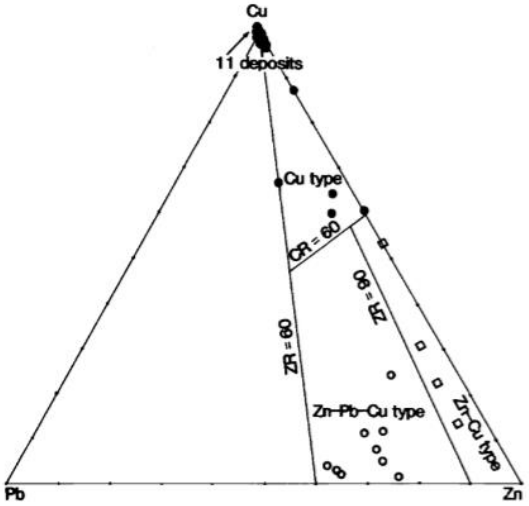

Figure 2-2 Classification based on the average base metal content in mass percent from Large (1992). ZR (zinc ratio) = 100*Zn/ (Zn + Pb). CR (copper ratio) =100*Cu/ (Cu + Zn). Cu-type in the upper part, Zn-Cu- and Zn-Pb-Cu-types in the lower right part. The mean grades of 30 Australian deposits is plotted with circles and squares (Large, 1992).

The third, and now widely used, classification of VMS deposits is based on the lithologies associated with the deposits in a given district. The concept was originally developed by Barrie and Hannington (1999) and later modified by (Franklin *et al.*, 2005). The original scheme by Barrie and Hannington (1999) was based on the lithologies up to about 1 km into the stratigraphic hanging-wall and about 3 km into the stratigraphic footwall, and up to 5 km in the strike direction of the VMS deposits. Franklin et al. (2005) modified this by taking into account the entire area affected by the volcano-sedimentary cycle in a given VMS district. This may concern anything from a few hundred square meters to over 20.000 km^2. They divided the VMS districts into 5 different lithostratigraphic types: Bimodal-mafic, mafic, pelitic-mafic, bimodal-felsic, and siliciclastic-felsic. In Table 1 the different lithostratigraphic rock types are listed with their main lithologies and the geological setting where these types were found. Barrie and Hannington (1999); Franklin *et al.* (2005); Morgan and Schulz (2012) are references below:

(1) *Bimodal-mafic* comprises at least 60% mafic lava, up to 25% felsic flows and the rest is siliciclastic rocks. Bimodal-mafic is thought to be related to volcanic arc settings and mantle plume environments. Mafic host rock is typically basaltic or tholeiitic, felsic are often rhyolites. Based on Canadian grade and tonnage, this type is the most abundant type. It has the highest average Cu-content of the subtypes. Examples of this is Noranda and Ural Mountains

(2) *Mafic type* consists of at least 75% mafic lava, less than 1% felsic and the rest is siliciclastic or ultramafic. Mafic type is often related to ophiolitic settings, ocean ridges and back-arc rifting. Predominantly tholeiitic mafic host rock. They are fewer in number, smaller, and they are often Cu-rich, and Pb-poor compared to other types. Examples of this type is Cyprus and Oman.

(3) *Pelite-mafic* is made up of about the same amount of felsic and mafic magma. These deposits are related to mature oceanic back-arc, rifted continental margin and sediment oceanic rift. They are often of Middle Protozoic age and younger and very deformed. It is not the most abundant type, but it has the second largest average tonnage, behind felsic-siliciclastic. Examples are Besshi and Windy craggy.

(4) *Bimodal felsic* consists of over 50% felsic lavas, less than 15% siliciclastic and the remnant is mafic. It is related to continental margin, arcs and back-arcs and rifted volcanic arc settings. Similar age as pelite-mafic. Host rock is typically calc-alkaline high silica rhyolite to calc-alkaline. It is the second most abundant type and contains the highest average content of Zn and Ag of the types and often contains barite. Examples are Skelleftea and Tasmania.

(5) *Felsic-siliciclastic* contains equal amount of volcanic and siliciclastic rocks, where felsic lava is more abundant than mafic. This is related to epicontinental back-arc and rifted continental arc settings. The felsic host rock is generally calc-alkaline, and the mafic is tholeiitic. The greatest tonnage is associated with these subtypes, and second largest in size. The average lowest Cu content and highest Pb content. Examples are Iberia and Bathurst.

Table 1 Classification system of VMS-deposits based on lithology and tectonic setting

ROCK TYPE (FRANKLIN *ET AL.*, 2005)	**CONTENT (BARRIE AND HANNINGTON, 1999)**	**GEOLOGICAL SETTING (BARRIE AND HANNINGTON, 1999; FRANKLIN *ET AL.*, 2005)**
BIMODAL-MAFIC (1)	>3% Felsic >50% mafic The rest is siliciclastic.	- Primitive volcanic arc - Rifted primitive volcanic arc setting - mantle plume environments
MAFIC (2)	>75% mafic <1% felsic <10% siliciclastic or ultramafic rock, or both	- Ophiolitic setting - Ocean ridge - Advanced back-arc rift - Supra subduction zone
PELITIC-MAFIC (3)	Subequal of mafic and siliciclastic.	- Mature oceanic back-arc

	Felsic volcanic rocks are minor or absent.	- Rifted continental margin - Sediment oceanic rift
BIMODAL-FELSIC (4)	>50% felsic volcanic < 15% siliciclastic Mafic volcanic and intrusive rock the remnant.	- Continental margin arcs and related back-arc - Rifted volcanic arc settings
FELSIC-SILICICLASTIC (5)	Equal volcanic and siliciclastic rocks, felsic volcanic more abundant than mafic.	- Mature epicontinental back-arc - Rifted continental arc setting

2.2.2 Tectonic setting

Several authors claim that all VMS-systems that are preserved are from extensional regimes resulting in graben subsidence, marine transgression, development of deep marine environments and injection of mafic magma from the mantle into the crust. The modern systems that are active today are mostly at mid-ocean spreading ridges. (Allen *et al.*, 2002; Galley, Hannington and Jonasson, 2007)

The old and preserved systems related to extensional regimes are thought to have formed in oceanic seafloor spreading and arc environment, and mainly in oceanic and continental nascent-arc, rifted arc, and back-arc settings. A fault plane is often the main pathway for the hydrothermal ore-forming fluids and the most common environment for VMS deposits is the formation of calderas related to bimodal mafic extrusive succession in arc environments. Volcaniclastic-rich bimodal felsic extensional regimes are often related to rifting of continental arcs (Barrie and Hannington, 1999; Galley, Hannington and Jonasson, 2007). In Figure 2-3, made by Galley, Hannington and Jonasson (2007), are all the tectonic environments where a VMS-deposit can form represented. They are natural parts of the formation of the Earth's crust. In Table 1, different types of VMS deposit listed with the content and geological settings. Types 1,2 and 3 are related to ocean-ocean subduction. Type 1 represent early arc rifting and may be related to an underlying mantle plume. Types 2 and 3 are formed in mature back-arc settings, and types 4 and 5 in an ocean-continent margin and/or continental back-arc-rifting systems. Type 4 is in the early supra-subduction arc-rifting stage, while type 5 is in the mature epicontinental back-arcs. Type 1 may also form in komatiitic environment, and type 3 in mafic alkalic terranes (seamount construction or late back-arc volcanism) (Franklin *et al.*, 2005; Galley, Hannington and Jonasson, 2007).

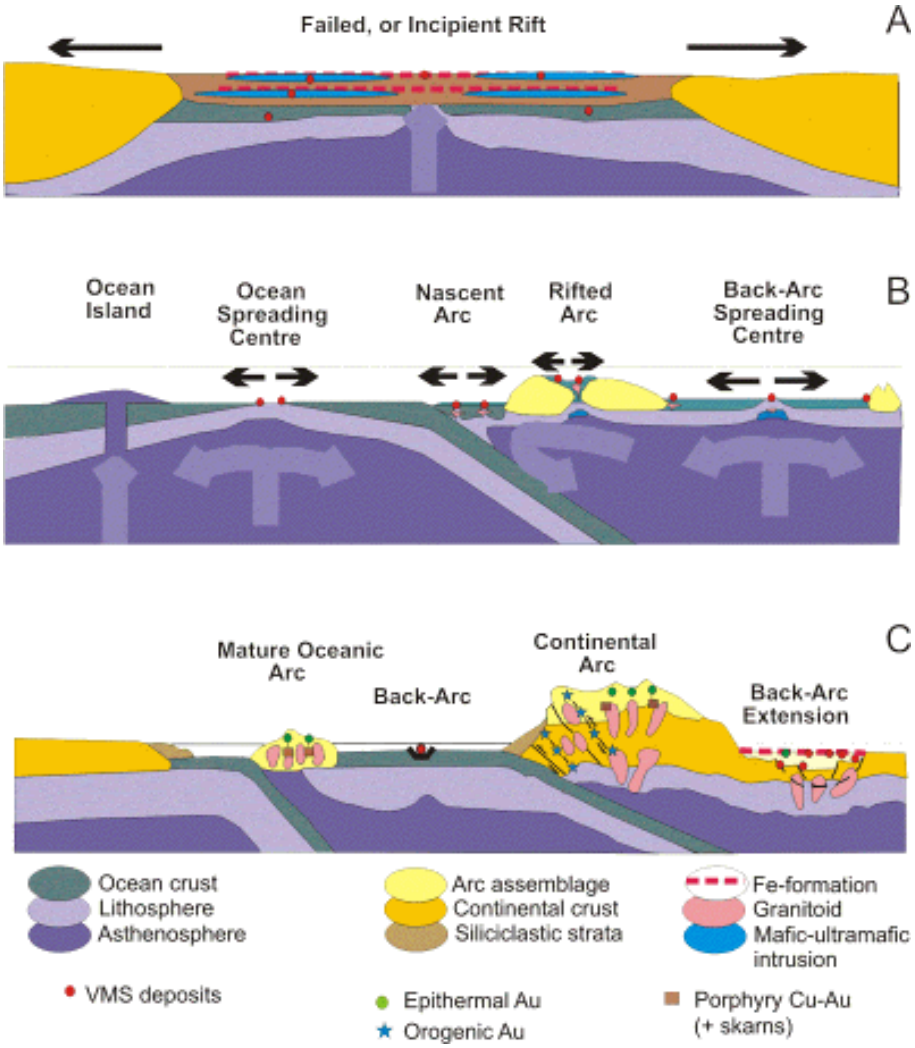

Figure 2-3 A idealized evolution of the formation of the Earth's crust and the tectonic environment VMS-deposits is formed. A) Early stage of the formation of the crust comprises plume activity, rift events and formation of basins with ocean crust and siliciclastic infill, Fe-formation and mafic-ultramafic sills. Type 3 may be formed here. B) Formation of ocean basins, ocean spreading centres, subduction zones resulting in ocean arc formation and associated extensional domains. Types 1,2 and 4 is formed in these kinds of regimes. C) In the end there is formation of mature arcs, back-arcs and continental volcanic arc assemblage because ocean-continent subduction. Types 4 and 5 are often formed in these regimes. (Galley, Hannington and Jonasson, 2007)

2.2.3 Hydrothermal alteration of host rock

The host rock surrounding the deposits that interact with the hydrothermal fluids gets altered in a greater or lesser extent. It may affect up to hundreds of kilometres along strike, down to the intrusion and up to the ambient sea floor. The alteration patterns are important evidence of the physical and chemical properties of hydrothermal fluids forming the deposit. Also, it may provide evidence for the origin of the metals. The zonation and mineral assemblage may also be a clue to find new and unexplored deposits. Shanks III (2012) claims that it is a characteristic zonation pattern in VMS-deposits that may be used as a guideline to find a deposit.

The stockwork vein system and the outer alteration zone (see Figure 2-1) forms by interaction between the hydrothermal fluid, circulating seawater, and subseafloor rocks. The rock and minerals experience metasomatism or metamorphism in contact with a hydrothermal fluid. Potassic, argillic, phyllic/sericitic, and propylitic alteration have all been observed in relation to VMS deposits. There may be different alteration types in one deposit arranged in a zonation pattern(Shanks III, 2012). Hydrothermal alteration of the host rock replaces the primary minerals with new minerals stable in the conditions of alteration, the temperature may range from 150-400°C. The typical mineral assemblage in the stockwork's core vein mineralisation is Fe–chlorite–quartz–sulphide ± sericite ± talc ± epidote mineral assemblage. Outward the zone is typically rich in sericite, phengite, Mg-chlorite, ±albite, ±carbonate, and ±barite. (Galley, Hannington and Jonasson, 2007)

2.2.4 Ore mineralogy in VMS-deposits

A VMS deposit is made in extensional regimes, and because of crustal thinning and mantle decompression, or magmatic intrusion into the continental crust may the continental become partially melted. The melt may mix with connate water (or other type of waters), become buoyant and rise toward the seafloor. The fluid finds the easiest way, and often follows a fault plane. On its way it circulates and leach the host rock for metals. It may mixes with the cold, near neutral pH, seawater further up and begin to circulate in the crust where the metals are leached from the host rock with progressively changing T, pH and Eh of the hydrothermal fluids (Allen *et al.*, 2002; Koski, 2012). A massive sulphide deposit may form at or near the seafloor when the non-boiling metal-rich fluid are cooled by erupting at the seafloor resulting in quenching by seawater or by steep thermal gradients near the seafloor (Barrie *et al.*, 1999).

The mineral assemblage in VMS deposits depends on the chemistry (pH, fO_2) and temperature of the hydrothermal fluids, the exchange reactions with the host rocks and the changes in these parameters that happens when the fluids migrates towards the surface decides which elements that ends up in the fluid and in will make up the deposit further up. The most important factor controlling the mineralogy of the ore deposit is thought to be the chemistry of volcanic rocks in the foot wall. The metal speciation may reflect the mineralogy of the leached host rock through hydrothermal alteration (Allen *et al.*, 2002; Koski, 2012; Large, 1977). According to Barrie and Hannington (1999) and references therein, it is the decomposition of minerals from the host rock that provides the source of the ore minerals. From destruction of ferromagnesian minerals and magmatic sulphide in mafic rocks, the fluid may get enriched in Cu. The felsic rock has feldspars enriched in Pb and Ba. In felsic magmatic and sedimentary rocks there are feldspars enriched in Pb, Ag and Zn.

Together with the host rock classification by Barrie and Hannington (1999), the geometry, size, composition and depth of the intrusion and permeability of the host rock are important factors in the making of a VMS-deposit. For a VMS deposit to get as large as possible it is favourable if the heat source, i.e. the intrusion, is deep and long lived to maintain a long living hydrothermal system. The permeability of the host rock is an important factor for the fluid migrating to the surface. Fault, fractures, dikes and sills are often crucial for maintenance of a fluid pathway. (Barrie *et al.*, 1999)

The formation of the mineral assemblage associated with the ore-deposit depends on multiple parameters. Early formed minerals are replaced by new minerals as the temperature of the hydrothermal activity is increasing or decreasing. The most common

sulphides are pyrite, pyrrhotite, chalcopyrite, sphalerite, and galena. The most dominant in all subtypes is either pyrite or pyrrhotite, and the next most abundant is sphalerite or chalcopyrite. Galena is abundant in bimodal-felsic and felsic-siliciclastic settings. Magnetite, hematite, cassiterite and barite are often associated gangue minerals. Idealized typical zonation patterns in bimodal-felsic and bimodal-mafic are chalcopyrite + pyrite ± magnetite in the upper stockwork, in the massive sulphide part it is dominated by pyrite + chalcopyrite. Sphalerite ± galena (± barite) is dominated in the upper and outer margins (Koski, 2012) and references therein. (Morgan and Schulz, 2012)

Koski (2012) and references therein have made a list over the most abundant minerals in the different subtypes based on the host rock:

- Mafic dominant host rock: Often dominated by pyrite, subordinate amount of chalcopyrite sphalerite, trace amount of galena.
- Siliciclastic-mafic: Pyrrhotite is more abundant relative to pyrite than in the mafic dominated. Lead poor.
- Bimodal-volcanic (felsic/mafic): often an assemblage intermediate between mafic and felsic. Major minerals are often pyrite, pyrrhotite, sphalerite and chalcopyrite. Minor amount of galena and arsenopyrite
- Rhyolites and dacite host rock: Mostly pyrite, chalcopyrite, and sphalerite, but significant amounts of galena. Often zones of ore dominated by sphalerite and galena.

2.2.5 Gangue minerals

The gangue minerals of a VMS-deposit represent all other minerals than economical minerals. Which assemblage of gangue minerals we get depends on age, metamorphic grade, and geological setting. But also, composition of the hydrothermal fluids, fluid/rock ratio, P-T history, and post ore recrystallization. In deposits of greenschist facies, the gangue mineral assemblage typically is quartz + chlorite + sericite ± carbonate ± barite ± albite. At higher metamorphic grade, the assemblage may be quartz + garnet + amphibole ± rutile. (Slack, 2012)

Metamorphic facies	**Main minerals**	**Subordinate**
Below greenschist facies	quartz, barite, carbonate, white mica, and (or) chlorite	magnetite, sodic plagioclase, epidote, tourmaline, analcime and gypsum
Higher	Chloritoid, garnet, amphibole, cordierite, gahnite, staurolite, kyanite and andalusite	Rutile and/or titanite

Some gangue minerals are broadly linked to the presence or absence of some gangue minerals. Especially barite and K-feldspars with high concentrations of Ba occurs in several Archean deposits, but also Phanerozoic deposits.

Zonation of gangue minerals is not much discussed in previous studies. Slack (2012) referring to Galley, Hannington and Jonasson (2007); Large (1992) suggested some generalization with quartz most abundant in the cores of the sulphide mount and barite and/or anhydrite at the margins. In the lower and upper parts of the sulphide mounds may chlorite and sericite be concentrated.

2.2.6 Deposits in Norway and around the world

In the Scandinacian Caledonides

Volcanic massive sulphide deposits have been reported from four different paleotectonic environments in the Scandinavian Caledonides; ophiolities (Løkken), immature arc (Skorovas, Stekenjokk - Levi), mature arc (Fosen), mixed sedimentary-volcanic sequences (Røros and Sulitjelma). These are most likely deposited in the end of the continental rifting and ocean floor spreading and, in the beginning of the plate convergence and ocean closure. The immature types are most likely deposited on each side of the ocean, one on the Baltik margin (Stekenjokk-Levi) and one on the Laurentian margin (Skorvas). Stekenjokk-Levi is deposited in a bimodal-felsic sequence and a thick tuffite sequence that often contains graphite. (Grenne, Ihlen and Vokes, 1999)

Bleikvassli deposit that lies about 50km south of Mo i Rana was long thought to be a sedimentary hosted massive sulphide deposit, but in recent studies by Bjerkgård *et al.* (1997) has litogeochemical analyses been done. The amount of volcanic rocks is bigger than previously thought and the setting is changed to be a volcanic massive sulphide deposit formed in a back-arc basin. The host and wall rocks is meta-volcanics and -sediments and amphibolites, and the massive deposit is a Zn-Pb-(Cu) deposit. (Cook, 1993)

In Figure 2-4 is one suggestion of how the Caledonian orogeny evolved, the massive ore deposits in the Caledonides is most likely formed during the continental rifting and ocean spreading and the early plate convergence and ocean closure. (Grenne, Ihlen and Vokes, 1999)

Keketale Pb-Zn VMS deposit in China

The Keketale deposit in the early Devonian sequence of the Kangbutiebao Formation of the Southern Altai Metallogenic Belt in China is a Pb-Zn VMS deposit. It is hosted by meta-sedimentary and volcanic rocks. The major sulphides are pyrite, sphalerite, galena, minor pyrrhotite and rare chalcopyrite. It consists of massive, banded and disseminated ore and has a typical VMS type hydrothermal alteration zone around the ore body. The host rock plots in the volcanic arc field, and the hydrothermal fluid was reducing. The observations indicate that is most likely is formed in a back-arc or arc basin. (Wan *et al.*, 2010)

New Brunswick No. 12, Canada

New Brunswick No. 12 is the world's largest underground mine and the fourth largest zinc producer. It is a Zn-Pb type massive sulphide deposit and is hosted by the Middle Ordovician bimodal volcanic and sedimentary sequence in the northern Appalachian of New Brunswick. The deposits were emplaced in an intra-continental back-arc basin. The massive sulphide occurs in layers and lenses with pyrite, sphalerite, galena, chalcopyrite and pyrrhotite. The grade is average 5.7% Zn, 2.4% Pb, 0.53% Cu, 75ppm Ag and 0.82ppm Au(McClenaghan *et al.*, 2009). The Brunswick area is a part of the Appalachian Mountains made by the Appalachian Orogenesis. The Caledonian mountains and the Appalachian mountains was the roots of the same Palaecoic orogenic belt and was separated by Iapetus, and when the Iapetus closes, these two mountain ranges was made, among others (TheEditorOfEncyclopaediaBritannica, n.d.).

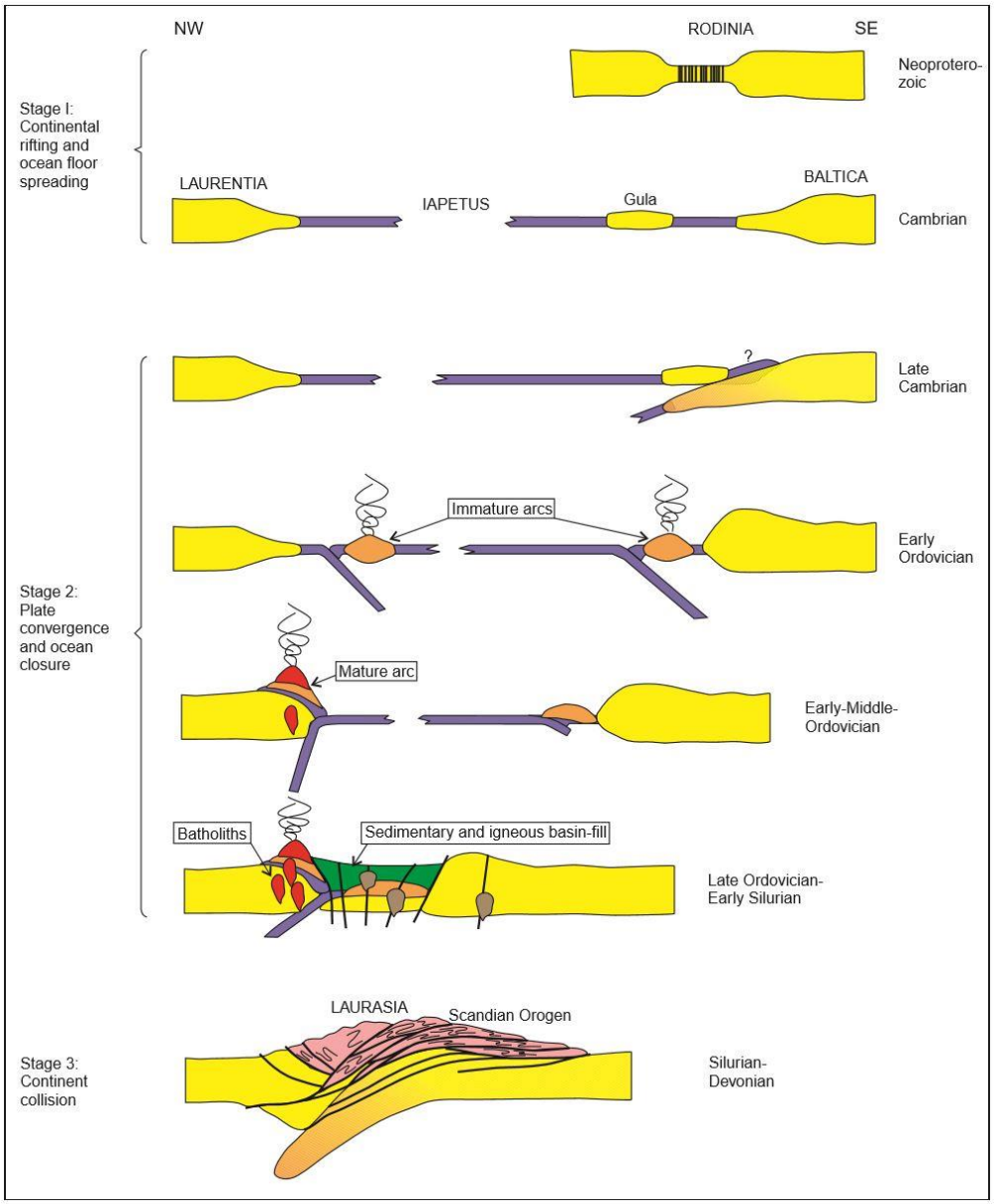

Figure 2-4 Grenne, Ihlen and Vokes (1999) suggestion of how the Caledonian orogency evolved. The massive ore are most likely made during stage 1 and early stage 2.

3 Methodology

3.1 Field work

Fieldwork was carried out for 3 weeks in August 2019. Most time was used at Hellerfjellet since more work have been done in the Hesjelia zone in previous studies done mostly by NGU as mentioned in Chapter 1.2. Also, Hellerfjellet covers a bigger area. In the field the mapping program FieldMOVE was used on an Apple iPad to get coordinates and write notes at the different localities. The bedrock maps MO I RANA (Søvegjarto *et al.*, 1988) and STORAKERSVATNET (Marker *et al.*, 2012) was used as a reference for where to go and which areas to focus on. The alteration zones, including the muscovite gneiss, the ores and the workings were studied since the ore-forming process and the lithologies affected by this is the focus in this thesis. Altogether 85 samples were collected with hammer and chisel, 24 of them were made thin section of and lithogeochemistry was carried out on all samples.

3.2 Drill core logging

One drill core from Hellerfjellet (BH4508) was logged in detail at NGU's National Drill Core and Sample Centre in Løkken in Trøndelag, Norway. 12 thin sections were made from the core and chemical analyses of the mineralized zone have been done with a portable XRF-analyser. It is also one core intersecting the Hesjelia-Hammertjønna zone at the storage, but the ore zone is missing, so this core was not studied in detail.

The portable XRF-analyser used is a **Thermo Scientific Niton XL3t goldd** owned by the Geological Survey of Norway.

3.3 Whole rock lithogeochemistry

All the samples collected in the field were shipped to Finland to MSALABS in Kempele for preparation and then to their lab in Canada for chemical analyses.

The WRA-360 method was used, which is a complete package for whole rock analyses at main and trace element level. The method included:

- Multi-element determination of mineralogical samples using four acid digestion and ICP-AES/MS finish
- Multi-element determination of mineralogical samples using two acid digestion and ICP-AES/MS finish
- Multi-element determination of mineralogical samples using a lithium borate fusion and ICP-MS finish
- Multi-element determination of mineralogical samples using lithium borate fusion and ICP-OES finish

For all the methods the samples were crushed and milled to 85% -75µm, dried and separated in batches.

3.3.1 Multi-element determination of mineralogical samples using four acid digestion and ICP-AES/MS finish

The homogeneous sample was digested in hydrofluoric acid (HCl), hydrochloric acid (HF), nitric acid (HNO_3) and perchloric acid ($HClO_4$). The sample was then mixed with deionized water to the correct volume for the analyses was reached. Almost all minerals will digest in this kind of solution, only the most highly resistant minerals will not be dissolved (e.g. zircon, and magnetite). Volatile elements (e.g. As, B, Pb, Ge, Sb) may be lost in the process (SGS, 2019). The sample solution was then analysed by Inductively Couple Plasma-Atomic Emission (ICP-AES) Spectroscopy and Inductively Couple Plasma Mass Spectrometry (ICP-MS). The elements analysed with this method is presented in Table 2. (MSAnalytical, 2017b)

Table 2 Quantitation limits for elements analysed in the 4-Acid ICP-AES/MS finish method (MSAnalytical, 2017d)

Element	Range	Element	Range	Element	Range
Ag	0.01-100 ppm	Hf	0.1-500 ppm	Sb	0.05-10 000 ppm
Al	0.01-50%	In	0.005-500 ppm	Sc	0.1-10 000 ppm
As	0.2-10 000 ppm	K	0.1-10%	Se	1-1000 ppm
Ba	10-10 000 ppm	La	0.5-10 000 ppm	Sn	0.2.-1000 ppm
Be	0.05 – 1000 ppm	Li	0.2-10 000 ppm	Sr	0.2-10 000 ppm
Bi	0.01-10 000 ppm	Mg	0.1-50%	Ta	0.05-100 ppm
Ca	0.01-50%	Mn	5-100 000 ppm	Te	0.05-500 ppm
Cd	0.02-1000 ppm	Mo	0.05-10 000 ppm	Th	0.2-10 000 ppm
Ce	0.02-500ppm	Na	0.01-10%	Ti	0.005-10%
Co	0.1-10 000 ppm	Nb	0.1-500 ppm	Tl	0.02-10 000 ppm
Cr	1-10 000 ppm	Ni	0.2-10 000 ppm	U	0.1-10 000 ppm
Cs	0.05-500 ppm	P	10-10 000 ppm	V	1-10 000 ppm
Cu	0.2-10 000 ppm	Pb	0.5-10 000 ppm	W	0.1-10 000 ppm
Fe	0.01-50%	Rb	0.1-10 000 ppm	Y	0.1-500 ppm
Ga	0.05-10 000 ppm	Re	0.002-50ppm	Zn	2-10 000 ppm
Ge	0.1-500ppm	S	0.01-10%	Zr	0.5-500 ppm

3.3.2 Multi-element determination of mineralogical samples using two acid (aqua regia) digestion and ICP-AES/MS finish

The homogeneous samples where digested in a mixture of hydrochloric acid and nitric acid while heated. The samples were then mixed with deionized water to the correct volume for the analyses. The solution was analysed by ICP-AES and ICP-MS. The elements to be analysed with this method is presented in Table 3. (MSAnalytical, 2017d)

Table 3 Quantitation limits for elements analysed in the 2-Acid ICP-AES/MS finish method (MSAnalytical, 2017d)

Element	Range	Element	Range	Element	Range
Ag	0.01-100 ppm	Ge	0.05-500 ppm	S	0.01-10%
Al	0.01-25%	Hf	0.02-500 ppm	Sb	0.05-10 000 ppm
As	0.1-10 000 ppm	Hg	0.005-10 000 ppm	Sc	0.1-10 000 ppm
Au	0.0005-25 ppm	In	0.005-500 ppm	Se	0.2-500 ppm
B	10-10 000 ppm	K	0.1-10%	Sn	0.2.-1000 ppm
Ba	10-10 000 ppm	La	0.1-10 000 ppm	Sr	0.2-10 000 ppm
Be	0.05 – 1000 ppm	Li	0.1-10 000 ppm	Ta	0.1-500 ppm
Bi	0.01-10 000 ppm	Mg	0.1-25%	Te	0.01-500 ppm
Ca	0.01-25%	Mn	5-50 000 ppm	Th	0.2-10 000 ppm
Cd	0.01-1000 ppm	Mo	0.05-10 000 ppm	Ti	0.005-10%
Ce	0.02-500ppm	Na	0.01-10%	Tl	0.02-10 000 ppm
Co	0.1-10 000 ppm	Nb	0.05-500 ppm	U	0.05-10 000 ppm
Cr	1-10 000 ppm	Ni	0.2-10 000 ppm	V	1-10 000 ppm
Cs	0.05-500 ppm	P	10-10 000 ppm	W	0.05-10 000 ppm
Cu	0.2-10 000 ppm	Pb	0.2-10 000 ppm	Y	0.05-500 ppm
Fe	0.01-50%	Rb	0.1-10 000 ppm	Zn	1-10 000 ppm
Ga	0.05-10 000 ppm	Re	0.001-50ppm	Zr	0.5-500 ppm

3.3.3 Multi-element determination of mineralogical samples using a lithium borate fusion and ICP-MS finish and ICP-OES finish

These methods are for the samples that are difficult to dissolve in acids, such as metal oxides and refractories. The samples were heated in a high temperature muffle furnace

at 1000°C with lithium borate flux. It was then cooled and dissolved in mineral acids. The remaining solution is analysed by ICP-MS and Inductively Coupled Plasma-Optical (ICP-OES) Emission Spectroscopy. The elements to be analysed with these methods is presented in Table 4 and Table 5. (MSAnalytical, 2017c; 2017a)

Table 4 Quantitation Limits for elements analysed with the Lithium Borate ICP-OES finish method (MSAnalytical, 2017a)

Element	Range(%)	Element	Range(%)	Element	Range(%)
Al_2O_3	0.01-100	K_2O	0.01-100	SiO_2	0.01-100
BaO	0.01-100	MgO	0.01-100	SrO	0.01-100
CaO	0.01-100	MnO	0.01-100	TiO_2	0.01-100
Cr_2O_3	0.01-100	Na_2O	0.01-100	LOI	0.01-100
Fe_2O_3	0.01-100	P_2O_5	0.01-100	*Total	97-103

*Total is dependent of the other base metals in the sample

Table 5 Quantitation limits for elements analysed with the Lithium Borate ICP-MS finish method (MSAnalytical, 2017c)

Element	Range (ppm)	Element	Range (ppm)	Element	Range (ppm)
Ba	0.5-10 000	Ho	0.01-1000	Ta	0.1-2500
Ce	0.1-10 000	La	0.1-10 000	Tb	0.01-1000
Cr	10-10 000	Lu	0.01-1000	Th	0.05-1000
Cs	0.01-10 000	Nb	0.1-2500	Tm	0.01-1000
Dy	0.05-1000	Nd	0.1-10 000	U	0.5-1000
Er	0.03-1000	Pr	0.03-1000	V	10-10 000
Eu	0.03-1000	Rb	0.2-10 000	W	1-10 000
Ga	0.2-1000	Sm	0.03-1000	Y	0.5-10 000
Gd	0.05-1000	Sn	5-10 000	Yb	0.03-1000
Hf	0.2-10 000	Sr	0.1-10 000	Zr	2-10 000

3.3.4 Calculation of metals in ppm from compound oxides

In the chemical results from MSAnalytical the values for some of the elements were shown as oxides. Some of these were recalculated to get the elements in ppm, and was done for, among others, BaO and MnO. Example of the calculation for BaO will follow. Ba was detected, but those with values over 10 000 ppm detected as oxides. These where calculated by converting BaO like this:

Component	**Atom mas (u)**
Ba	137,327
O	15,999
BaO	153,326
Ppm Ba	$\frac{137,327}{153,326} = 0,8957$ 0,8957 X weight% BaO X 10 000 =ppmBa

Example:

BaO (%)	Calculation	Ppm Ba
1,58	1,58 X 0,8957 X 10 000	14151,3

3.4 Thin section production

36 polished thin sections (dimensions 28x48mm) were made at the thin section laboratory at Berglaboratoriet at the Department of Geoscience and Petroleum, NTNU, Trondheim. 24 sections were from field samples and 12 from the drill core from Hellerfjellet.

3.5 Optical microscopy

Both transmitted and reflected polarized light was used for the optical microscopy. Microscopy was used to identify mineral, as well as the crystal shape, grain size, mineral behaviour, texture, and relation between minerals. Which samples to analyse with SEM and EPMA was also decided using optical microscopy.

With transmitted light microscopy it is possible to look at the thin section with both plane polarized light and crossed polarized light. In plane polarized light (PPL) the relief, cleavage, colour and pleochroism are important properties. With crossed polarised light (XPL) the interference colour, extinction and birefringence are the main properties to look at.

The opaque minerals are observed with reflected light microscopy. With reflected light microscopy the light is directed to the surface of the specimen, and the minerals will either reflect and/or absorb the light. The reflected light is captured by the objective and the minerals can be seen (Abramowitz and Davidson, n.d.). Important properties possible to see with reflected light is shape, size, colour, bireflectance, anisotropy and internal reflections of the opaque or nearly opaque minerals.

A **Nikon eclipse E600 microscope** with reflected light source **Nikon** and a **Spot Insight CMOS** camera was used at the Microscopy lab at Petroleumteknisk centre at NTNU, Trondheim.

All the thin sections were scanned in PPL, XPL and reflected light to get an overview of the thin sections. The scans were used mostly when looking at selected thin sections in SEM and EPMA to find the correct spots to analyse. For this work was an **Olympus BX51 microscope** with reflected light source **Prior Lumen200PRO** used at Microscopy lab at Petroleumteknisk centre at NTNU, Trondheim.

3.6 Scanning Electron Microscope (SEM)

Scanning Electron Microscope (SEM) can provide information on surface topography, crystalline structure, chemical composition, and electrical behaviour of a specimen. The specimen can be a polished thin section or polished section, and even small rock samples and single grains can be analysed. Up to 1000 000 X magnification can be achieved with 1nm resolution (Vernon-Parry, 2000). The basic principle of SEM is an electron gun that produce a focused beam of energetic electrons at the specimen which then produces secondary, backscattered and Auger electrons, x-rays and light (cathodoluminescence) and heat (see Figure 3-1to see the direction of the signals)(Vernon-Parry, 2000).

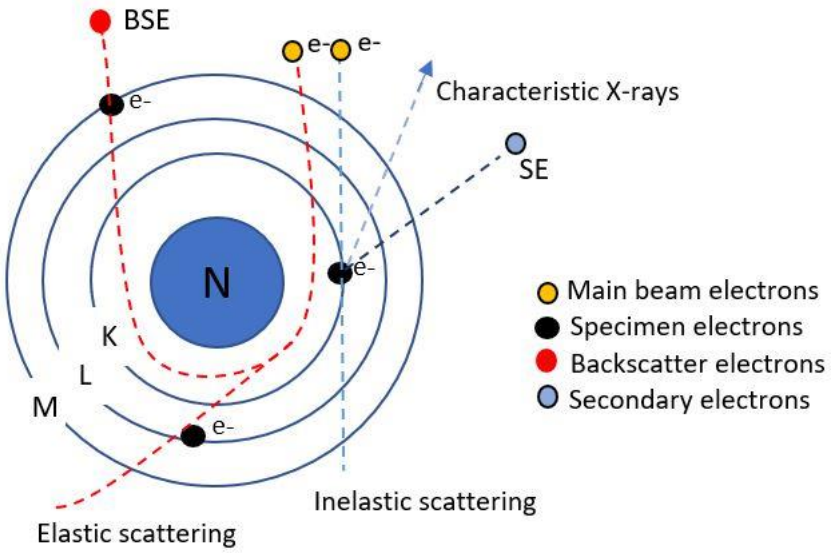

Figure 3-1 Interaction of the electron beam into an atom may be like this. The BSE goes through an elastic scattering, changes direction and escape the specimen again. The SE is electrons ejected out from an atom because of the incoming beam. The characteristic X-rays is the energy released when one electron replaces the vacant spot in an inner shell. Modified from(Huges, 2016).

The 10 thin sections that was to be analysed with SEM was coated with carbon before the analyses. A **Cressington carbon coater – 208carbon** with a **Cressington thickness monitor – mtm10** was used. 7 seconds per shock with 4,3 V. The thickness of the coating is between 15 and 20nm. This was done at the Microscopy lab at Petroleumteknisk centre at NTNU, Trondheim.

3.6.1 Secondary Electron (SE)

Secondary electrons are electrons in the atom that is ejected by the incoming beam when it goes through inelastic scattering (see Figure 3-1). The energies of the secondary electrons are below 50 eV. The beam is detected by an SE detector, and an image is made. This gives the image with highest resolution since the beam is only at or near the surface of the specimen, and it primarily gives topographic information. (Goldstein *et al.*, 2018; Vernon-Parry, 2000)

3.6.2 Backscattered Electron (BSE)

The incident electron beam shooting the sample causes both elastic and inelastic collision between electrons and atoms within the sample. Backscatter Electron(BSE) is when the incoming beam electrons interact with the sample without any significant change in the kinetic energy but completely changes direction and escape the specimen again (see Figure 3-1). The escaping beams are called *backscattered electrons* and a BSE detector is detecting the signal and an image is made. The BSE signal can give important information of composition, topography, mass thickness, and crystallography (Goldstein *et al.*, 2018; Goodge, 2016). It is most valuable in illustrating a compositional contrast in a sample. Bigger and heavier atoms, those with greater atomic number, have a bigger cross-section area and has greater chance of producing elastic collision. The brightness of a phase in a sample is the result of the average atomic number of the analysed spot. The higher atomic number, the brighter BSE intensity (Goodge, 2016). BSE images has less

resolution than SE images, but it goes deeper in the specimen and give more information (Vernon-Parry, 2000).

3.6.3 Energy Dispersive Spectrometry (EDS)

Energy dispersive Spectrometry (EDS) is the most common detector to use and gives qualitative results relatively fast. It also gives semi-quantitative results, but these can't always be trusted (Vernon-Parry, 2000). An EDS detector detects the characteristic X-ray for the elements and separate the elements into an energy spectrum, and then the software determines the abundance of the elements compared with standards and relative to other elements. The chemical components of a specimen down to a spot size of a few microns is possible to measure with an EDS detector. Also, a compositional map over a bigger area can be made (Goodge, 2017). It can detect photons from a threshold of about 40 eV to E_0. Analytical software is used to look at the results of the qualitative X-ray microanalysis. The most important thing this software do is to decide which element each peak in the spectrum represent. Different elements may have the same peak, so the operator should check and be sure that the right element is chosen for that phase and for the qualitative analyses. The quantitative analyses are based on the intensity of each peak relative to the other peaks and to standards. This is determined by peak fitting procedures (Goldstein *et al.*, 2018). The images SE and BSE detectors identifies is used as a background picture for the maps and analyses with the EDS.

The biggest limitation of SEM and EDS is that some elements have overlapping energy peaks. Especially between those with higher energies where some elements may have the same energy between different shells. Then the operator must decide which element that makes most sense. WDS with EPMA is a more precise method to use for chemical analyses, but SEM and EDS is faster (Goodge, 2017).

One example of overlapping peak is showed in Figure 3-2. The LA shell in Pb has overlapping peak with KB shell in As, but since Pb makes more sense to have here than As, is Pb chosen in this case. And also, there is no peak at any other shell for As.

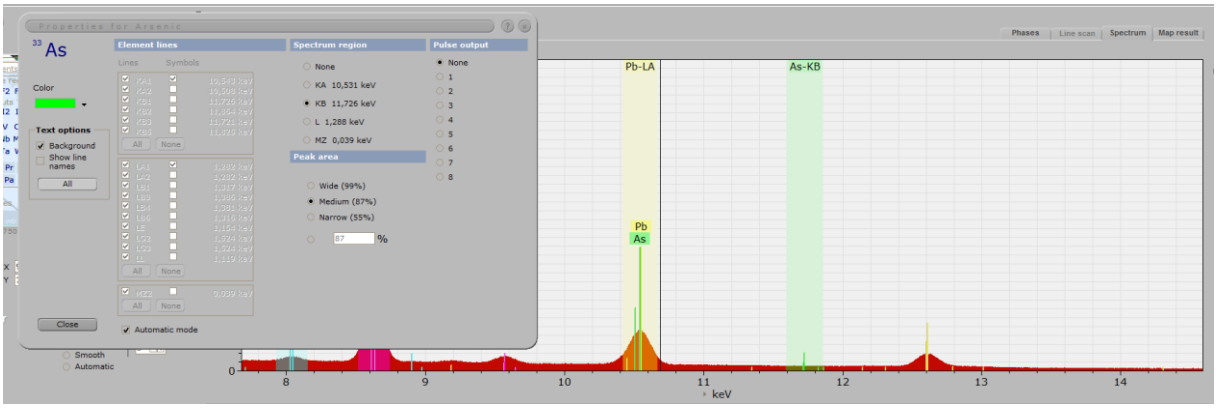

Figure 3-2 Example of overlapping peaks between Pb and As.

A **Hitachi SU6600 Scanning Electron Microscope** with Schottky-field emission electron source was used at the microscopy lab at Petroleumteknisk center, NTNU, Trondheim. Both SE, BSE and EDS, the setup can be seen in Table 6 and Table 7. SEM was used to get the chemistry of the sulphides and some of the gangue minerals to map out the differences and similarities between the different outcropping ore zones. Also, to be better prepared for EPMA.

Table 6 Setup for BSE for the SEM analyses.

Setup for BSE		
Electron beam	Vacc	20 kV
	Gun Brightness	Extraction voltage: 5-2.20kV
		Supressor voltage: 300V, medium, 15.0
		Probe current: Cond Lens 1 Cond Lens 2
Working distance	15mm	
Anode aperture	As recommended by the software:	Anode aperture: 3 Obj aperture: 2

Table 7 Setup for the EDS for the SEM-analyses.

Setup for EDS		
Point analyses	Analyse 10 seconds on each point	Acquire: Automatic PB-ZAF Quantify: interactive PB-ZAF or automatic PB-ZAF
Mapping	Analyse 5 minutes per map	

6 thin sections from the field samples and 4 from the Hellerfjellet drill core was analysed with SEM. Two samples from each locality was analysed. One of massive ore from the prospects and one of disseminated ore not far away from the prospects. The thin sections analysed from the drill core were from the wall rock (grey gneiss) and from the alteration close to the ore zone.

The field samples analysed was HES-04NGU and HS-05 from Hesjelia, HAM-04NGU and HAM-B2 from Hammertjønna and HF-10NGU and HF-x18 from Hellerfjellet. Samples from the drill core is from 14.25-14.40, 91.00-91.20, 102.90 and 141.50 meters below surface.

The results from SEM is semi-quantitative and was supposed to be followed up with Electron probe micro-analyser (EPMA). But because of the situation with lockdown of the country because of the pandemic COVID-19, was there no time or opportunity to do the last methods planned for this thesis.

3.7 ArcGIS Pro

The GIS program ArcGIS Pro has been used to plot the coordinates for the samples to get an overview of where they are collected. The map used is a bedrock map from GeologicalSurveyofNorway (n.d.) and a basemap from (Kartverket, n.d.).

This have been used when picking out samples for thin section. The samples from NGU and the drill core coordinates has also been plotted in the map.

3.8 Chemical diagrams – ioGAS-64

ioGAS-64 software is used to make the diagrams for the results of the chemical results. The software has various commonly used geological diagrams made by different authors. New diagrams can also be made. The results from the chemical analyses was plotted in different diagrams to find trends and useful information to get closer the answers this thesis is trying to figure out.

4 Results

4.1 Field observations

4.1.1 Lithological descriptions

There are several different lithologies in the two studied areas which also varies to some degree in composition, texture, and structure. The two zones studied are the Hellerfjellet and Hesjelia zones shown in the maps in Figure 4-1 and Figure 4-2. All together 6 different lithologies has been observed in the studied areas, and these will be described in detail in the following subchapters.

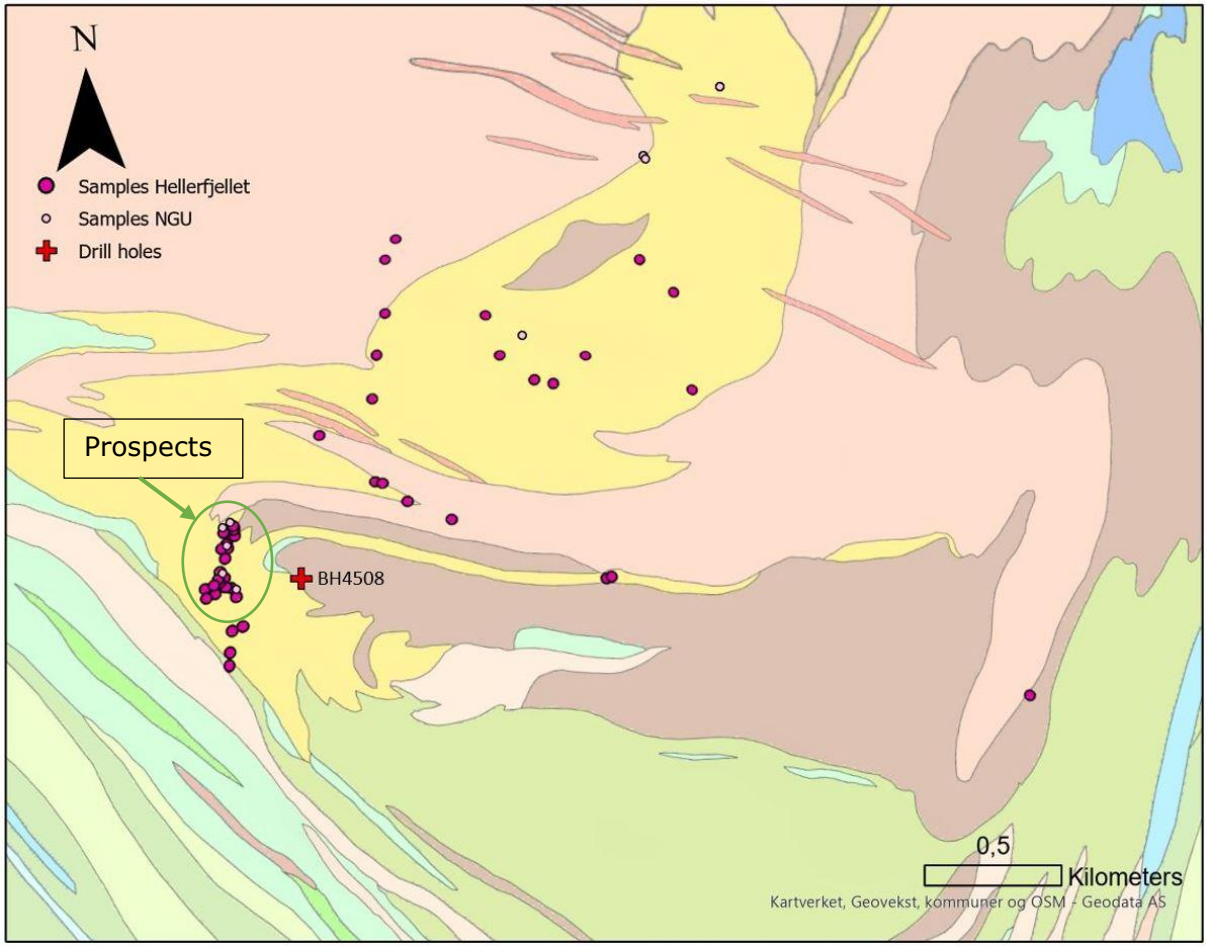

Figure 4-1 Hellerfjellet zone. The purple and yellow dots represent the samples collected in the area by me and NGU, the red dot is the drill hole made by GEXCO in 2009. Legend in Figure 4-2. Map from: NGU-bergrunnskart (Marker et al., 2012)

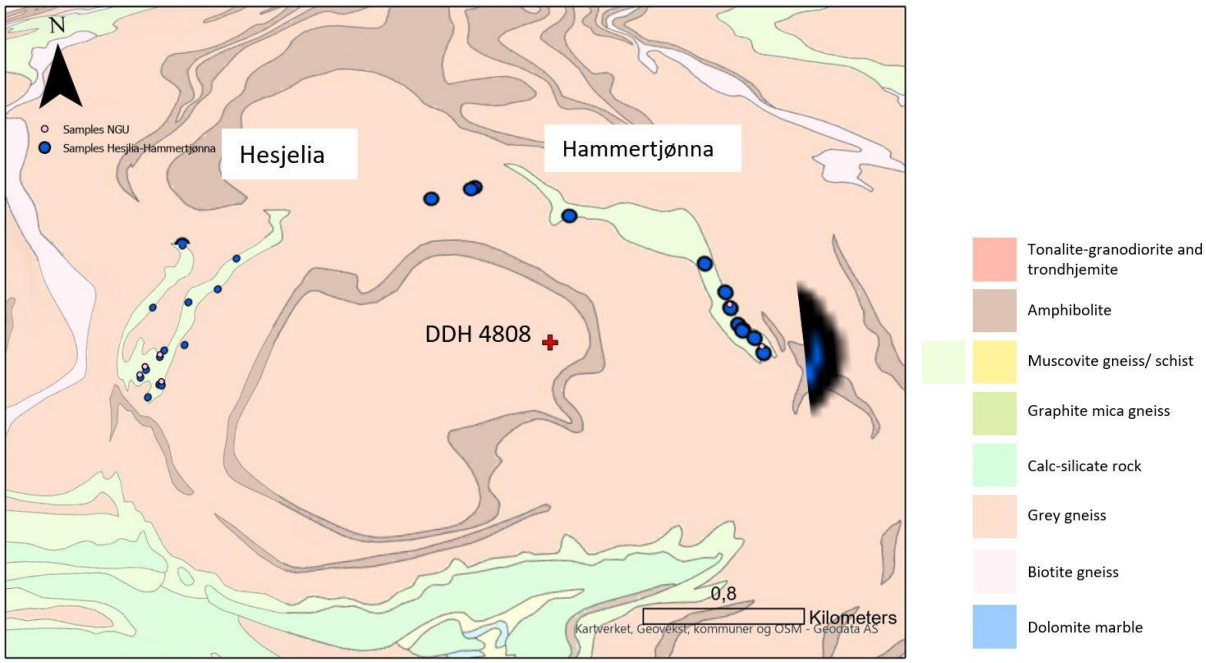

Figure 4-2 Map over Hesjelia zone, Hesjelia and Hammertjønna are the two areas with outcropping ore. The dots represent the samples collected in the area by me and NGU. Map from NGU (Søvegjarto et al., 1988).

Muscovite schist/ gneiss

The muscovite schist/gneiss was the main focus of this study since it is the host rock for the mineralisation's. It has been suggested that it is a result of alteration associated with ore-formation, but this will be discussed in details in the chemical results in Chapter 4.3. The muscovite schist/ gneiss is white to pale greyish and greyish when it contains graphite. It is typically strongly schistose and foliated and locally banded and can be both fine- and coarse-grained. In hand specimen it has a pearly lustre, due to the content of sericite. The main minerals are quartz and white muscovite (sericite), minor biotite and garnet and locally kyanite and chlorite. It has varying amounts of quartz and sericite, if mostly quartz, it is more gneissose, with more sericite it is more schistose. In the Hesjelia-Hammertjønna zone chlorite is abundant, while in the Hellerfjellet zone it may contain graphite and garnet. It often contains disseminated grains of sulphides, mostly pyrite or pyrrhotite.

The lateral extent of this rock at Hellerfjellet is up to 1.5km in the east-west direction and over 3km towards north from the prospects, see Figure 4-1. Several varieties of muscovite schist are present at Hellerfjellet. Far away from the massive ore the schist is typically whitish with almost only quartz and white muscovite (Figure 4-3a). Near the massive ore and the prospects is graphite-rich muscovite schist dominating, and this is only observed at Hellerfjellet. Bands of minor biotite appears throughout the area, and garnet is also present (Figure 4-3b). Throughout the area it contains sulphides (mostly pyrite or pyrrhotite), which either is concentrated in bands or is disseminated throughout the rock. In Figure 4-4 and Figure 4-5 is examples of how the muscovite schist/gneiss appears in the field at Hellerfjellet. Here, it is more schistose at Hellerfjellet than in the Hesjelia zone.

The muscovite gneiss/schist is outcropping in two places in the Hesjelia zone, in the areas of sulphide mineralisations at Hesjelia and Hammertjønna, see Figure 4-2. The maximum extent of the zone is 300m in the east-west direction, and about 1 km towards

north, this applies to both outcropping zones. The dip direction of the layers is towards south. In the Hesjelia zone the muscovite schist/ gneiss is generally coarser grained than in the Hellerfjellet zone and contains more quartz (Figure 4-3c). It may have layers of biotite and in the Hammertjønna area chlorite is observed (Figure 4-3d). It may contain disseminated sulphides, mostly pyrite, away from the massive ore. Figure 4-6 and Figure 4-7 are examples of muscovite gneiss/schist seen in the field in the Hesjelia zone, it is not as schistose as in the Hellerfjellet zone probably because of higher quartz contents. In Figure 4-7 can we see the yellow colour this rock type has when it is small amounts of sulphides.

In Figure 4-8 and Figure 4-9 are examples of muscovite schist from both zones in thin section. In these examples we can see that the muscovite gneiss/ schist from the Hesjelia zone(Figure 4-8) is coarser grained than the muscovite gneiss/schist from the Hellerfjellet zone(Figure 4-9). The grain size of quartz varies more in the Hesjelia zone than in Hellerfjellet, the Hellerfjellet zone is generally more fine-grained. Figure 4-10 show the muscovite gneiss from the Hesjelia zone in the microscope. The quartz grains show signs of recrystallization with undulose extinction and triple junctions. The grain contacts are irregular, and the grain sizes varies considerably. Figure 4-11 is examples from Hellerfjellet where we can see that sericite is partially replacing the plagioclase feldspars which is a common type of sericite alteration.

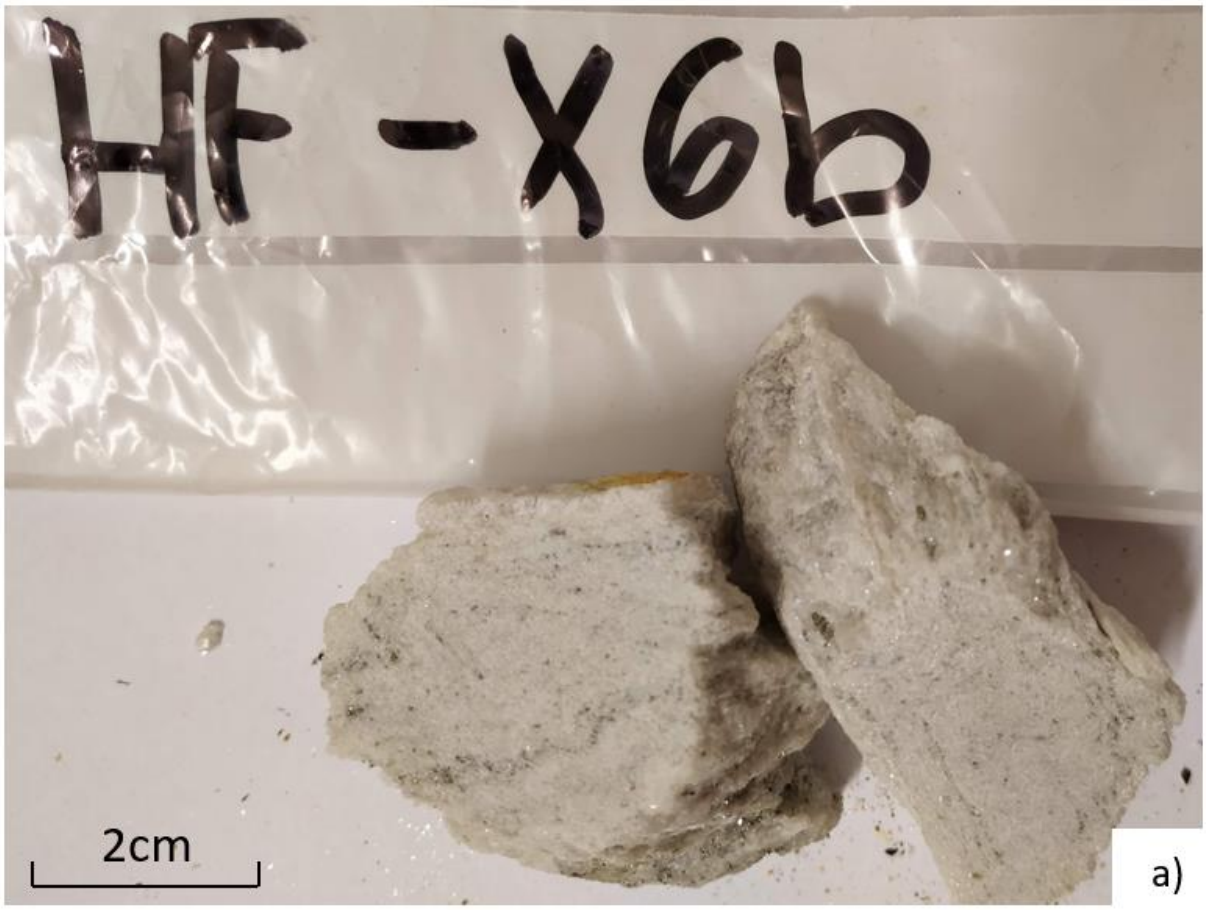
HF -X6b
2cm
a)

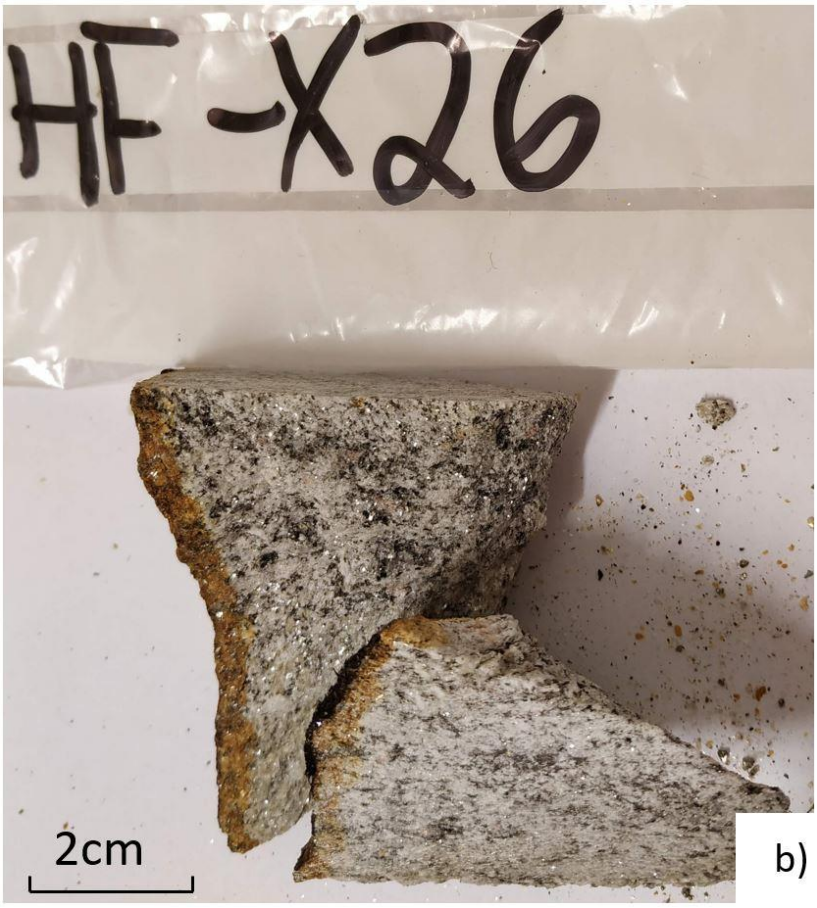
HF-X26
2cm
b)

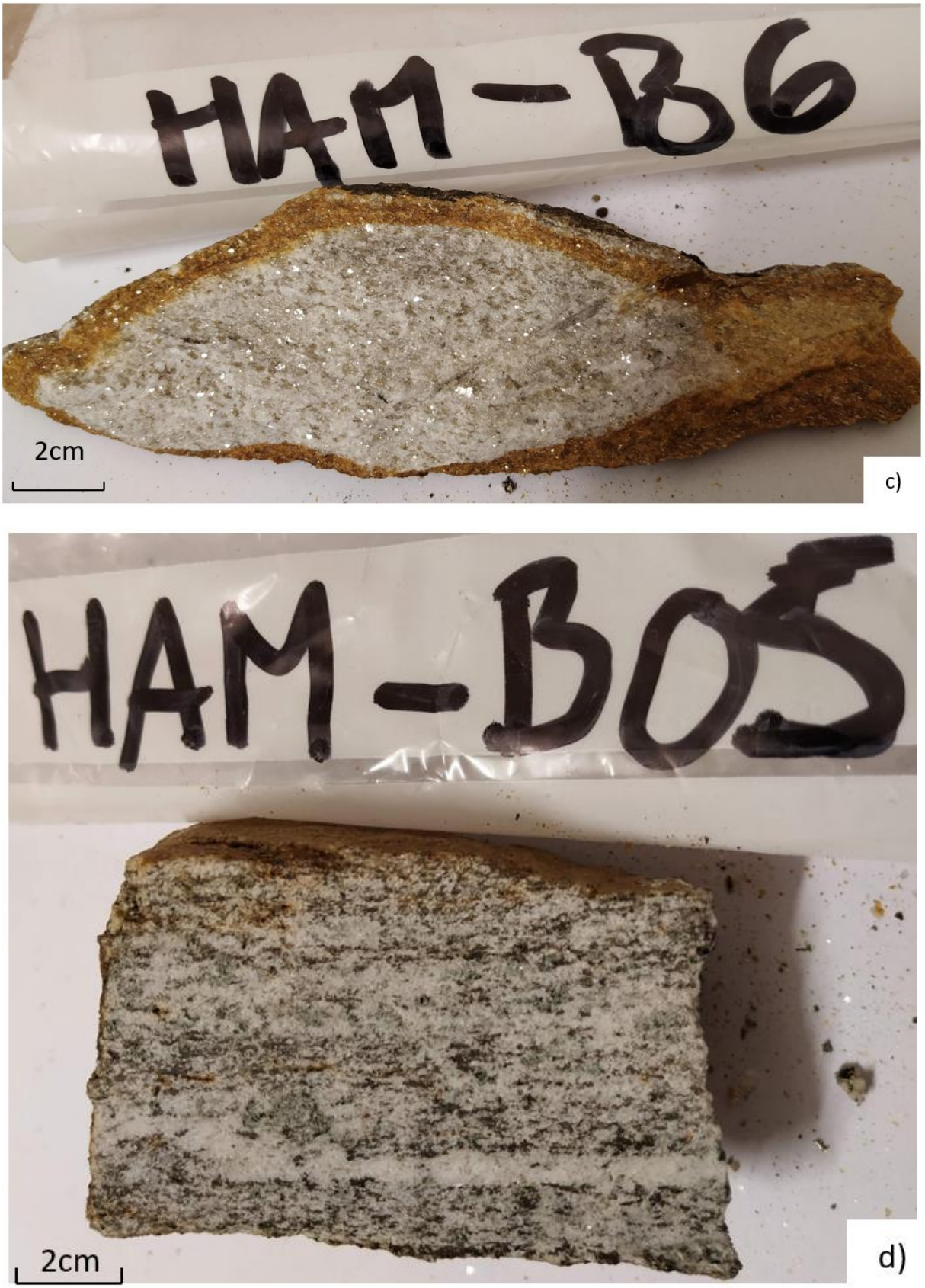

Figure 4-3 Samples of muscovite gneiss/schist collected in the field. a) perfect example of a white muscovite gneiss with more sericite from Hellerfjellet, and it also are mineralized with pyrrhotite. b) sample from Hellerfjellet with minor biotite and garnet. c) an example from Hammertjønna, and this is richer in quartz compared to sericite. d) sample from Hammertjønna with chlorite and biotite.

Figure 4-4 Muscovite schist seen in the field at Hellerfjellet. It is very schistose and probably contains more mica than quartz.

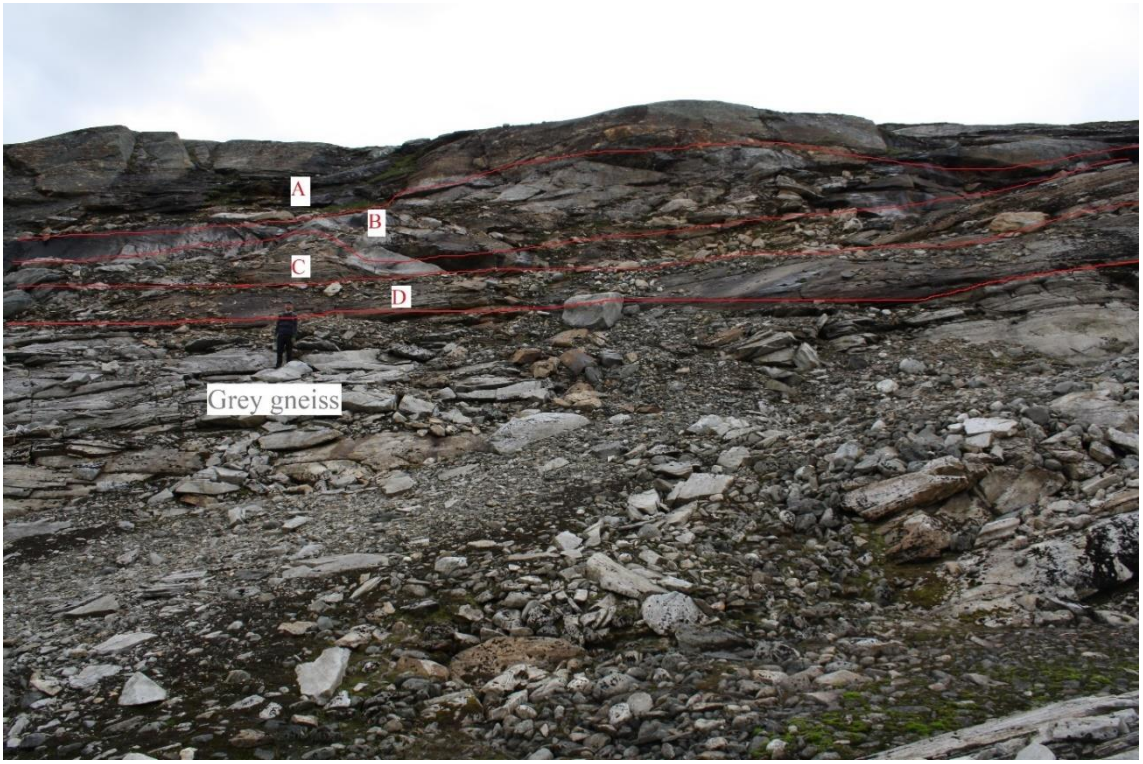

Figure 4-5 From Hellerfjellet. In this wall there is 3 different variations of muscovite gneiss. A Muscovite gneiss with fine-grained quartz and white muscovite, mineralized with pyrite and/or pyrrhotite. B: Trondhjemite dyke. C: Muscovite gneiss with traces of graphite. D: Biotite bearing muscovite gneiss

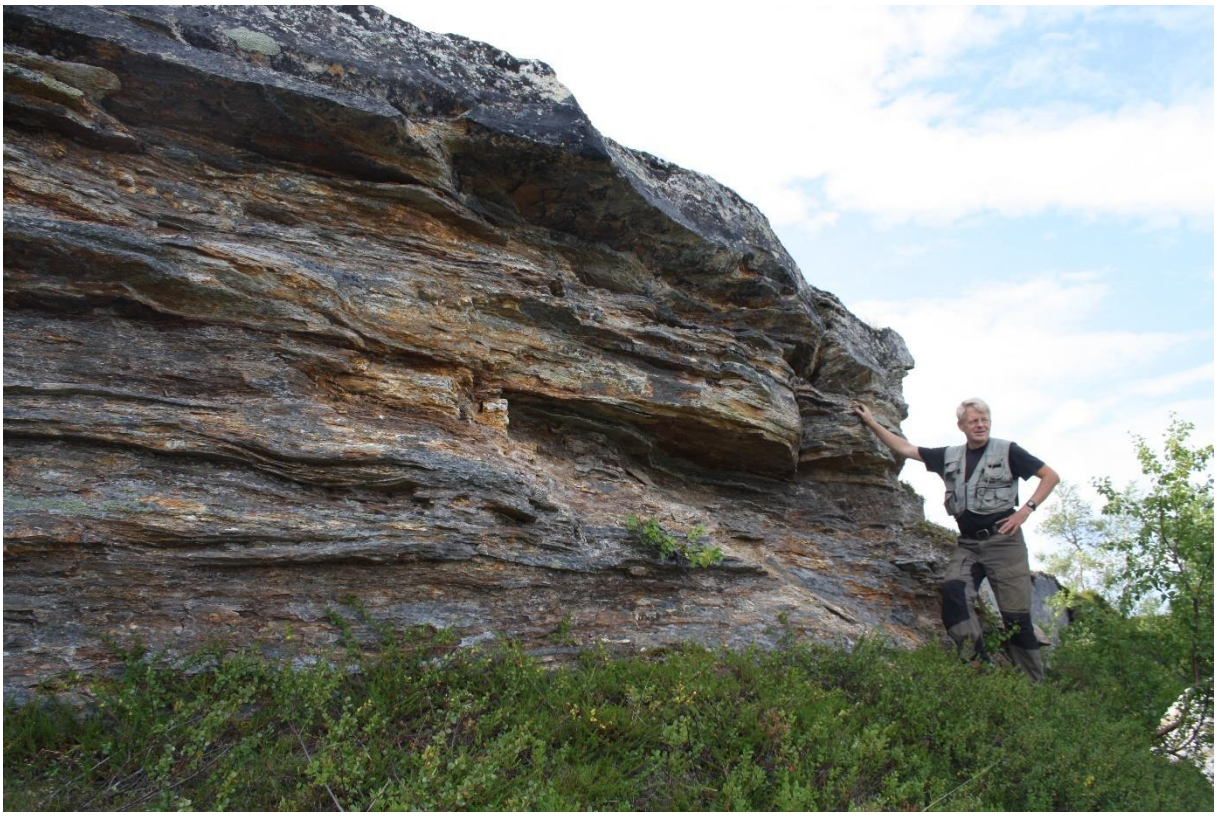

Figure 4-6 Example of muscovite schist in the Hesjelia zone. It is mineralized with disseminated pyrite. Above the schistose muscovite schist one can see the more massive grey gneiss.

Figure 4-7 Example of muscovite gneiss in the Hesjelia zone, this is close to Hammertjønna. The yellow colour is typical for this rock type and is due to small amount of iron sulphides.

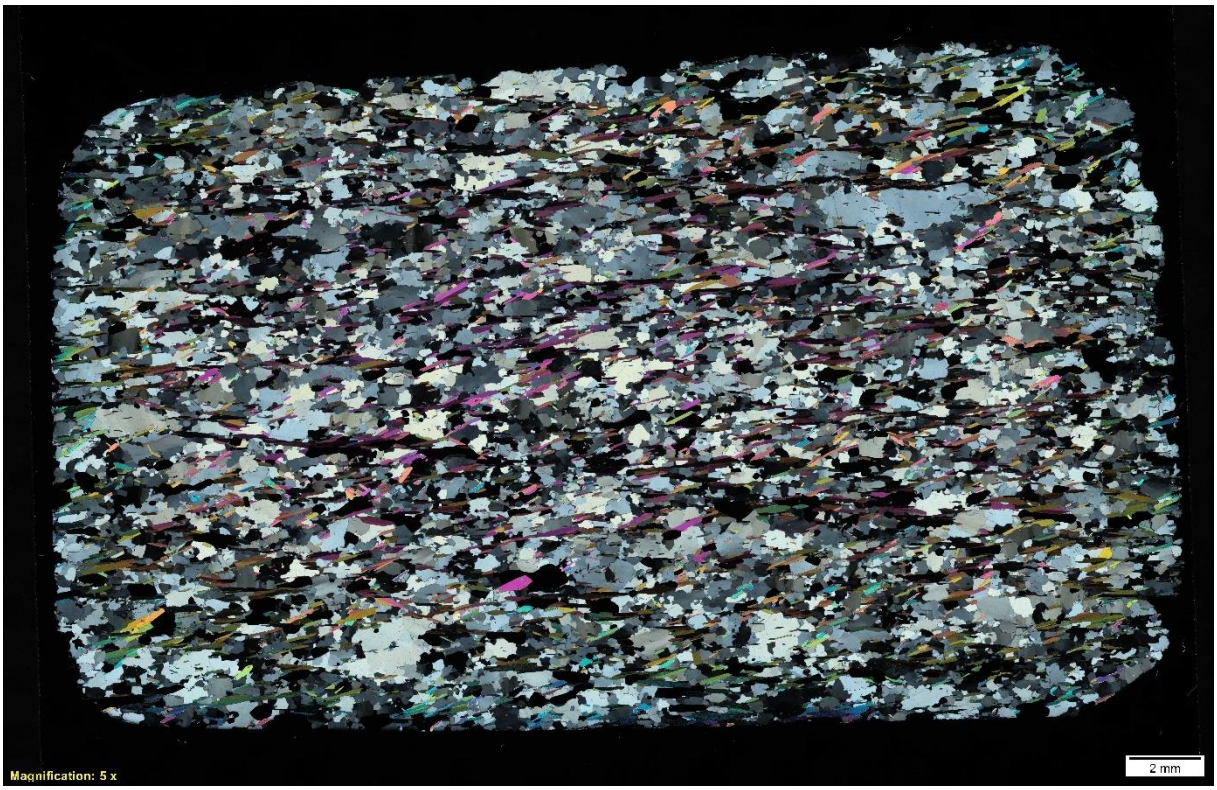

Figure 4-8 . Example of muscovite gneiss from the Hesjelia zone (sample HS-5). It is generally coarser grained compared to samples from Hellerfjellet.

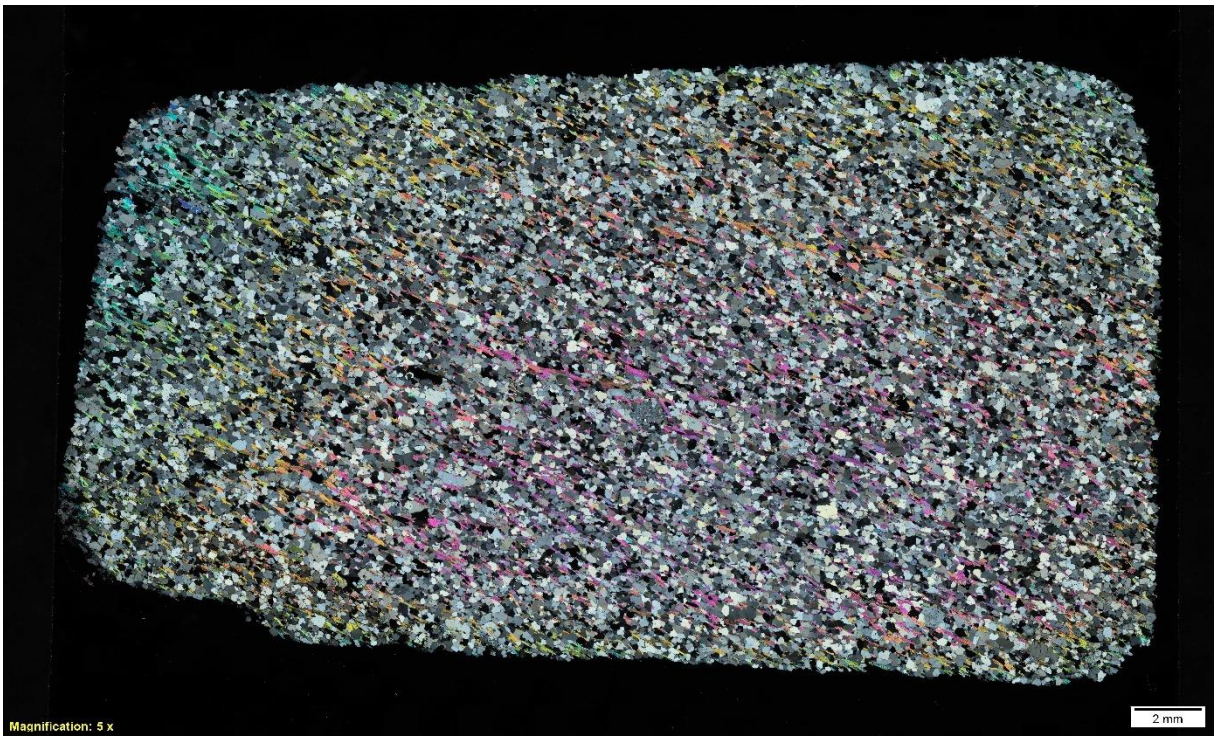

Figure 4-9 Example of a sample of muscovite gneiss from Hellerfjellet (sample HF-x22a). It is very fine-grained which is typical for Hellerfjellet. Lepidoblastic muscovite defines the foliation.

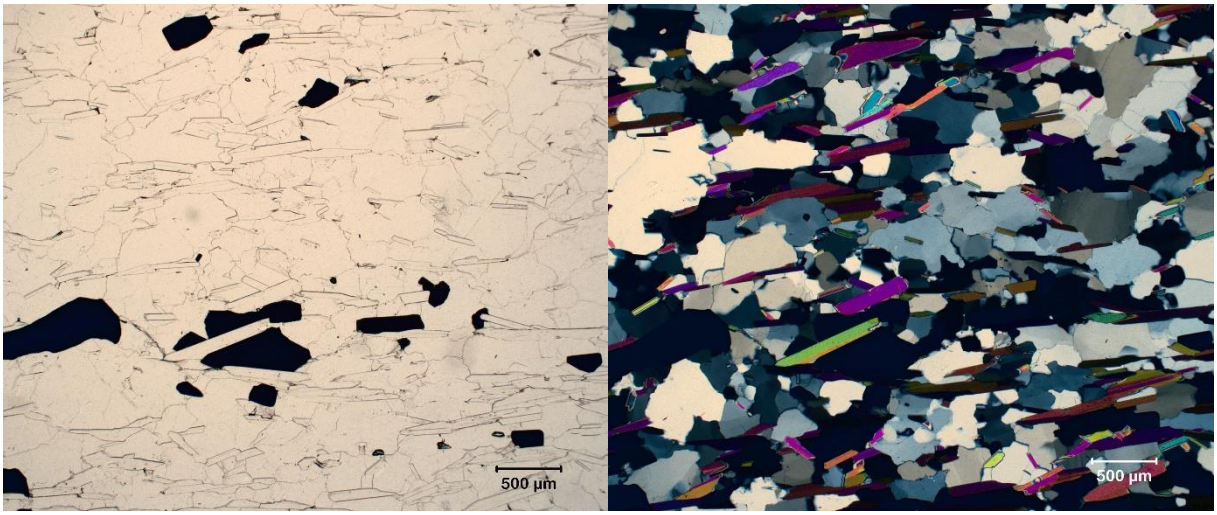

Figure 4-10 Example of muscovite gneiss from the Hesjelia zone (sample HS-6) in PPL and XPL. It contains dominantly quartz and white muscovite and disseminated grains of pyrite. The right picture demonstrates weak undulose extinction of quartz

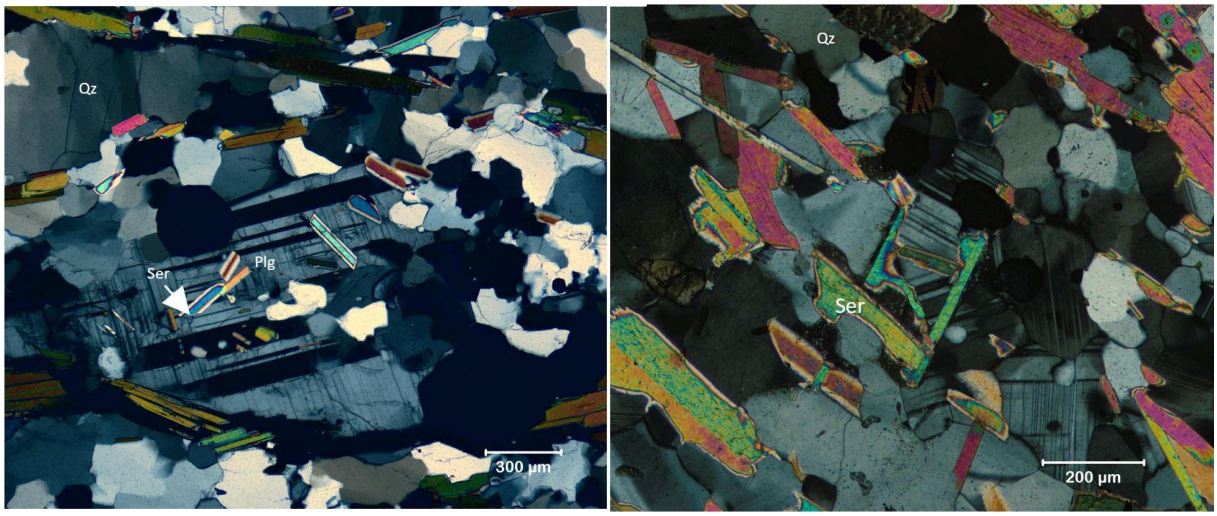

Figure 4-11 Plagioclase feldspar in muscovite gneiss from the Hesjelia zone (left picture, sample HAM-B1) and Hellerfjellet zone (right picture, sample HF-x26). Sericite is partly replacing the feldspar grains (sericitic alteration).

Mica schist

Mica schist is a light to dark grey lithology that is foliated and banded. It contains biotite and muscovite in varying proportions and may be muscovite-dominated or biotite-dominated. Other minerals are quartz, and subordinate garnet, graphite, feldspar, and hornblende. It may also contain grains of pyrite and/or pyrrhotite. The proportions of this rock type are difficult to define since it occurs among the grey gneisses and intercalated with the muscovite gneiss/ schist. It may be defined as one of those types, but since it generally contains more feldspar and less biotite than the average grey gneiss or muscovite schist it is defined as a separate rock type.

Bjerkgård *et al.* (2013a) observed that the biotite-dominated type may also contain hornblende, some kyanite, garnet and staurolite, whereas the muscovite-dominated generally do not contain these minerals. Some varieties may contain pyrite.

It is observed most frequently at Hellerfjellet but is also present locally in the Hesjelia-Hammertjønna area. Figure 4-12 is an example of amphibolite from Hellerfjellet with 1cm grains of garnet, and it also contains graphite. Figure 4-13 is a thin section of the same sample. The garnets are poikiloblastic in this example of mica schist and is probably pre-kinematic since the foliation defined by the biotite goes around the grains. In hand-specimen in Figure 4-12 it appears that the garnet has a reaction rim around the grains, this is not very clear in the thin section picture. It is less biotite around the grains, but not significantly.

Figure 4-12 Exampled of mica schist from Hellerfjellet. The garnets have a reaction rim around the grains.

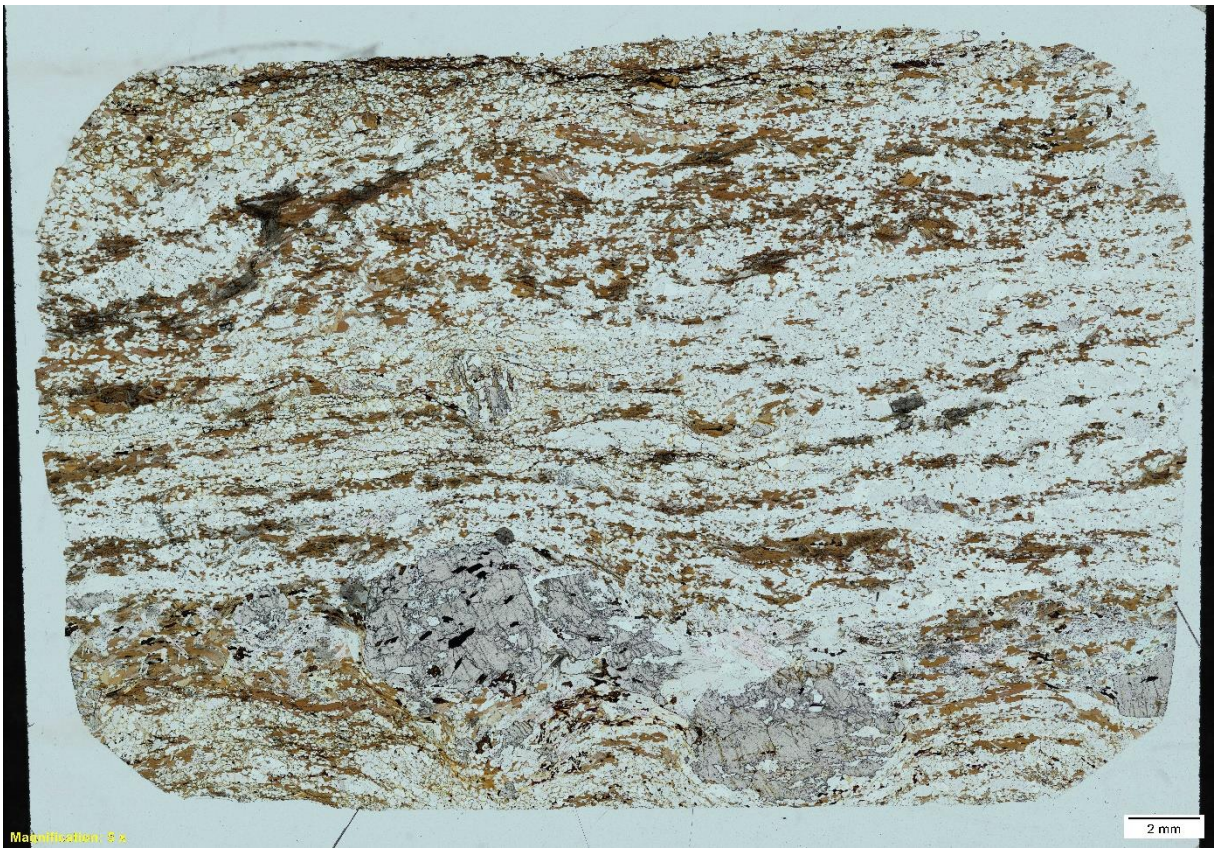

Figure 4-13 PPL microscope picture of sample HF-x17 of mica schist from Hellerfjellet.

Graphite mica gneiss/ schist

A schistose, black, fine- to medium-grained rock with graphite, quartz, biotite, muscovite, and garnet. This rock type is observed only at Hellerfjellet above the prospects and towards the top of Hellerfjellet which lies south-east of the prospects. Close to the mineralisation it may be mineralised with pyrrhotite and traces of chalcopyrite and sphalerite. The extent of this rock type was not mapped out in the field, but the rock type was found in the green circle in the map in Figure 4-14. The bedrock map shows a unit with graphite mica gneiss some meters from where the samples were collected, alias it might belong to this unit. Near the massive ore there is a muscovite gneiss with graphite and further away and closer to the graphite mica gneiss unit, it gradually becomes more graphite rich. The sample in Figure 4-15 is from the green circle in the map. The graphite is fine-grained and appears as a cloudy shadow amongst the other minerals. Figure 4-16 is a zoomed in picture of the thin section in the previous picture; here we can see the graphite that lies as black dust among the minerals. It is very fine grained and is probably not usable for anything.

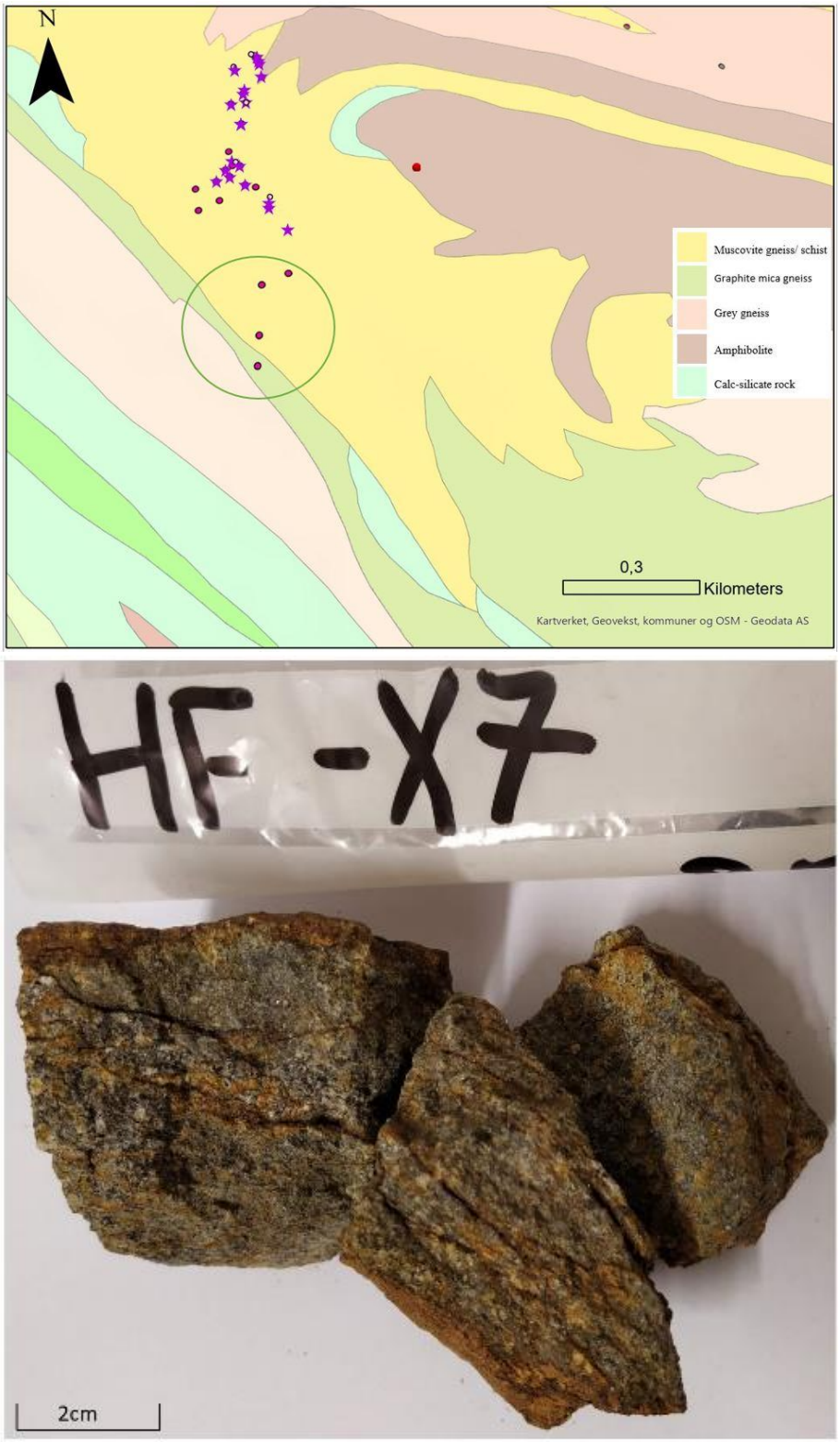

Figure 4-14 Upper picture. a map of the part of Hellerfjellet where graphite is observed. It is observed in the muscovite gneiss all around the prospects (the stars), but the graphite mica gneiss was found in the area defined by the green circle. The green rock type on the map is a graphite mica gneiss unit. lower: an example of a graphite mica gneiss from Hellerfjellet.

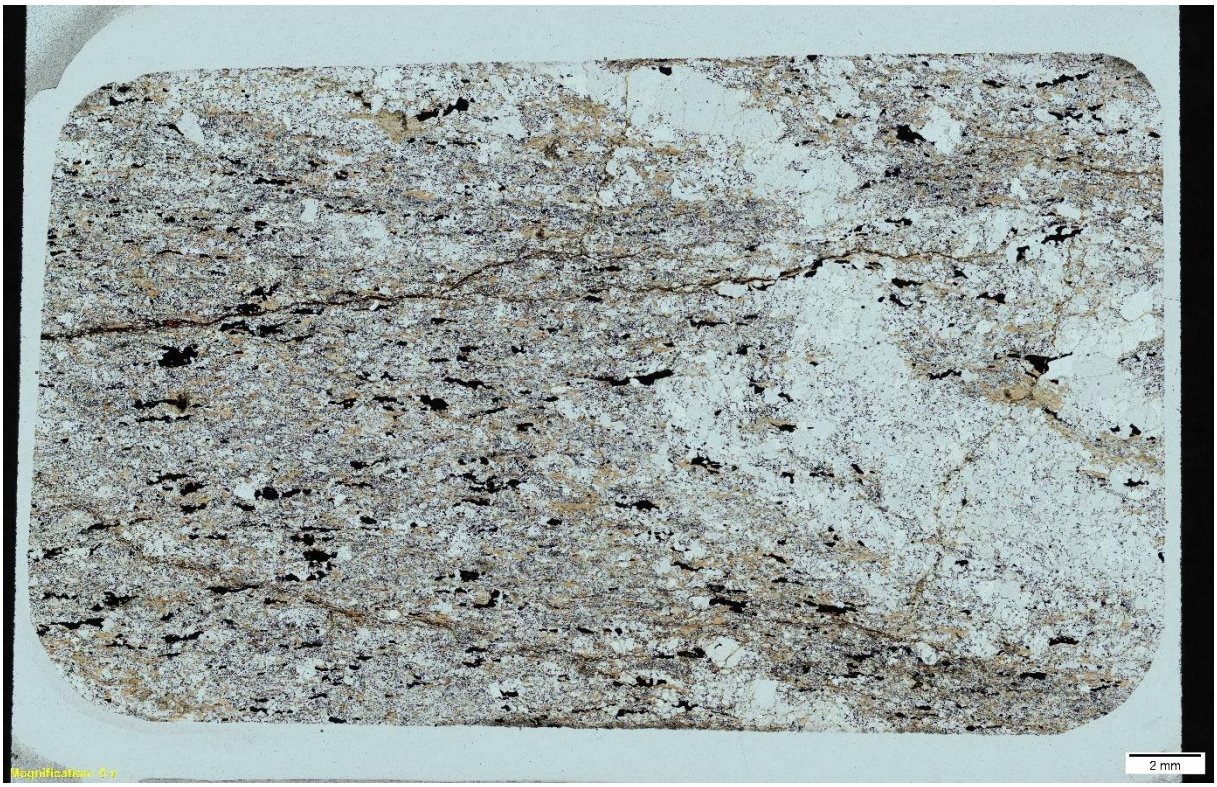

Figure 4-15 Example of graphite mica gneiss from Hellerfjellet (HF-x18) collected in the muscovite schist unit near the boundary to the graphite mica gneiss unit according to the bedrock map in Figure 4-14. The graphite is very fine grained.

Figure 4-16 A zoomed in figure of sample HF-x18 from Hellerfjellet. The graphite is the black minerals that look like dust on the other minerals. The other black minerals are other sulphides.

Amphibolite

The amphibolite is a dark grey to dark green massive rock and is coarse-grained where the biggest grains can be 1 cm. The minerals are amphibole, epidote, garnet, plagioclase, minor biotite, and quartz. Amphibolite is present in both the Hellerfjellet and Hesjelia zones but was not mapped in detail. At Hellerfjellet is it observed close to the prospects, but it is not in contact with the mineralisation. The samples in Figure 4-17 are examples of amphibolite collected in two of the prospects without mineralisation at Hellerfjellet. It probably lies above the ore according to evidences in the field.

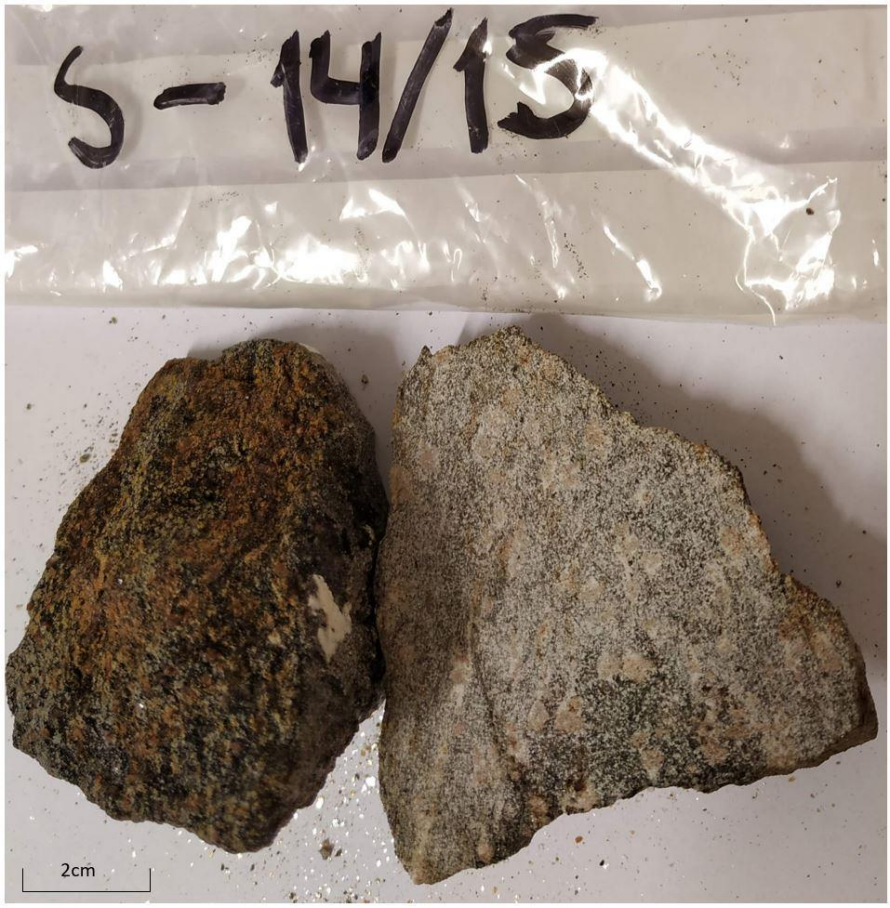

Figure 4-17 Example of amphibolite from Hellerfjellet (sample S-14/15, in two prospects). Contains big grains of garnets.

Grey gneiss

The grey gneiss is a pale grey, fine-grained rock and varies between massive and schistose when observing it in the field. It is dominated by plagioclase and quartz, whereas muscovite and biotite occur in subordinate to accessory amount. Other minerals are garnet, hornblende and locally carbonates and clasts of feldspar (probably K-feldspar) and quartz. The variation with carbonates were recognised in the field where holes in the gneiss were formerly filled with carbonate. It is more schistose where there is a bigger amount of mica.

Grey gneiss is the most abundant rock type in the Mofjell group. It is the dominating lithology both at Hellerfjellet and in the Hesjelia-Hammertjønna areas. So, the extend of this rock is hard to define, but it covers a large area in both zones. Figure 4-18a is an example of grey gneiss from the Hesjelia zone where the rock type is both massive and schistose or layered, this is probably due to varying content of mica. Figure 4-18b is an example from Hellerfjellet where the grey gneiss is folded in a recumbent fold, it is massive, but still shows layering. Figure 4-19a is another example from the grey gneiss in the Hesjelia zone when seen in outcrop. Figure 4-19b is an example of strongly deformed grey gneiss with clasts at Hellerfjellet, this may be a deformed conglomerate. Grey gneiss with clasts and carbonates is only observed at Hellerfjellet.

In the Hellerfjellet drill core several variations of grey gneiss were observed. Figure 4-20 and Figure 4-21 show scanned thin section images of the grey gneiss. Garnets contents

varies the most throughout the core, this will be described in more details in the chapter 4.2. Other variations in the grey gneiss are the biotite and amphibole content that decrease when we get closer to the ore zone.

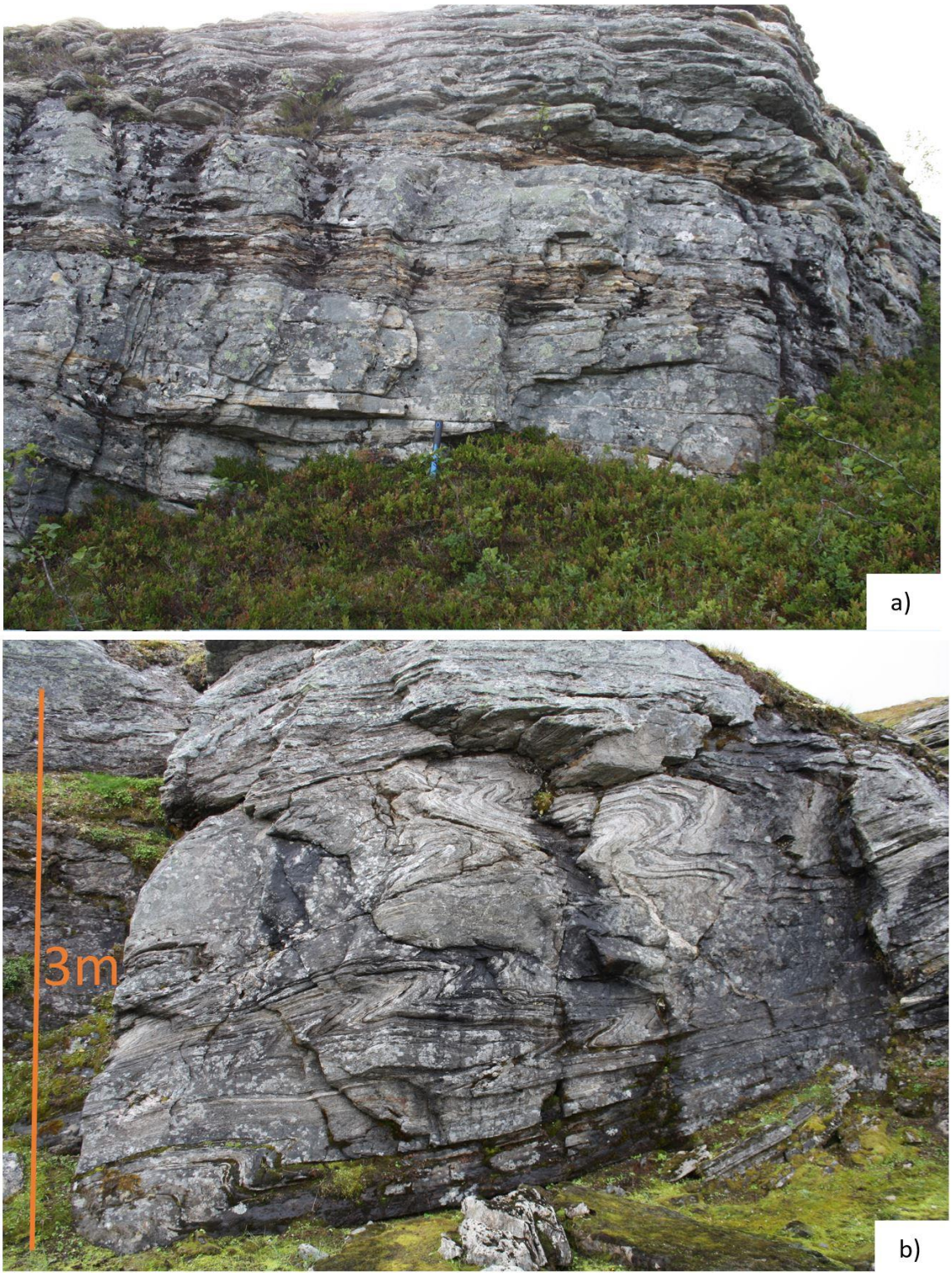

Figure 4-18 Exampled of grey gneiss in the field. a) grey gneiss in the Hesjelia-Hammertjønna zone with a hammer as scale. A wall where the rocktype is alternating massive and schistose. b) grey gneiss in the Hellerfjellet zone folded in recumbent fold (most likely F3 structures).

Figure 4-19 a) another example from the Hesjelia zone, this is how it typically look like from above. A light grey rock with moss on top. Sample HS-3 is from this locality. B) A schistose example from Hellerfjellet with clasts of quartz and feldspar. Hammer as scale.

Figure 4-20 Sample of grey gneiss from Hellerfjellet drill core, this is from 14.25-14.40 below the surface. The garnets have boikiloblastic texture.

Figure 4-21 Sample of grey gneiss from Hellerfjellet drill core, this is from 80.70-80.90 below the surface. The garnets follow the foliation and the folds in this sample.

Tonalite-granodiorite

Throughout the area there are numerous dikes of different sizes that crosscut the foliation and other internal structures in the rocks, showing that these are late intrusions. The dikes are dominated by plagioclase and quartz, with small amounts of K-feldspar and mica. This mineralogy classifies them as tonalite-granodiorite and trondhjemite. Figure 4-22 shows an example of one of the smaller dikes at Hellerfjellet. It is only observed at Hellerfjellet and often extends several km with a width from 20cm to 2 meters.

Figure 4-22 A tonalitic dike (defined by the blue line) that crosscut grey gneiss at Hellerfjellet. Photo: Simon F. Gundersen

4.1.2 Observation of the mineralisations

Outcropping mineralisations are found at one area at Hellerfjellet and at two different areas in the Hesjelia zone, at Hesjelia and Hammertjønna. At all these localities exploration has been carried out, mainly before 1950, including test mining, trenching and diamond drilling. There are 22 small prospects at Hellerfjellet, 6 prospects at Hesjelia, and Hammertjønna has 4 prospects. All the prospects are described in Appendix A and all minerals observed in the thins sections in Appendix B.

Hesjelia zone

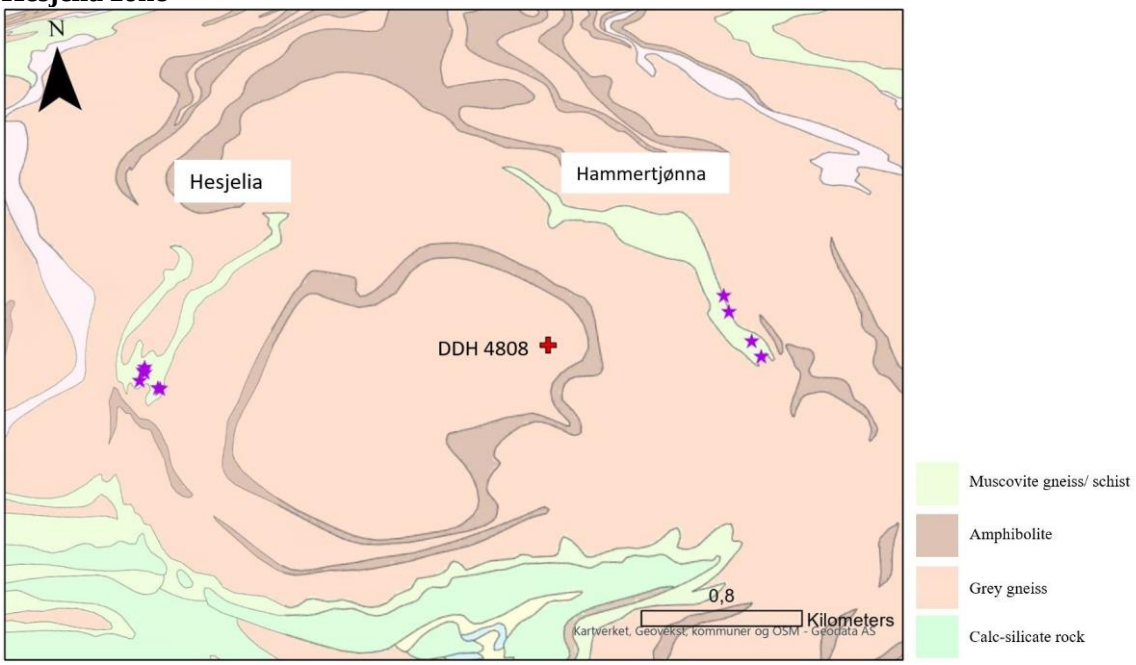

Figure 4-23 The Hesjelia zone. The stars represent the samples taken from the prospects. The red dot is the drill hole by GEXCO in 2008.

The Hesjelia zone lies on the southern slope of Mofjellet and has a total length of 2.9km and makes up a recumbent fold structure with orientation east west and closure towards south. There are two outcropping mineralisations in the zone, Hesjelia and Hammertjønna (Figure 4-23), that lies in the muscovite gneiss. GEXCO drilled between Hesjelia and Hammertjønna in 2008 and found mineralisations and host rock that had the same signature as in both outcropping mineralisations. This confirmed the connection between Hesjelia and Hammertjønna that probably is connected through the recumbent fold (Bjerkgård *et al.*, 2009). Kruse (1980) claims that the ore zone may be about 450 000 m^2 with an average thickness of 3 meters, this correspond to 1.25 M tons of ore. The average grade of the ore measures in the drill core are 0.25% Cu and 3.39% Zn.

The host rock for the mineralisation is a muscovite schist where the major minerals are quartz, muscovite, and minor biotite and amphibole, there may also be hornblende, chlorite, and feldspar.

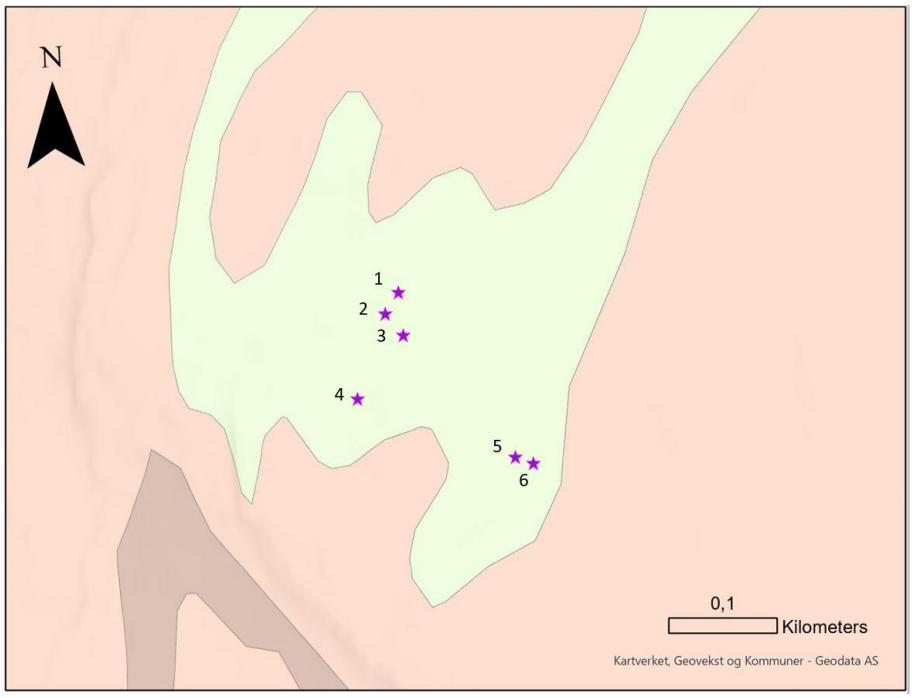

Figure 4-24 Geological map from Hesjelia. The stars represent the places where tha sample from the prospects was taken. The numbers are the prospect names. See legend in Figure 4-23.

Hesjelia (Figure 4-24) represents the west part of the Hesjelia zone and the mineralisation extents more than 200m with ore found in six prospects. The six prospects are mineralized with semi-massive to massive ore and some is disseminated. The mineralisation appears in layers and lenses that are 10-50 cm thick with mineralisation of mostly pyrite and pyrrhotite, whereas sphalerite is subordinate, galena and chalcopyrite are accessory. Often one layer is massive and those around semi-massive and disseminated. The mineralisation's in the prospects has a thickness of up to 0.5m and can be followed for maximum 10-15 meters. Reports from the drilling in 1959 reports up to 4.9m thick layers of the massive ore and with an average thickness of 2.95m (Kruse, 1980). Of the six prospects semi-massive to massive ore occur in prospect 3, 4, 5 and 6. Prospect 1 and 2 consists of muscovite gneiss with thin bands of pyrite or pyrrhotite. Prospect 3, 4 and 5 has massive and disseminated ore in layers and in lenses (Figure 4-25, Figure 4-26 and Figure 4-27). It is mineralized with pyrrhotite, pyrite and sphalerite. Above and below is a muscovite gneiss with disseminated mineralisation. Prospect 6 consists of massive lenses of pyrite, see Figure 4-28 and Figure 4-29. The pyrite occurs as idiomorphic minerals some places and as hypidiomorphic aggregates other places with the other sulphides and silicates as a matrix.

Figure 4-30 and Figure 4-31 are thin sections of samples from prospects 3 in Figure 4-26 and disseminated ore. The mineralisation in the massive ore mostly appear as sub- to anhedral/xenomorphic masses of pyrrhotite, pyrite and sphalerite as major, galena and chalcopyrite as minor and accessory. Pyrite is often observed more euhedral and bigger than the other minerals, this is probably because of metamorphism, and the pyrite is what is called idiomorph. It is normal that high energy minerals, as pyrite, recrystallizes to get a higher contrast to the low energy matrix; galena, chalcopyrite, sphalerite and pyrrhotite. The resulting porphyroblasts of pyrite often have inclusions of sphalerite and gangue minerals (mostly quartz and sericite). The other sulphides do not have the same idomorphic tendencies as pyrite (Craig *et al.*, 1981; Vokes, 1969). Few pyrite grains have

accomplished a perfect cubic crystal shape, but many of them has a few sharp sides and others is more diffuse. Pyrite often have the sharpest contact towards pyrrhotite and a more diffuse contact towards the matrix of mostly pyrrhotite and sphalerite. Inclusion in pyrite is probably trapped when the pyrite was recrystallizing. The presence of inclusions may indicate outward growth or recrystallization that leads to closing of embayment. Sphalerite appears as a matrix, pyrrhotite appears both as a matrix and as separate grains. Galena appears as an infill mineral, especially with sphalerite. Chalcopyrite tends to concentrate and form at grain boundaries randomly throughout the ore. The biggest grains of pyrite and pyrrhotite is 5mm as seen in Figure 4-30. That is one example of how the ore occur in the Hesjelia zone, other samples have more sphalerite in the matrix.

The disseminated ore in the Hesjelia zone mainly consists of pyrite (Figure 4-31). They have sub- to euhedral shape probably caused by recrystallization during metamorphism. The elongation of the crystals is also made by the deformation during the regional metamorphism. The gneissic texture in less massive ore is a typical metamorphic texture for pyrite according to Vokes (1969). Gangue minerals are subhedral grains of quartz, amphibole, and feldspar. The quartz often has triple junction against each other and some grain show undulose extinction as seen in the small picture in Figure 4-31, this is metamorphic structures.

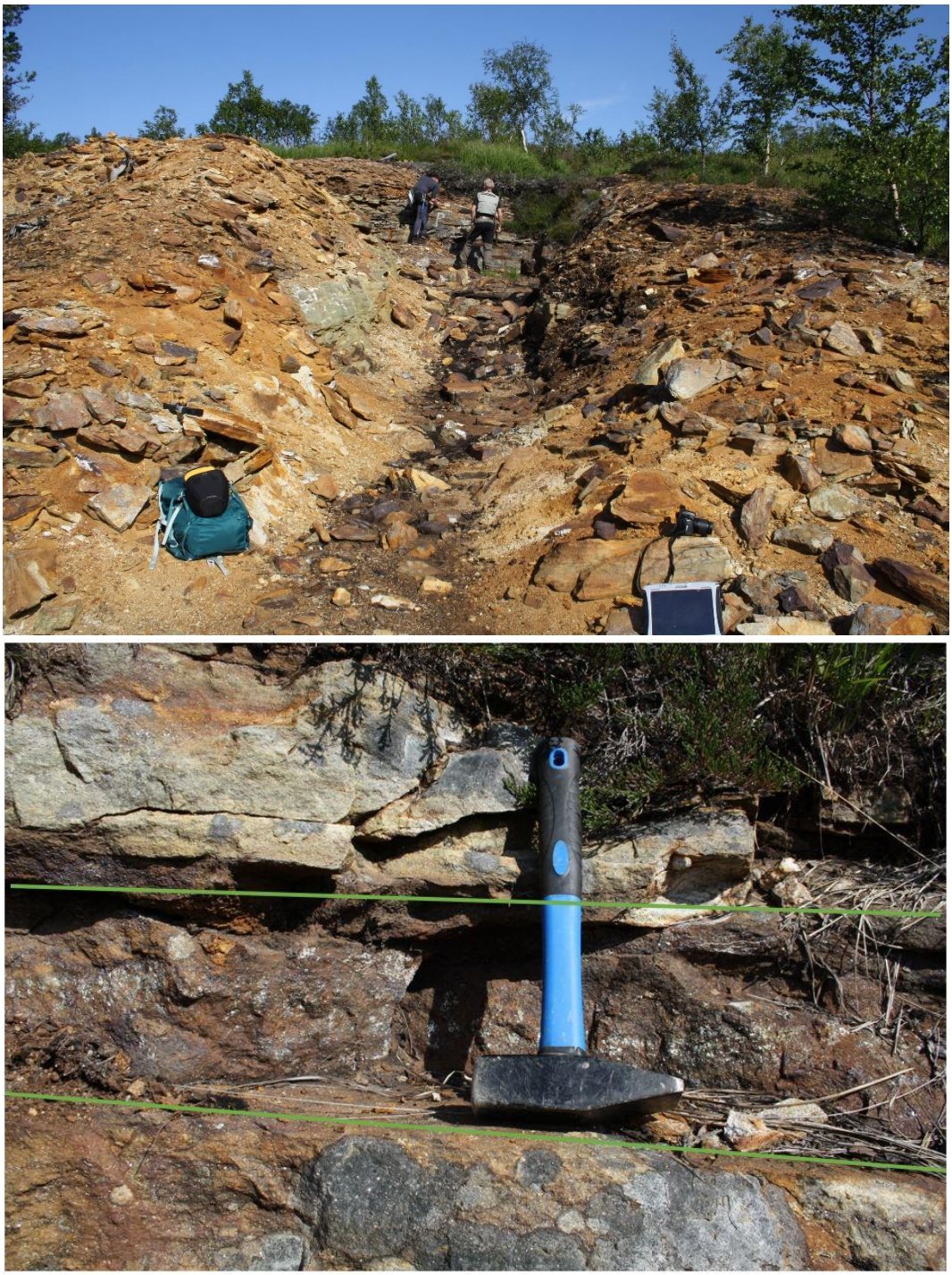

Figure 4-25 Pictures from prospect 3 in Hesjelia. a) is a picture of the whole prospect which is the biggest in Hesjelia. The ore is outcropping where my field-partners are standing. b) one example of massive ore in layer of about 10 cm.

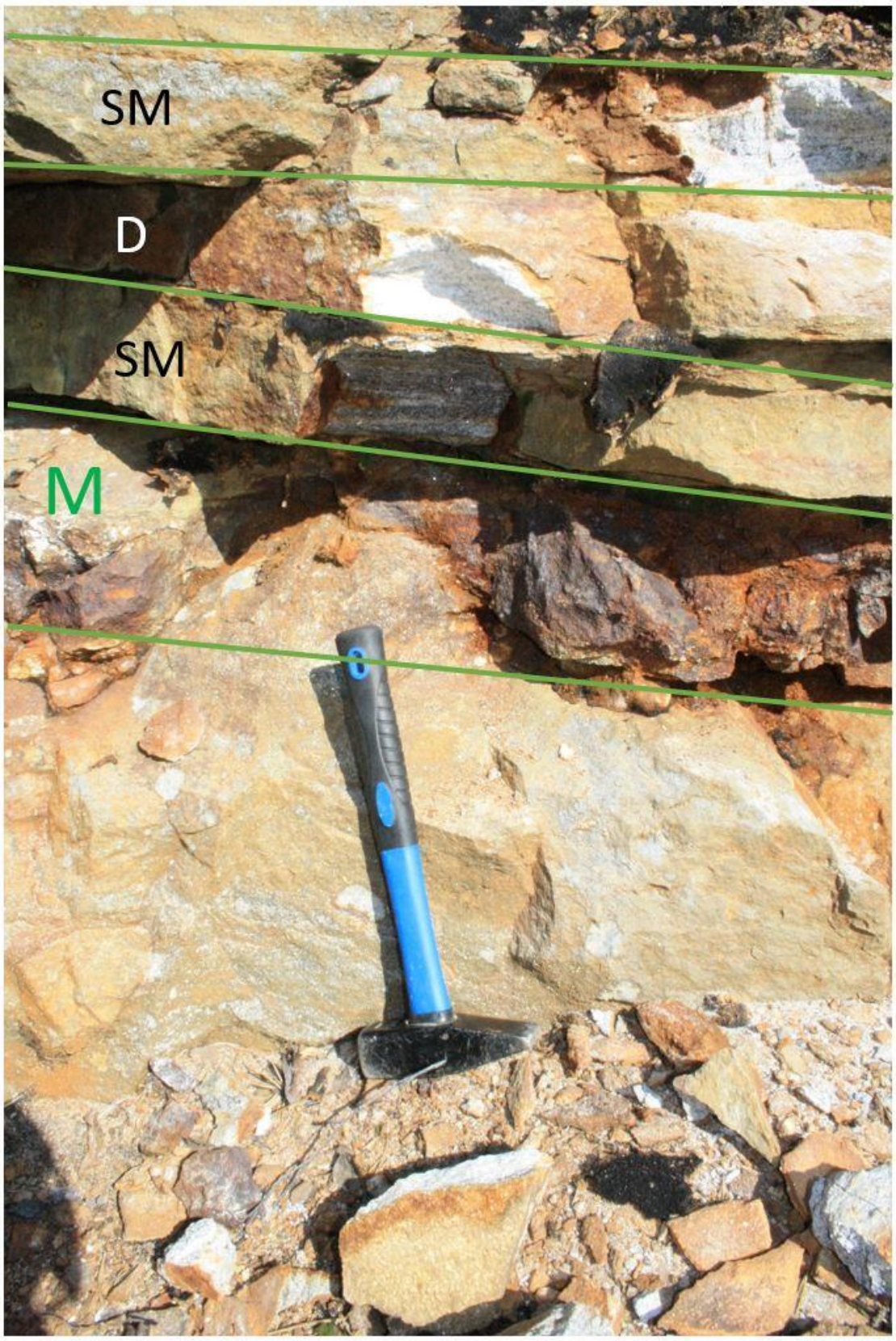

Figure 4-26 From prospect 3 in Hesjelia: different ore grades in different layers. The upper layer is of semi-massive ore, next is disseminated, next is semi-massive and the lower is of massive ore. The ore occurs as lenses in the most massive layer.

Figure 4-27 From prospect 4 in Hesjelia. The semi-massive to massive ore is outcropping 1.5-2m thick and 15m along the strike direction

Figure 4-28 From prospect 6 in Hesjelia where there was one layer that was 10cm to 1 m thick with a lot of pyrite.

Figure 4-29 From prospect 6 in Hesjelia. Here we ca see that the massive ore appears in lenses as defined by the blue line

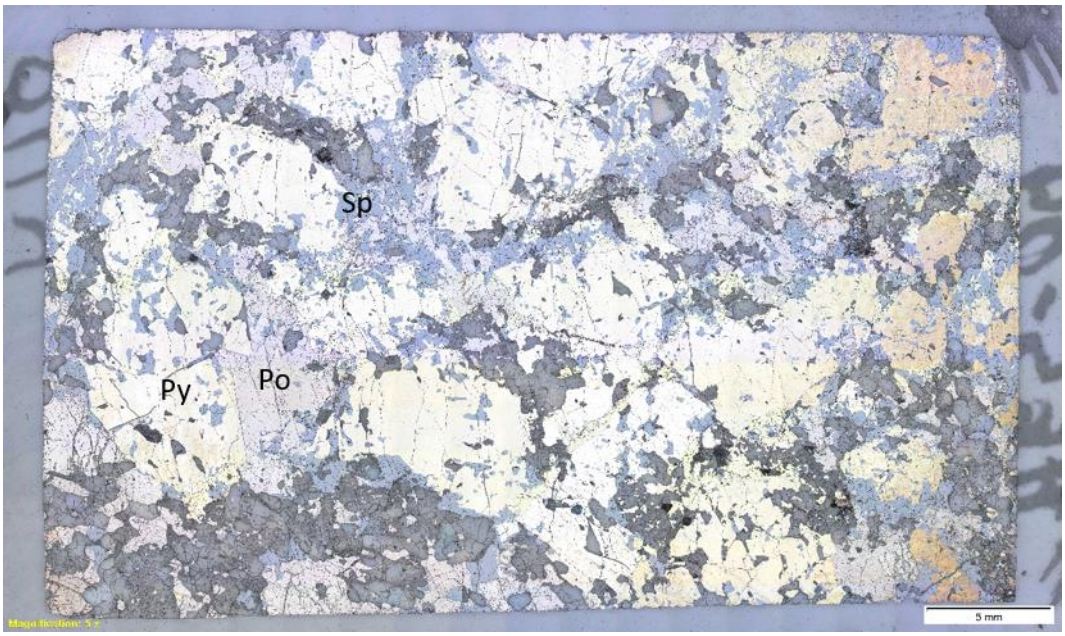

Figure 4-30 Thin section(HES-04NGU) of a sample from prospect 3 in Hesjelia. Massive ore consisting of pyrite, pyrrhotite, sphalerite and minor galena.

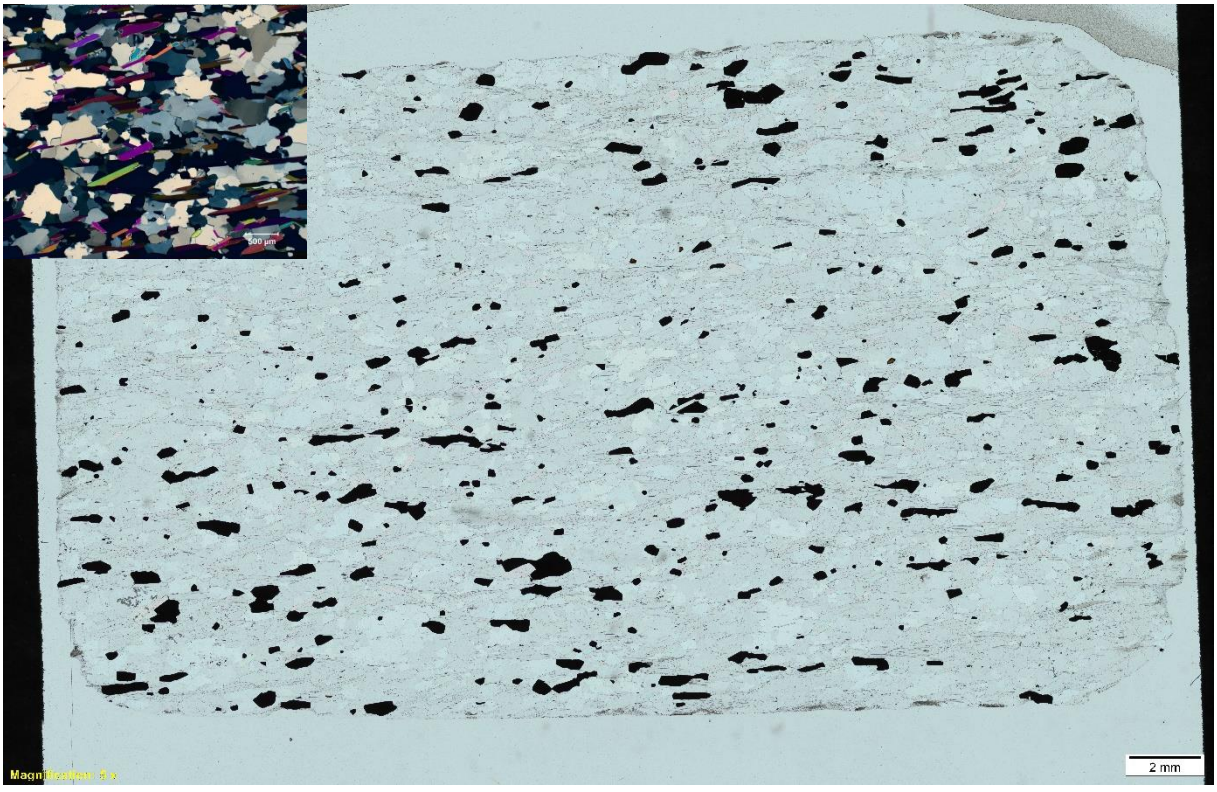

Figure 4-31 Thin section(HS-5) of a sample of disseminated ore in Hesjelia. The sulphides are pyrite, gangue minerals are mainly quartz and muscovite, some feldspar. In the upper left corner, there is a XPL picture from this sample, here can triple junction, undulose extinction and lepidoblastic textures be observed.

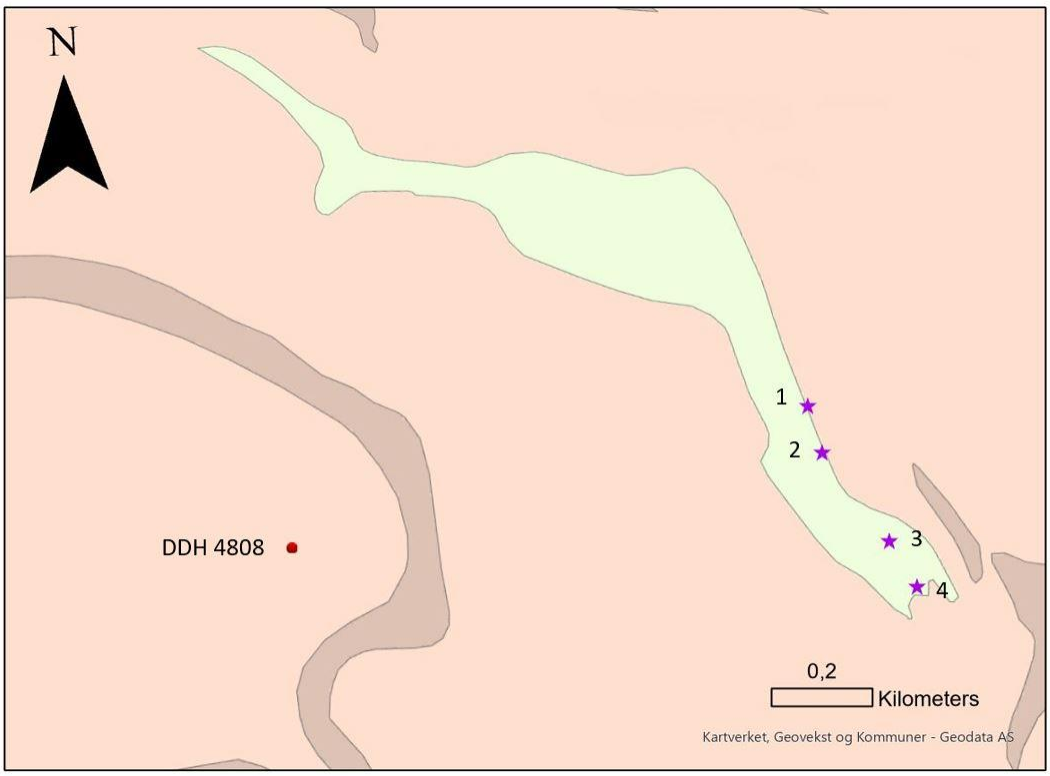

Figure 4-32 Geological map of Hammertjønna. The stars represent where samples were taken from the prospects and the numbers are the prospect's name. The red dot is the drill hole made by GEXCO in 2009. See legend in Figure 4-23.

Hammertjønna represents the eastern part of the Hesjelia zone. The mineralisation covers a length of about 350m and outcrops in four small prospects (map in Figure 4-32). The ore is semi-massive to massive, and some is disseminated and appears in layers from 10 to 30 cm and in lenses. Kruse (1980) reports from drilling in the 1950s that found the mineralisation to be from 0.6 to 3.85 m's thick.

Figure 4-33, Figure 4-34 and Figure 4-35 are 3 different prospects at Hammertjønna with the ore outcropping in lenses and layers. The maximum thickness seen in the prospects is about 50 cm's of massive ore. In Figure 4-36 from prospect 4 is the ore seen in layers and in an open fold. The main minerals are pyrrhotite or pyrite and sphalerite, with chalcopyrite and galena as subordinate to accessory. Figure 4-37 is a thin section of a semi massive sample from prospect 4 in Hammertjønna. The sulphides occur together in sub- to anhedral masses/ xenomorphic, also called polymineralogic masses. Galena often acts like an infill mineral that lies on the rim of other sulphides, often sphalerite. Chalcopyrite occur randomly and in small clusters. The gangue minerals are quartz, kyanite, chlorite, biotite, and plagioclase.

The disseminated ore in the area have sub- to euhedral grains of mostly pyrite, but also complexes of sphalerite, pyrite/pyrrhotite and chalcopyrite. The examples in Figure 4-38 are from two different samples where the gangue minerals in HAM-B2 are quartz, muscovite and kyanite. In HAM-B1 is the gangue almost only quartz and some muscovite. The pyrite grains are aligned in the foliation direction and has made a gneissic texture. The quartz often has triple junction and some grains with undulose extinction which is made by metamorphism.

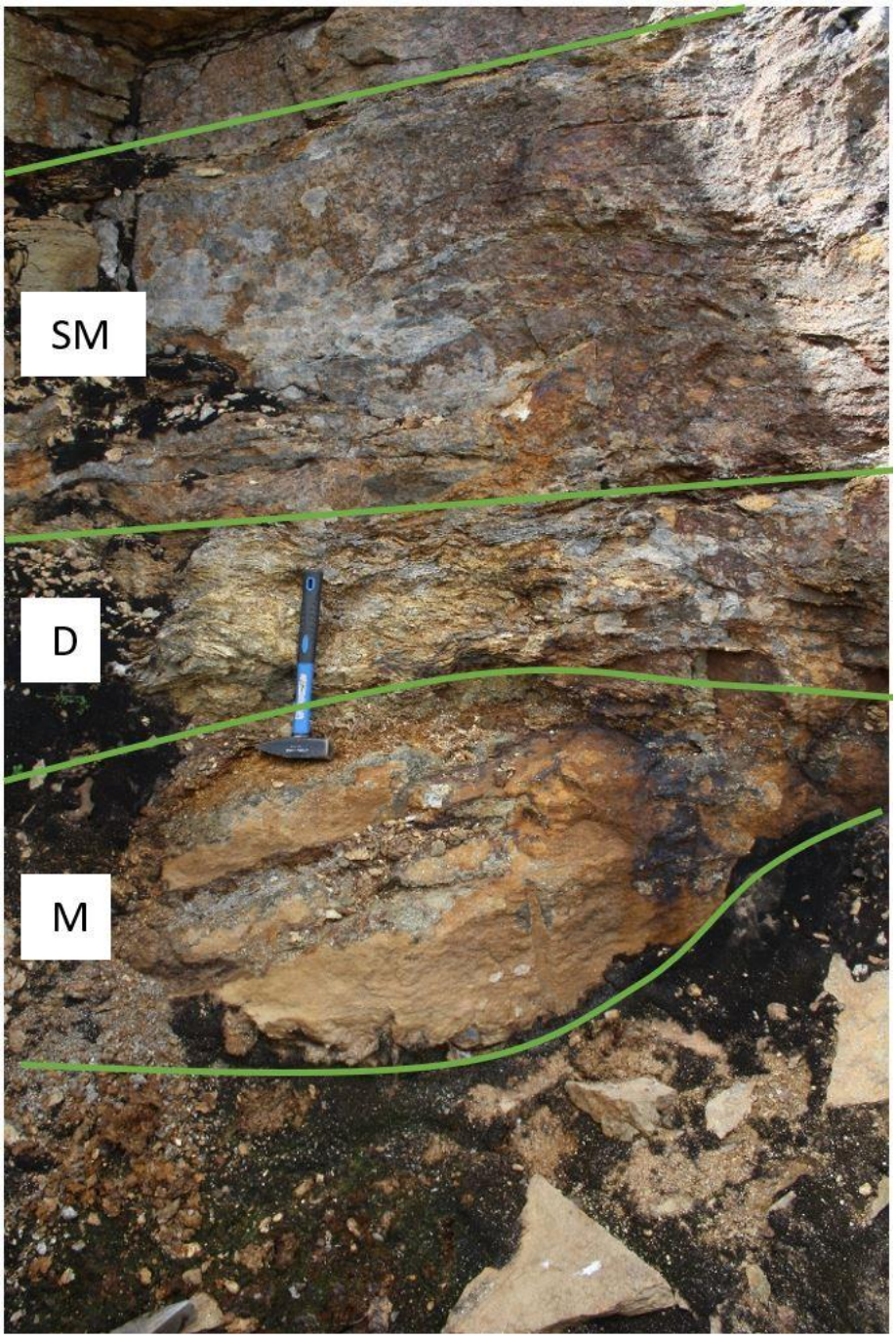

Figure 4-33 From prospect 2 at Hammertjønna. The ore are in layers and lenses. M: massive, D: disseminated, SM: semi massive.

Figure 4-34 Prospect 3 at Hammertjønna. Massive ore in a lens with mostly galena, some chalcopyrite and sphalerite, in a matrix totally dominated by chlorite. Above there is another layer of massive to semi-massive ore. The upper layers are of disseminated ore.

Figure 4-35 Prospect 4 at Hammertjønna. Massive ore occurs in a layer about 50 cm in thickness (red marked outcrop).

Figure 4-36 Near prospect 4 at Hammertjønna. Prospect 4 is a part of a very open fold. The ore can be seen in layers along the fold in the picture.

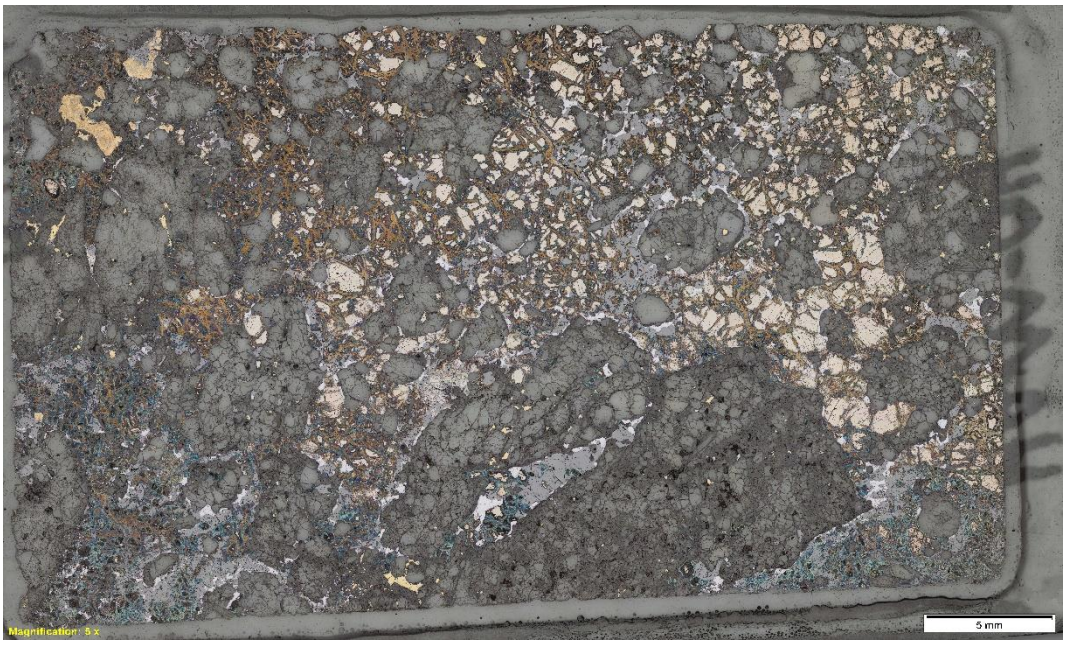

Figure 4-37 Thin section (HAM-04NGU) of a sample from prospect 4 at Hammertjønna. The sulphides appear as anhedral masses. It consists of pyrrhotite and sphalerite, minor galena and traces of pyrite and chalcopyrite. The matrix (gangue minerals) are feldspar, quartz, amphibole, chlorite, and biotite.

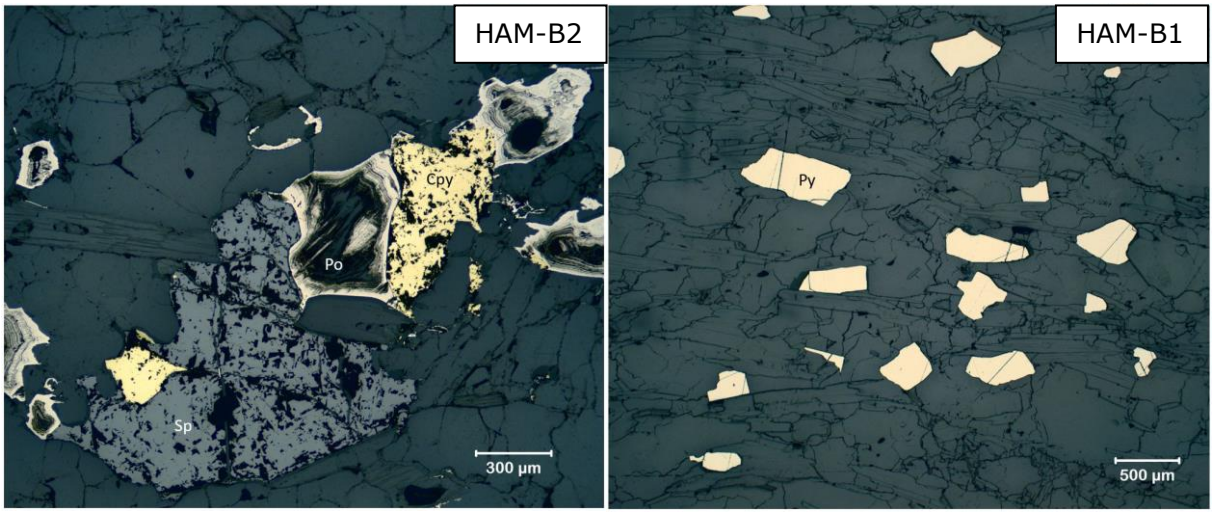

Figure 4-38 Example of the sulphides in disseminated ore in Hammertjønna (sample HAM-B2 and HAM-B1). In HAM-B2 the sulphides make complexes of pyrrhotite, chalcopyrite and sphalerite. In HAM-B1 it is sub- to euhedral grains of pyrite. The matrix is mainly quartz, sericite, and feldspar.

Hellerfjell zone

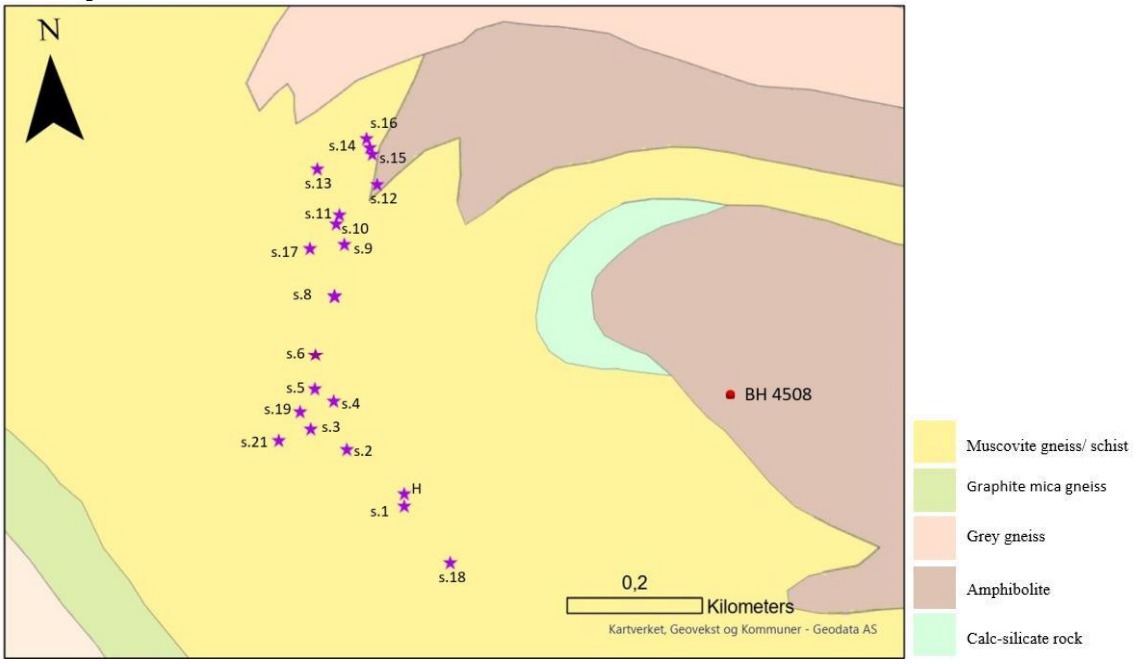

Figure 4-39 Geological map from a small part of Hellerfjellet. The stars represent where the samples from the prospects are taken. The numbers are the prospect names given by NGU.

Hellerfjellet represents the southern part of what is called the Stangfjell-Hellerfjell zone by (Bjerkgård *et al.*, 2013a), but only Hellerfjellet is studied in this thesis. The outcropping mineralisation at Hellerfjellet consists of 22 prospects of different sizes over a length of more than 200m (Figure 4-39). The sulphides occur in lenses up to 1.5m thick and a few meters long and the mineralised zone by the prospects is thought to be between 1.5 meters thick. TEM data indicates that the extent of the mineralised zone is at least 1.5 km along strike from the prospects (Bjerkgård *et al.*, 2013a). The host rock here is muscovite gneiss, somewhere with layers and lenses of graphite close to the mineralisations.

The massive ore at Hellerfjellet occur in lenses of different size and in layers. Figure 4-40 and Figure 4-41 shows three of the prospects at Hellerfjellet and in two of them the lenses can be seen clearly. The thickest lenses and the most massive ore occur in prospect 4, 6 and the main prospect (H), they are about 1.5m thick. The massive ore in the prospects are dominated by sphalerite and pyrrhotite, whereas chalcopyrite and galena are accessory to minor. The other prospects have disseminated to semi-massive ore in small lenses and in layers from 5 to 50 cm. Bands of graphite appears in most of the prospects. The main sulphide minerals vary from prospect to prospect, but often it is sphalerite and galena and subordinate chalcopyrite. Pyrrhotite is the main sulphide and appears in most prospects.

The sulphides in the massive ore occur mostly as xenomorphic masses that acts like a matrix of sphalerite, pyrrhotite, and minor galena and chalcopyrite, freibergite as accessory, this can be called polymineralogic masses (Figure 4-42. In some samples pyrrhotite occur as sub- to euhedral grains (see Figure 4-43) with sphalerite as matrix, and this is probably due to metamorphic recrystallisation. Galena and chalcopyrite often lie in the contact between pyrrhotite or sphalerite and the gangue minerals. The biggest grains of pyrrhotite are up to 3mm, these often has inclusions, especially of sphalerite. Freibergite is found as an accessory phase in the massive ore at Hellerfjellet, most

common as inclusions in galena. Embayment structures can be seen in the massive ore both in the sulphides and the gangue minerals.

In disseminated ore outside the prospects the mineralisation is dominated by pyrite and/or pyrrhotite, with some sphalerite and galena and rare chalcopyrite (Figure 4-44). The pyrrhotite and pyrite often appear as sub- to euhedral grains and is most likely recrystallized during metamorphism. Gangue minerals includes quartz, amphibole, muscovite and celcian, graphite, biotite, ilmenite, feldspar and staurolite in lesser amounts. Generally, is graphite bearing muscovite schist observed above the ore and below is muscovite schist without graphite.

Figure 4-40 Prospect number 11 at Hellerfjellet. The ore are about 2 m thick and 1,5m wide and mineralised with thin bands of pyrite, chalcopyrite, sphalerite, and galena in a graphite bearing muscovite gneiss/schist.

Figure 4-41 Prospect number 6(upper picture) and the main prospect (lower picture) at Hellerfjellet. These are two of the biggest prospects and have massive ore occurring in lenses (Photo: NGU).

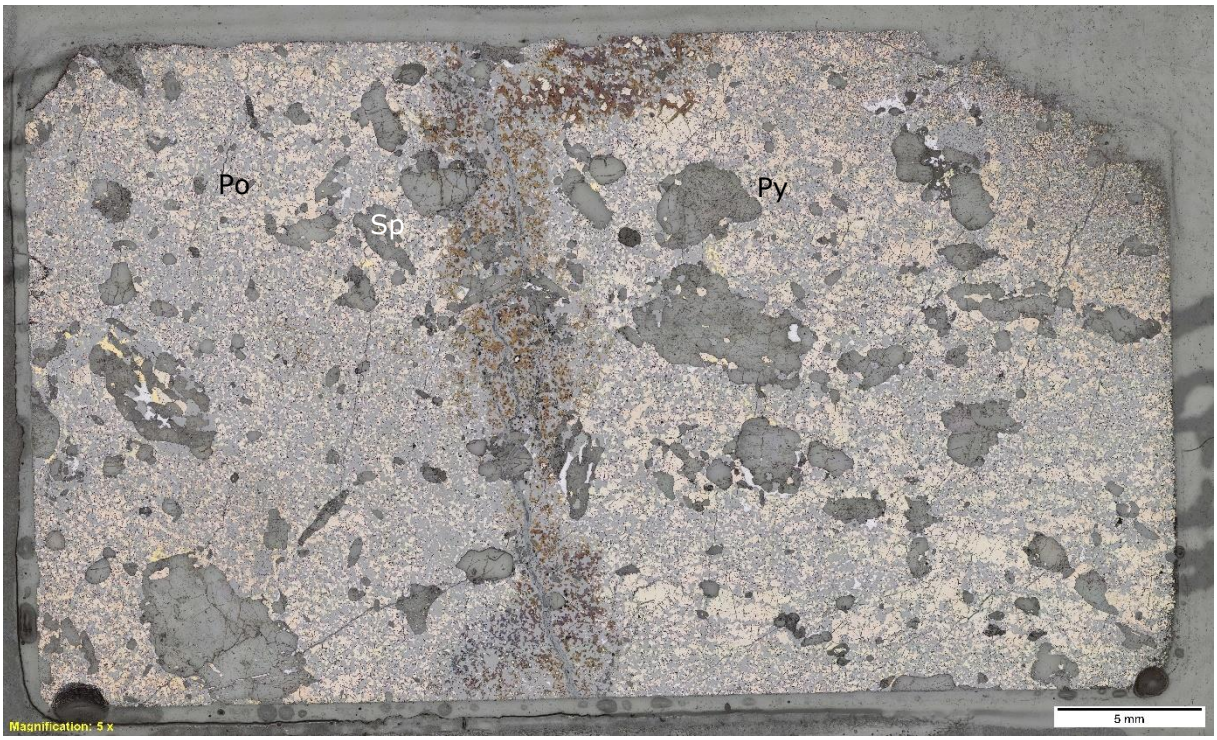

Figure 4-42 Thin section of a sample from prospect 4 (HF-7NGU) at Hellerfjellet. It consists of anhedral masses of sphalerite and pyrrhotite, minor galena, accessory chalcopyrite, and traces of freibergite.

Figure 4-43 Thin section of a sample from the main prospect at Hellerfjellet (HF-10NGU). Main minerals are pyrrhotite and sphalerite, minor galena, accessory of galena and traces of freibergite.

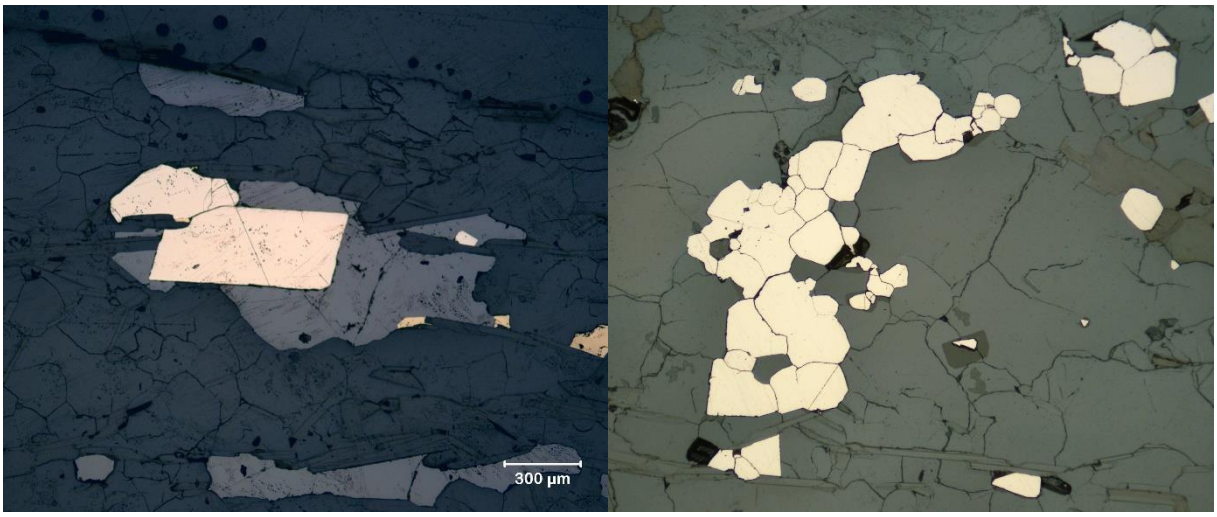

Figure 4-44 left: disseminated ore (HF-x6c) from Hellerfjellet. Euhedral pyrrhotite grain in a sphalerite grain. Right: same scale as the left figure. From disseminated ore at Hellerfjellet (HF-x26). Sub- to euhedral pyrite.

4.2 Drill core logging

Drill core BH4508 drilled by GEXCO in 2008 on the Hellerfjellet deposit was logged in detail and analysed by a portable XRF for every 10 cm throughout the core. More detailed description together with the results from the XRF analyses can be found in Appendix C and D. The drill core is about 190m long. In Figure 4-45 of the core log we can see that most of the core consists of different variations of grey gneiss and muscovite schist. The ore zone is from around 116 to 134 meters below the surface (mbs.). Table 8 comprises a brief description of the different parts of the drill core and the variations in them.

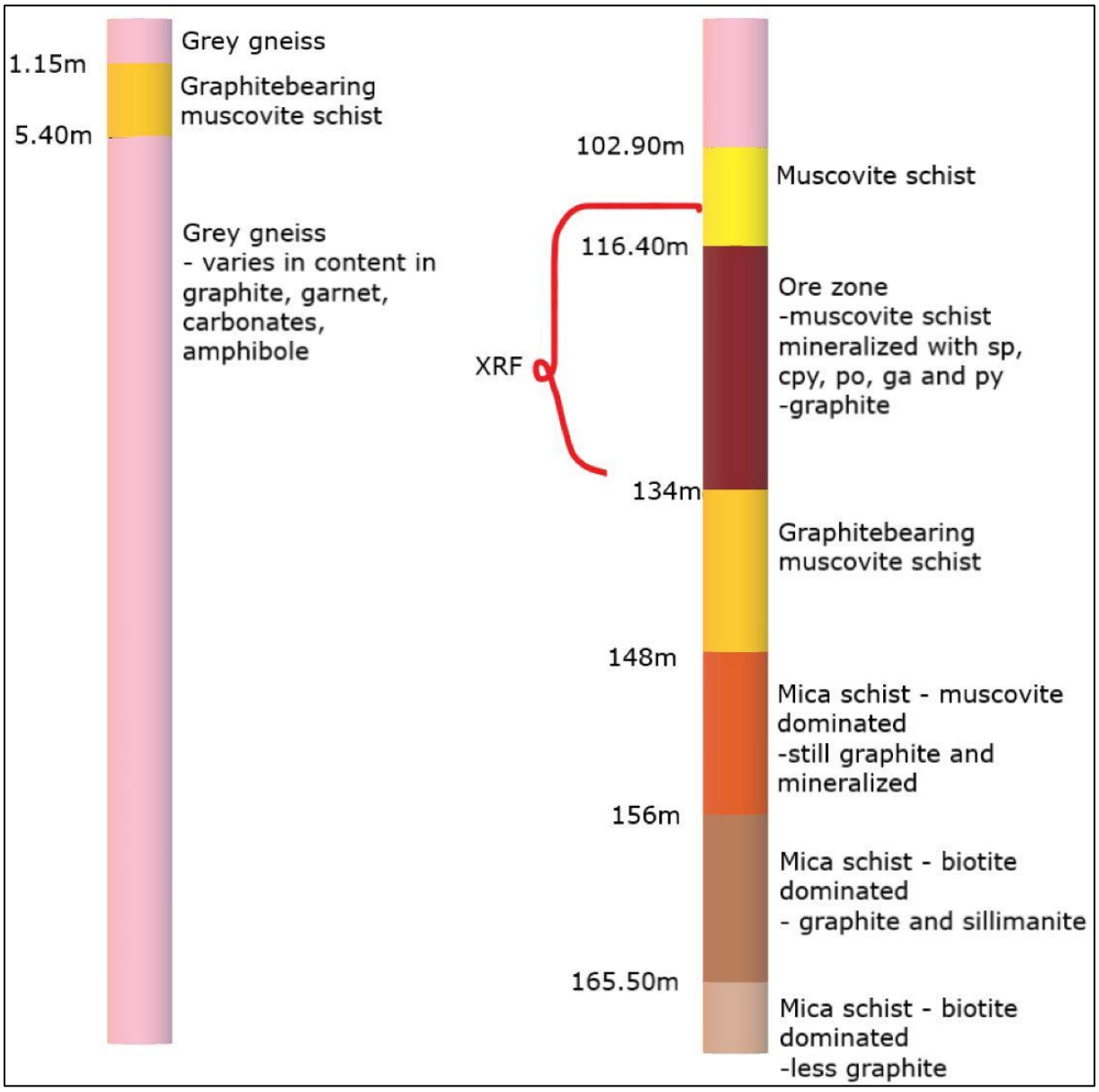

Figure 4-45 Core log of drill core BH4508 at Hellerfjellet. The drill core is to about 190 meters below surface.

Table 8 Brief description the observations done in the drill core at Hellerfjellet. The colours represent the fields in the core log in Figure 4-45. Qz – quartz, plg-plagioclase,

bt-biotite, gr-graphite, ms-muscovite, grt-garnet, po-pyrrhotite, chl-chlorite, amp-amphibole, cpy-chalcopyrite, ser - sericite

	Meters down the core	Minerals	Details	Rock type
	0-1.15	Qz, plg, bt, gr	Homogeneous, changing pale and darker layers	Grey gneiss
	-5.40	Qz, plg, ms, bt, gr, po	Foliated and banded rock	Mica schist with graphite and pyrrhotite
	-102.90	Qz, plg, grt, ms, bt, gr, amp, chl, cpy	Alternating colours and grain size, banded. Richer in bt further down.	Grey gneiss
	-116.40	Ser, qz, ms, gr, grt	Banded	Muscovite gneiss
	-134	Gr, qz, ser, sulphides (sp, cpy, po), chl	Various amount of different minerals, sulphides both disseminated and in bands	Ore zone – graphite bearing muscovite gneiss with mineralisation
	-148	Gr, qz, bt, ms, grt	Below the ore zone	Graphite bearing muscovite gneiss
	-156	Ms, bt, qz, flp, gr, po	Banded, alternating ms- and bt-rich	Micas schist
	-165.50	Ms, bt, qz	Transition from ms- to bt- rich	Mica schist
	~190	Bt, gr, qz		Mica schist

Garnet was one of the main minerals in focus in the core to see how it varies when we are moving closer to the ore zone. The garnets vary in size, shape and texture. Examples of garnets in thin section and in hand specimen can be seen in Figure 4-46, Figure 4-47 and Figure 4-48. The size is from 0,2mm to 4mm with the biggest grains closer to the surface and smaller closer to the ore. The colour in hand specimen is from pale pink to red and some with halos of quartz and feldspars around it, this can also be observed optically. The shape of the garnet's changes from anhedral to euhedral and it looks like it has grown over the other minerals and the foliation. Garnets are porphyroblastic although some are poikiloblastic (Mommio, n.d.-b). It generally is fractured and contain inclusions of other minerals. The biggest quanta and size of the garnets are observed together with other Fe-Mg minerals, like biotite and amphibole, that have the right elements for the garnet to grow. The garnets are probably either pre- or syn-kinematic, since in some places the foliations wrap around the garnets and some places the mica goes around the garnet grains. Garnet is euhedral in places and subhedral in other parts, i.e. showing evidence for several growth episodes.

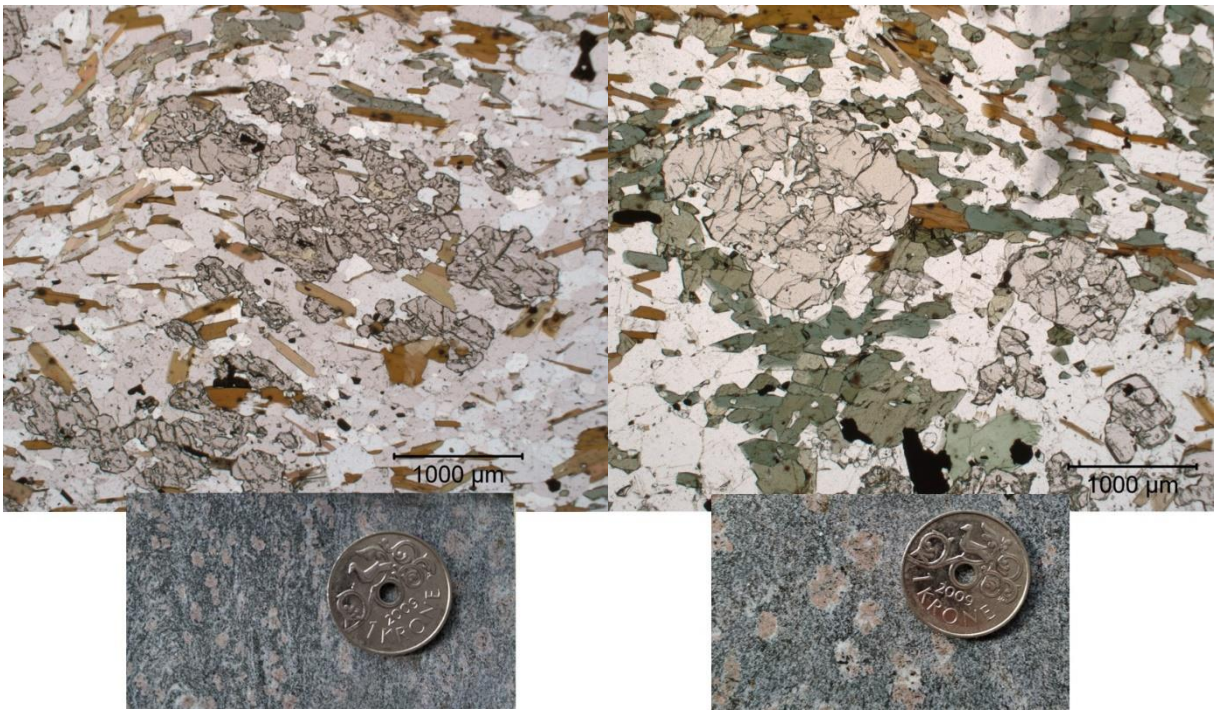

Figure 4-46 Garnet in thin section and in hand specimen from the drill core at Hellerfjellet (BH4508). The left picture is from 5.50-5.65 meters below the surface and the right is from 14.25-14.40 meters below the surface.

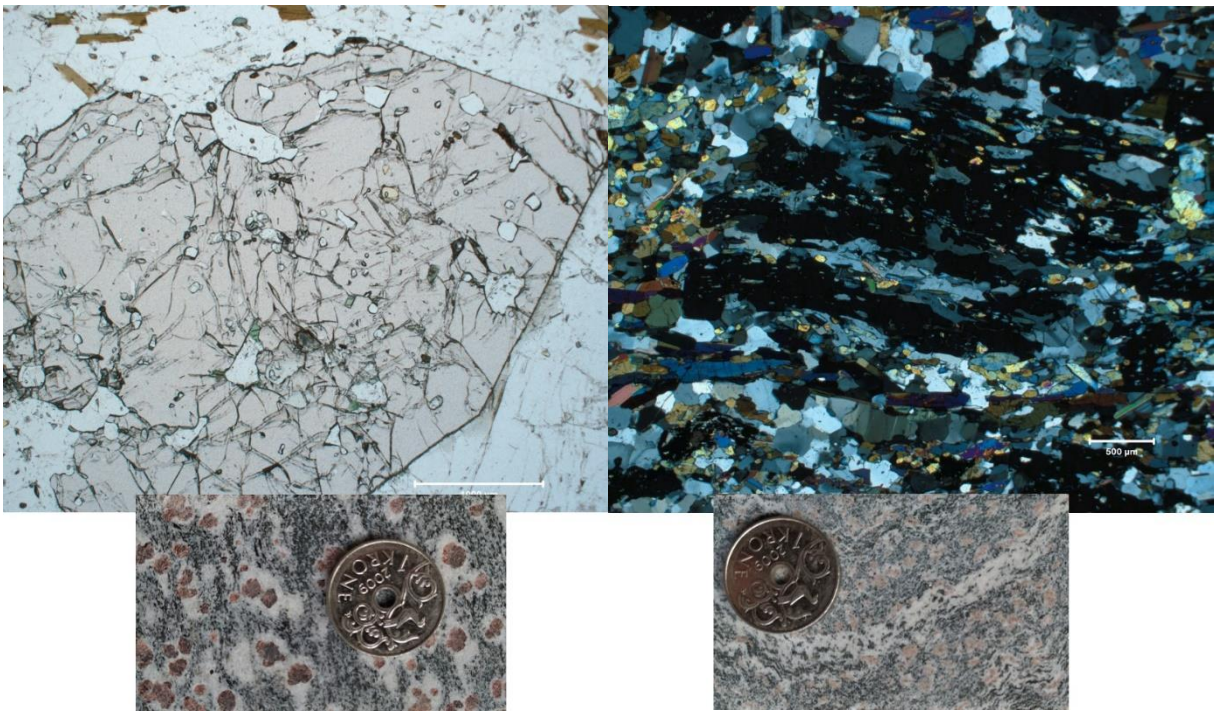

Figure 4-47 Garnet in thin section and in hand specimen from the drill core at Hellerfjellet (BH4508). The left pictures are from 55.40-55.55 meter below the surface, and the right is from 80.70-80.90 meters below the surface.

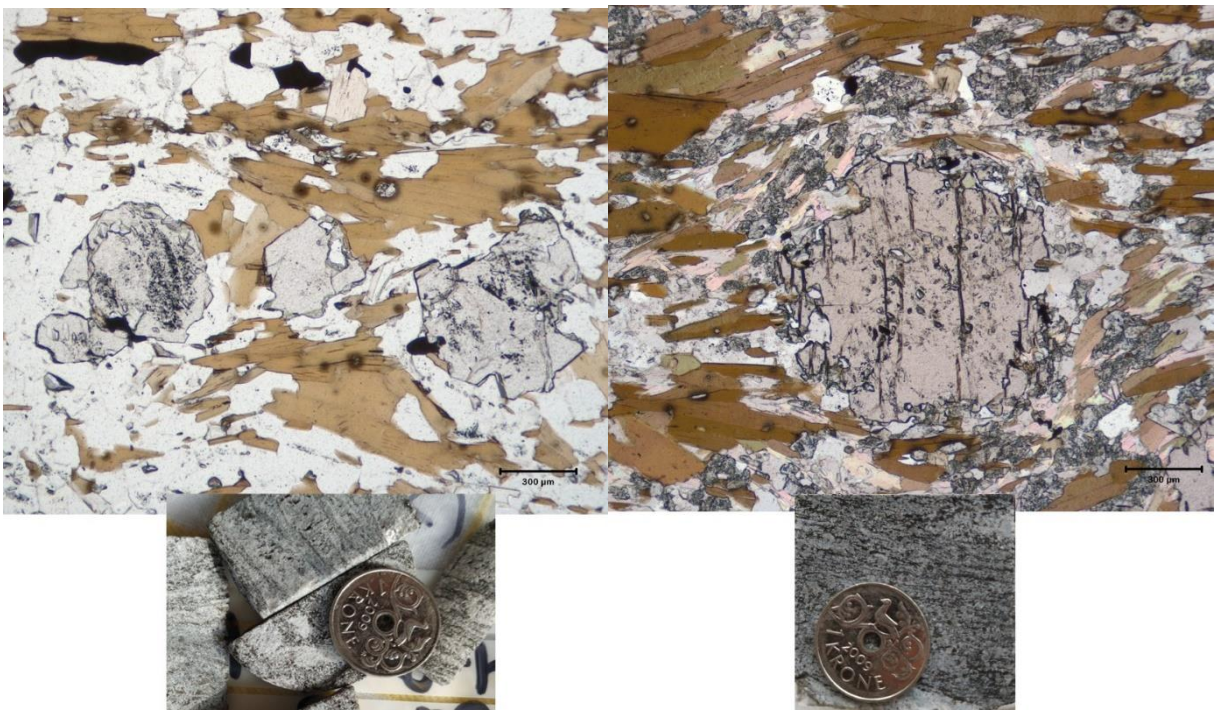

Figure 4-48 Garnet in thin section and in hand specimen from the drill core at Hellerfjellet (BH4508). The left picture is from 102.9 meters below the surface and the right is from 141.5 meters below the surface. The garnets are not as easy to see in hand specimen in these samples because of their small size and the light colour.

The portable XRF revealed the ore zone (116-134 mbs.) and the proportions of, especially, the various ore-forming elements and some of the most common rock-forming elements. The most abundant metals are Zn, Cu and Pb (Figure 4-49). Silver (Figure 4-50) is mostly below detection limit but enriched in some parts of the ore zone with the average value of 65g/t. One analysis has 1398 g/t, this is probably of a silver mineral grain. The ore zone generally has a high barium content (Figure 4-50) and especially in and close to the ore zone. One goal with the XRF analyses was to find zonation patterns when getting close to the ore. There is no clear zonation, but it may look like the barium content increase in a few hundred ppms when we get closer to the ore. It is generally a small decrease in the elements often found in the gangue minerals, like Ca and K (Figure 4-51). The iron content is decreasing a few hundred ppm towards the ore zone and the S content is about the same through the whole analysed area (Figure 4-50). All the elements vary more in the ore zone compared to just above and below.

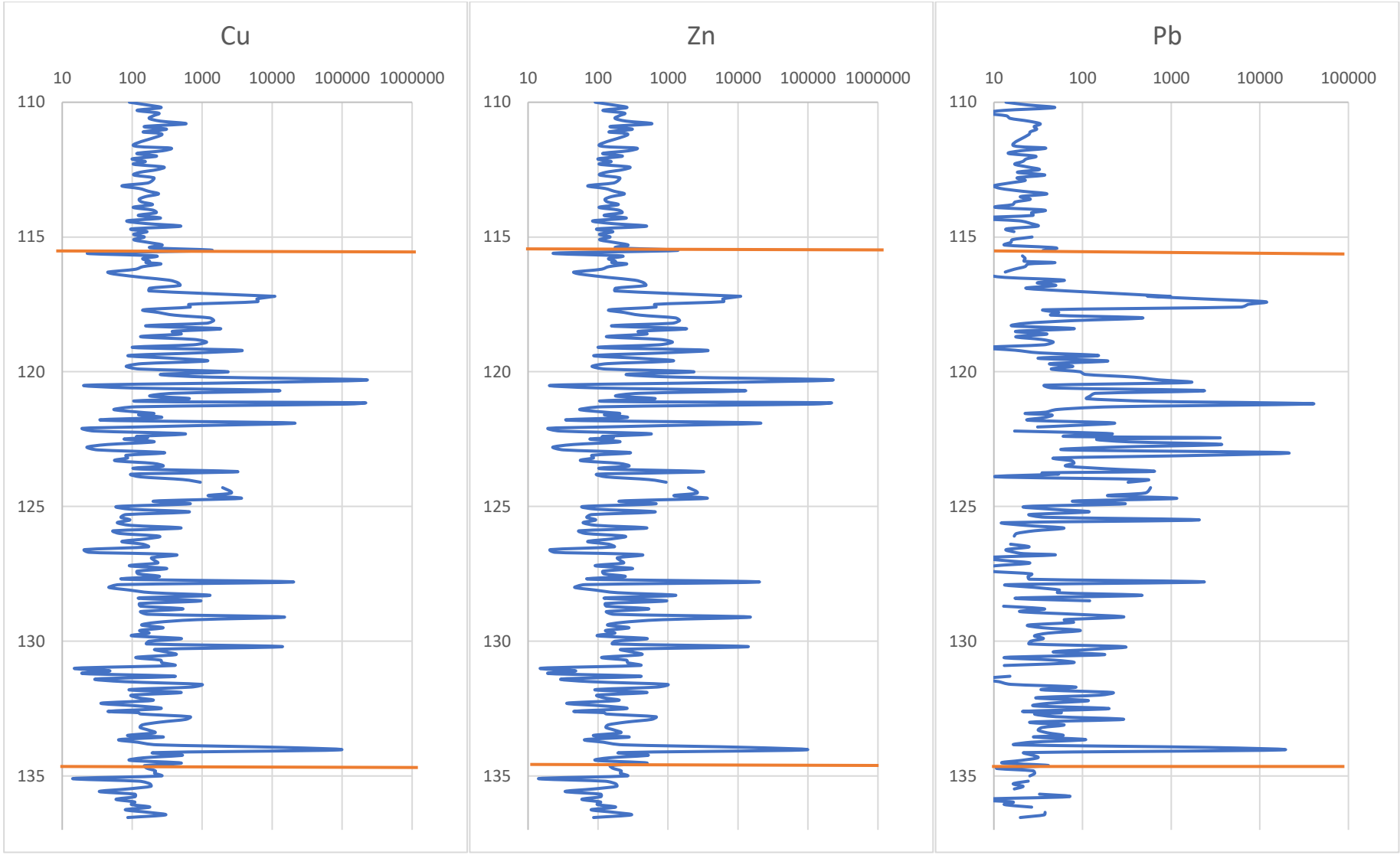

Figure 4-49 Portable XRF results of the drill core. These are the most important metal; Cu, Zn and Pb. Logarithmic ppm values in the x-axis, meters down the core on the y-axis. The field between the two orange lines represents the ore zone.

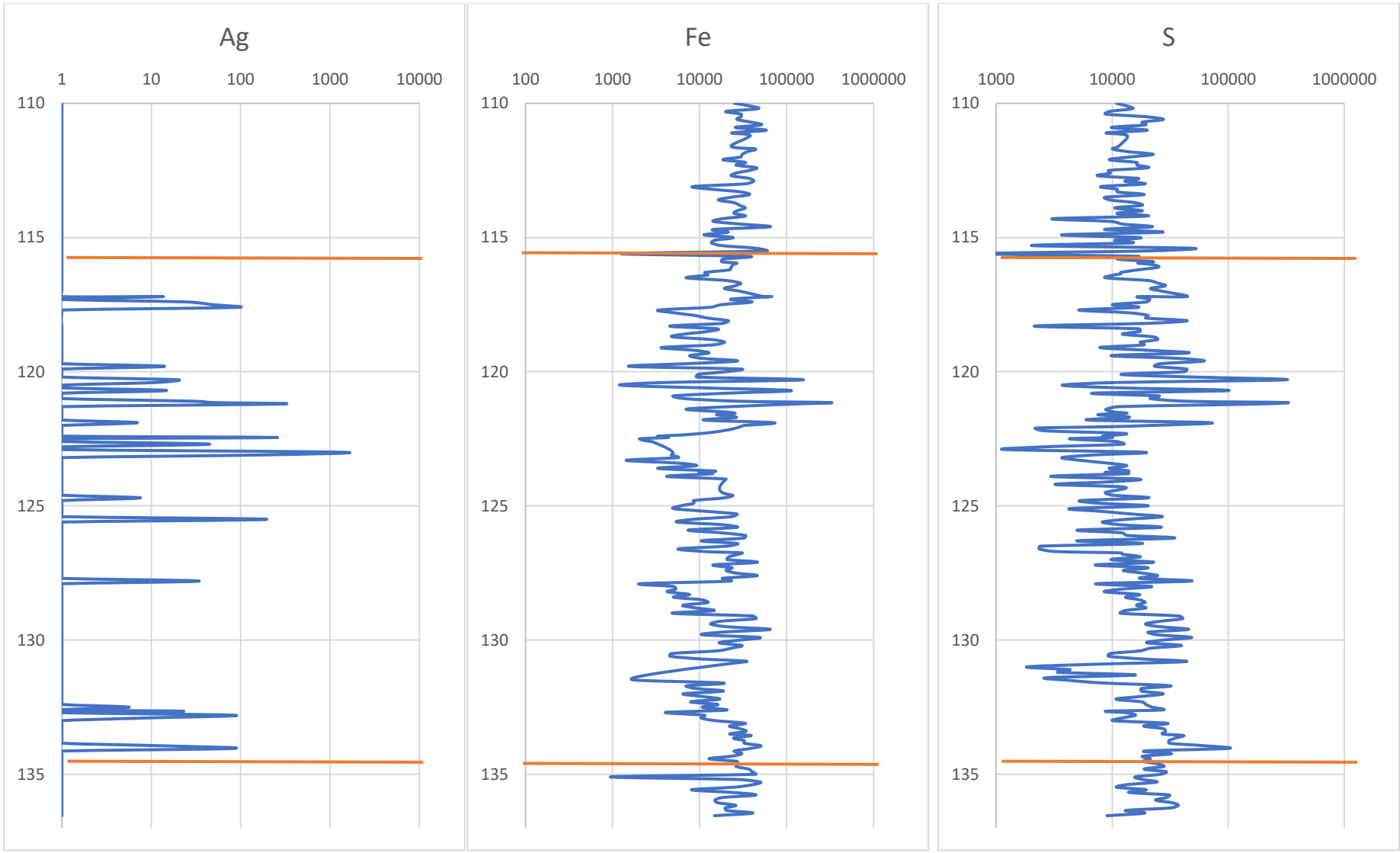

Figure 4-50 Portable XRF-results of the drill core. Results for Ag, Fe and S. Logarithmic ppm values in the x-axis, meters down the core on the y-axis. The field between the two orange lines represents the ore zone.

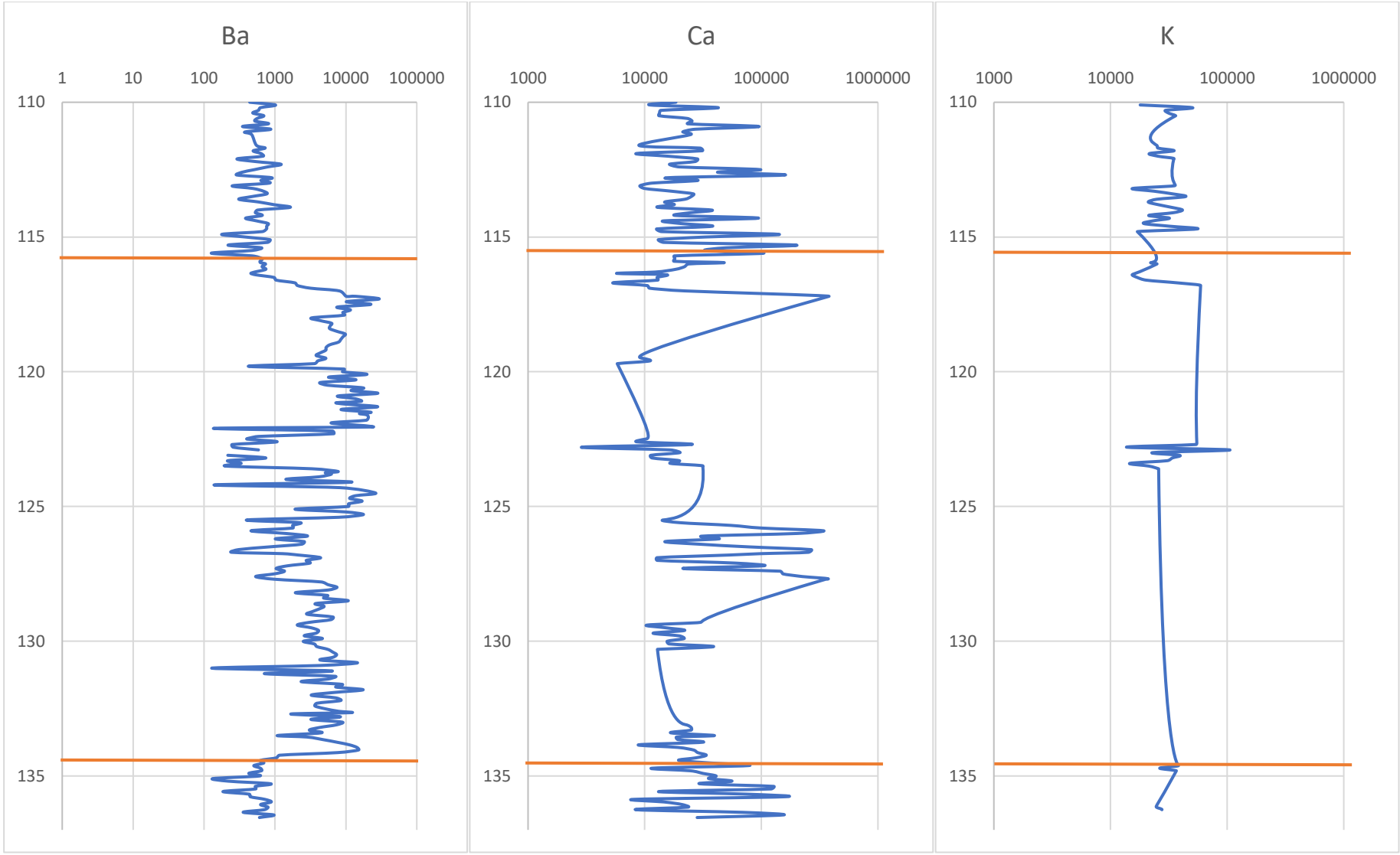

Figure 4-51 Portable XRF-results of the drill core. Ba, Ca and K. Logarithmic ppm values in the x-axis, meters down the core on the y-axis. The field between the two orange lines represents the ore zone.

4.3 Chemical analyses

The chemical analyses concern the field samples collected in the field the summer of 2019. These have been analysed with different ICP methods as explained in the methodology chapter (3.3). Chemical result of grey gneiss and amphibolite from NGU has also been used. All the chemical results for the field samples are listed in Appendix E.

Grey gneiss

The grey gneiss unit covers the biggest area of the two zones studied in this thesis, and the origin of this rocky type is useful for deciding the origin of the ore.

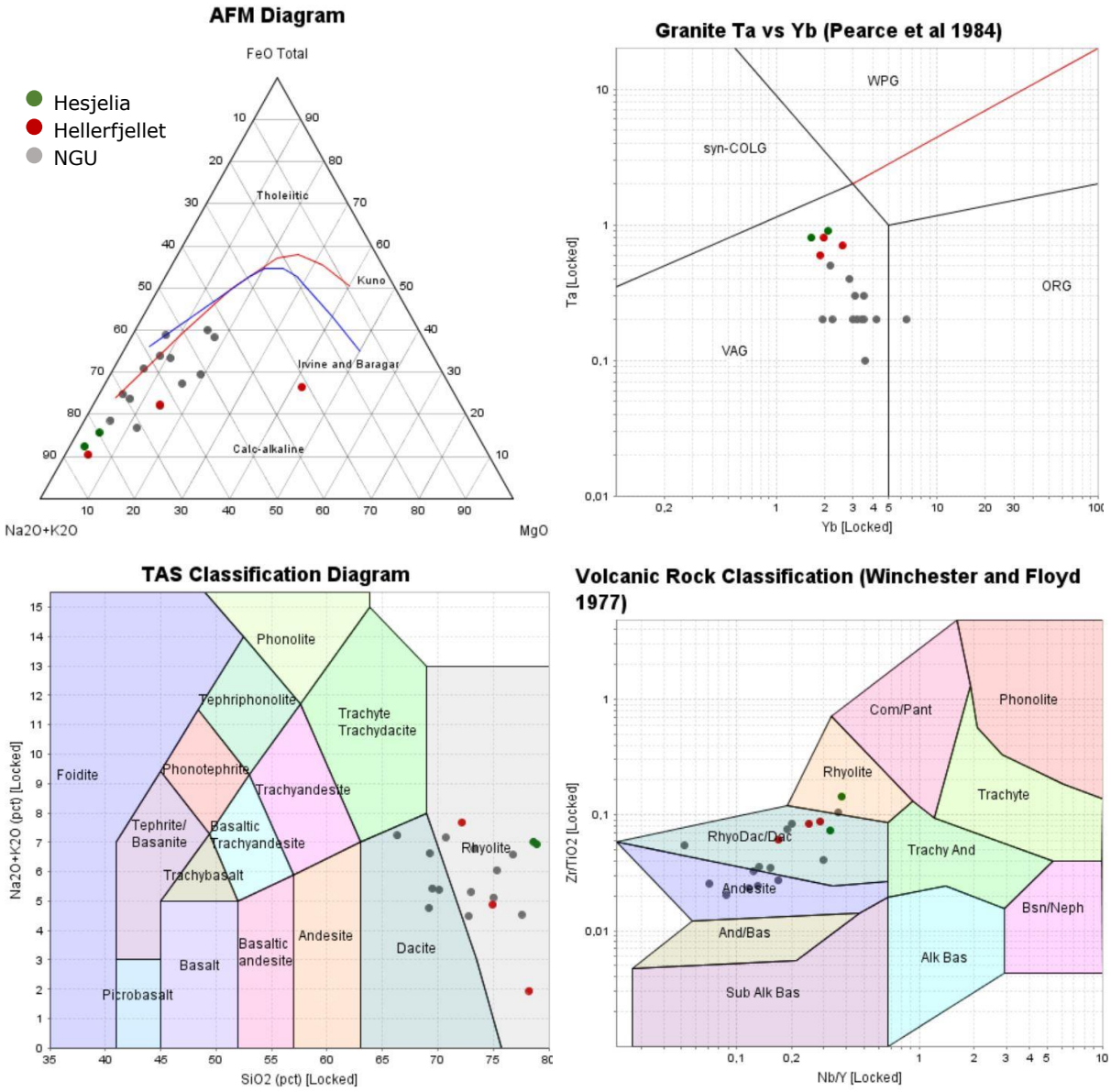

Figure 4-52: Composition of grey gneiss plotted in various classification diagrams. Composition of grey gneiss plotted in different classification diagrams. Diagrams are from Irvine and Baragar (1971); Kuno (1969), (Pearce *et al.*, 1984), Le Maitre et al. (1989), (Winchester and Floyd, 1977).

Few samples of grey gneiss were collected in the field this summer, but in earlier studies by NGU are more sample of grey gneiss analysed. All the chemical analyses available will be used in this thesis to get a better overview of the grey gneiss.

In the AFM diagram the grey gneiss plots on and near the boundary between tholeiitic and calc-alkaline (Irvine and Baragar, 1971; Kuno, 1969) and has a tholeiitic trend. This is typical for volcanic arc environments according to Chin *et al.* (2018). This is also confirmed by the Ta vs Yb granite classification diagram (Pearce, Harris and Tindle, 1984) where the grey gneiss plots in the volcanic arc field. According to Lentz (1998) referring to Barrett and MacLean (1999) can the Zr/Y ratio be used to separate what is calc-alkaline and what is tholeiitic sequences in a felsic volcanic sequence. If Zr/Y ratio is between 2 and 4 it is tholeiitic, ≥7 it is calc-alkaline and if it is transition group, it is between 4 and 7. The Zr/Y ratio of the grey gneiss in Table 9 in the Mofjell group is between 2 and 8, so the grey gneiss will be a transition group, but more towards a tholeiitic affinity than a calc-alkaline. The samples from Hellerfjellet and Hesjelia are in all the three groups.

Table 9 Zr/Y ratio of the grey gneiss from Hellerfjellet and Hesjelia. The MO samples are from all over the Mofjell group (NGU's samples)

Sample	Zr/Y
HF-01	5,223214286
HF-02	8,133333333
HF-12	3,95
HS-2	4,114285714
HS-3	8,380952381
MO 020	3,056603774
MO 061	3,907563025
MO 041	2,893772894
MO 053	1,789473684
MO 054	3,365384615
MO 067-1	2,814814815
MO 092	5,458937198

In the TAS and volcanic rock classification diagram (Le Maitre *et al.*, 1989; Winchester and Floyd, 1977) the grey gneiss plots in the rhyolite, andesite and dacite field. This is a confirmation that the grey gneiss varies in the content and that we have a bimodal volcanic system.

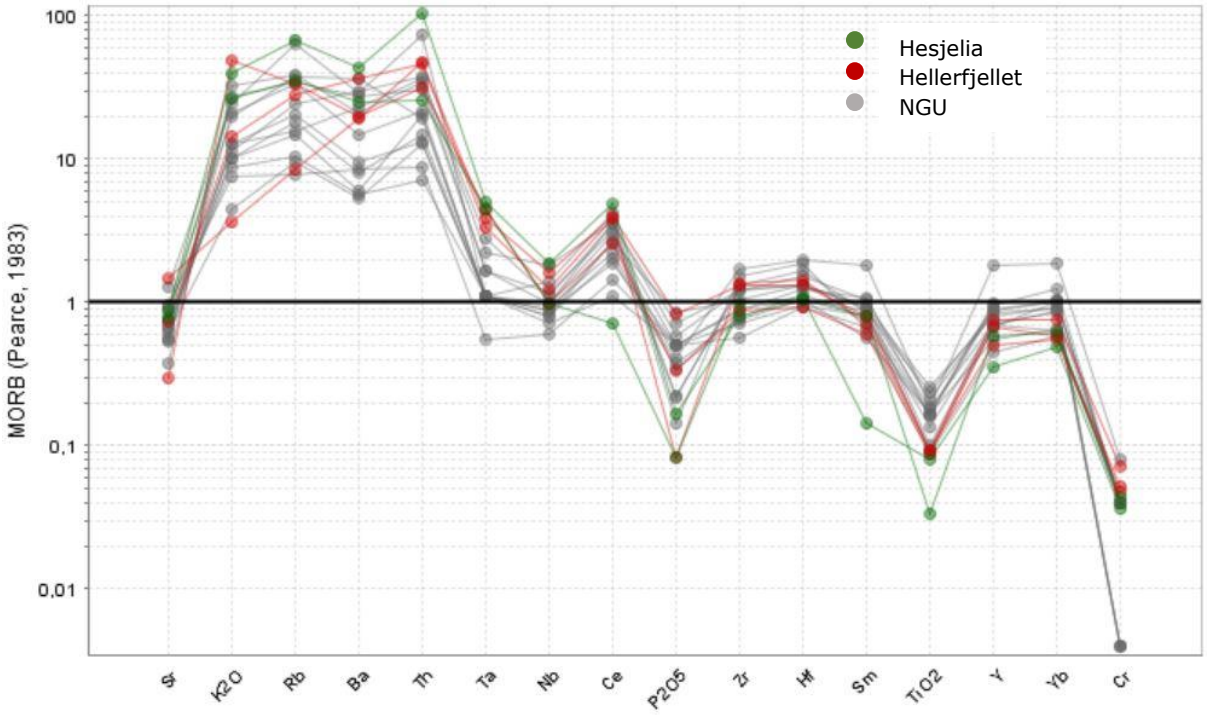
Hesjelia
Hellerfjellet
NGU
MORB (Pearce, 1983)
100
10
1
0,1
0,01
Sr
K2O
Rb
Ba
Th
Ta
Nb
Ce
P2O5
Zr
Hf
Sm
TiO2
Y
Yb
Cr

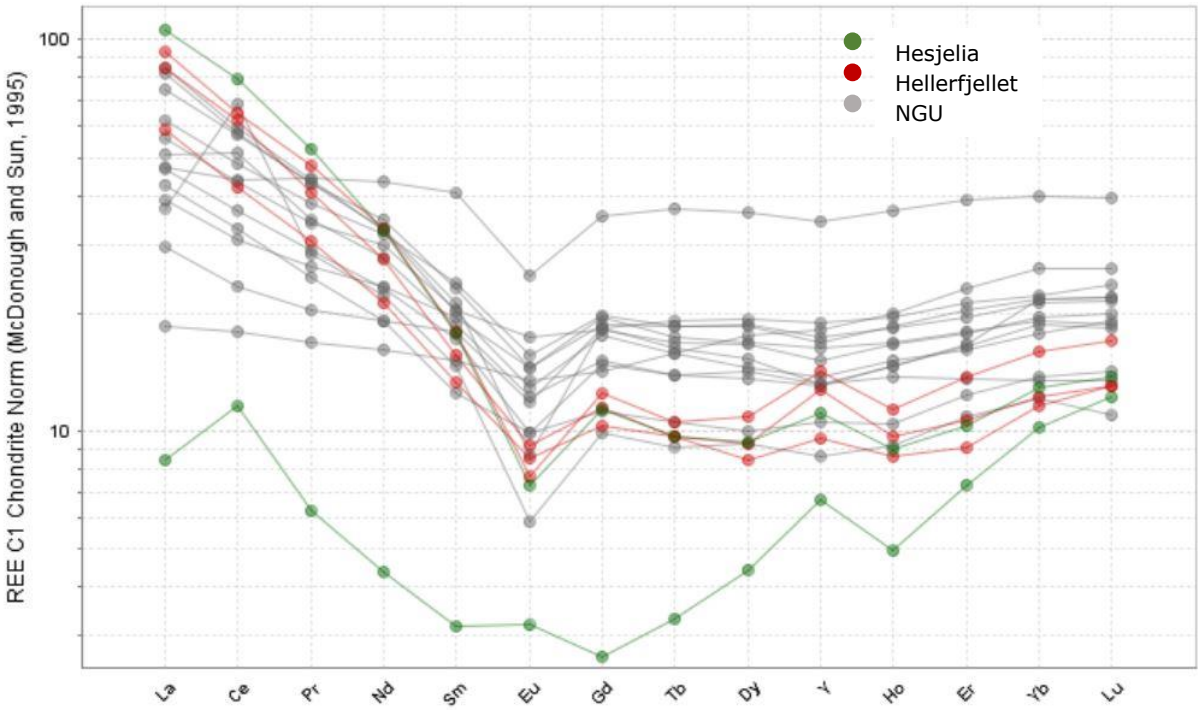
Hesjelia
Hellerfjellet
NGU
REE C1 Chondrite Norm (McDonough and Sun, 1995)
100
10
La
Ce
Pr
Nd
Sm
Eu
Gd
Tb
Dy
Y
Ho
Er
Yb
Lu

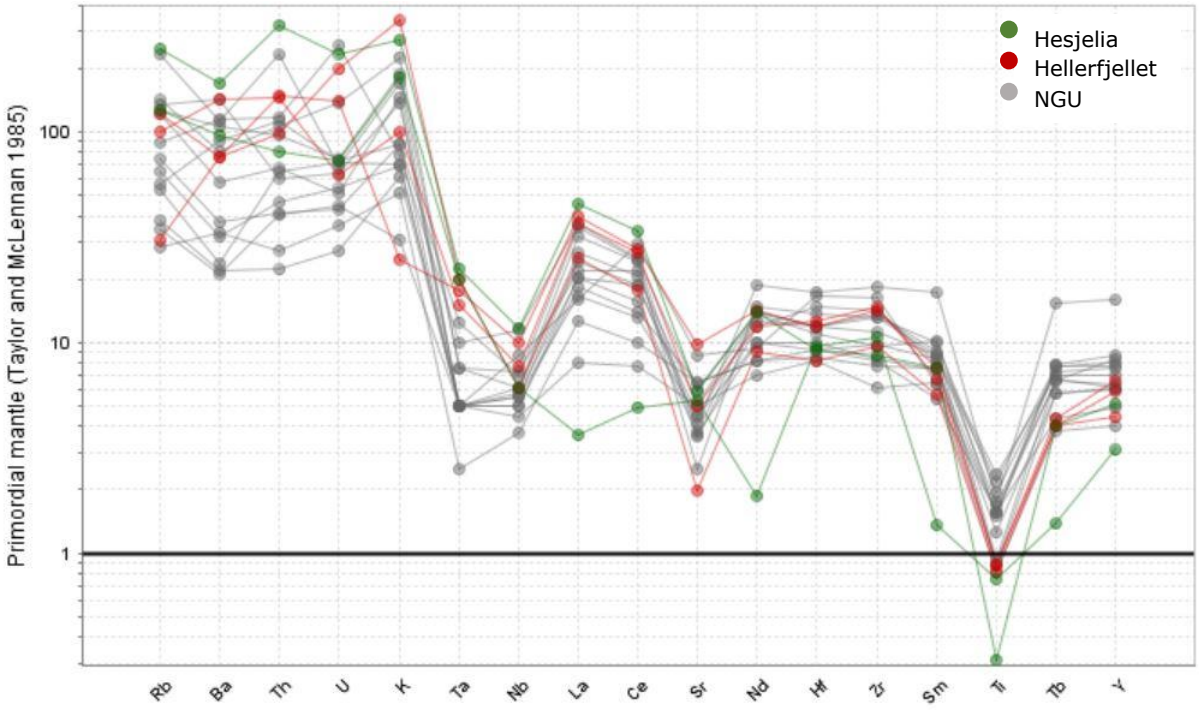

Figure 4-53 MORB normalized diagram, REE chondrite normalized diagram and primitive mantle normalized diagram from McDonough and Sun (1995); Pearce (1983); (Taylor and McLennan, 1985).

In the MORB normalized spider diagram (Pearce, 1983) does all the samples more ore less follow the same trend. It is enriched in K, Rb, Ba and Th and depleted in P, Ti and Nb. This pattern is typical for volcanic-arc tectonic setting according to Bjerkgård *et al.* (2013a).

In the REE diagram are the grey gneiss more enriched in LREE than HREE and has a weak negative Eu-anomaly. According to Defant and Drummond (1990) is this together with Al_2O_3 <15wt% typical for partial melting metabasalt in the lower crust. The values of Al_2O_3 for the grey gneiss has the average of 13wt.%. Also, in this diagram there is one sample of grey gneiss does not follow the trend of the other samples and does not have an Eu-anomaly typical for volcanic rocks. This sample is most likely a sedimentary variation of the grey gneiss. Those samples with a flat trend are the dacite and andesite samples, and the ones with a steeper curve are the rhyolites.

The spider diagram with grey gneiss normalized to primitive mantle (Taylor and McLennan, 1985) show relatively high LIL and HFS elements, negative anomaly in Ta, Nb, Sr and Ti. This trend, together with the Granite Ta vs Yb classification diagram has a similar trend to the Kuroko district in Japan (fig. 3a in Lentz (1998)) and Keketale VMS deposit in China district in Tasmania, both formed in an island-arc setting(Wan, Zhang and Xiao, 2010).

M**uscovite gneiss**

The muscovite schist/ gneiss is the host rock to the sulphide deposits and are thought to result from circulation of the same fluid depositing the mineralisation. The origin is thought to be the same because of the similar chemistry and evidence in the field. The muscovite gneiss is most likely an altered rock and are suggested to originally have been grey gneiss and amphibolite by Bjerkgård *et al.* (2013a). This will be more unravelled here.

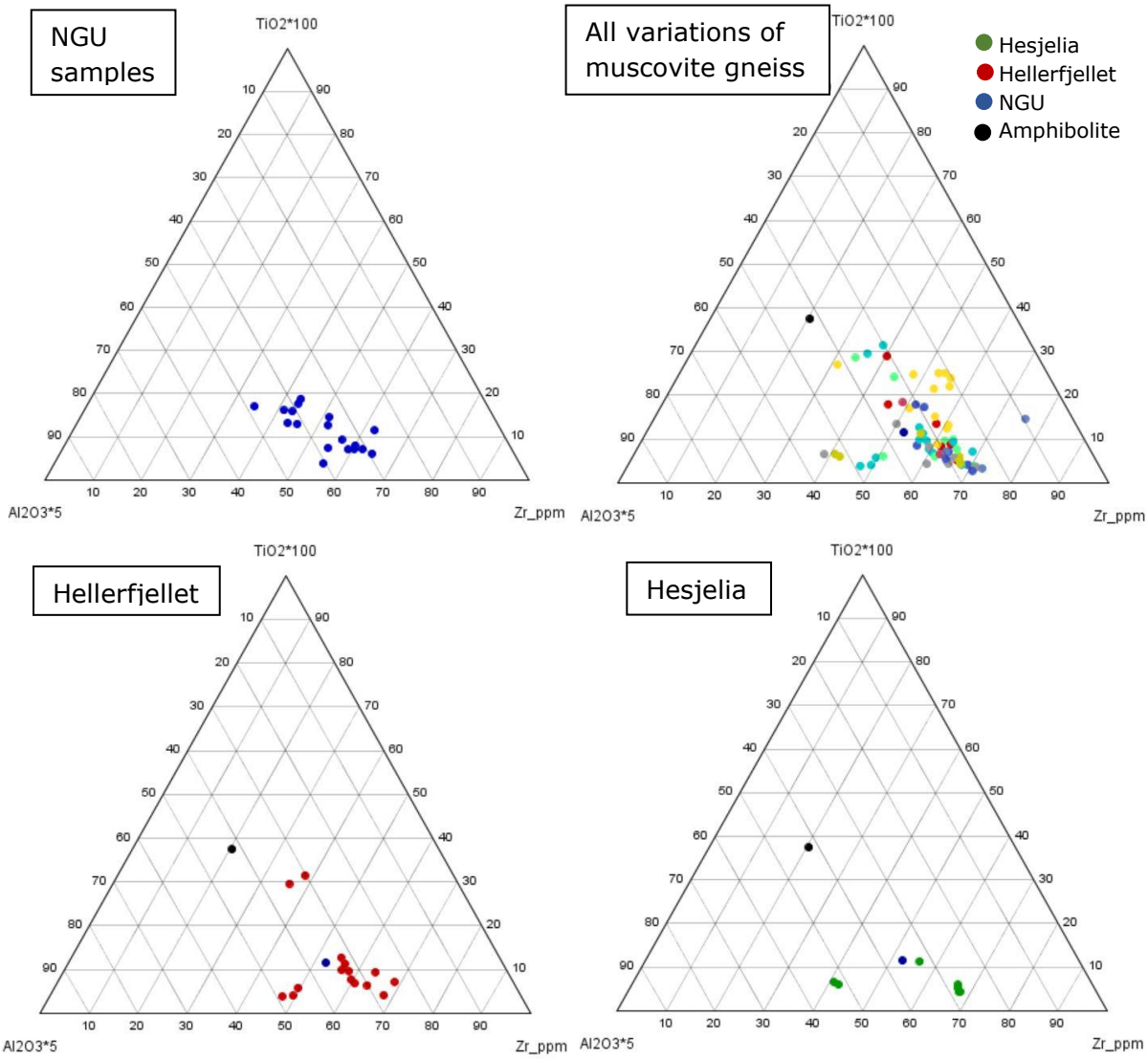

Figure 4-54 Ternary diagram of Ti, Al and Zr that are considered as immobile elements in this system. All the grey gneiss sample (left) and the variations of muscovite gneiss (±biotite±graphite±mineralisation) (right) are plotted in the two upper diagrams. In the two lower diagrams are plain muscovite gneiss (mostly quartz and muscovite) plotted together with the average amphibolite and grey gneiss.

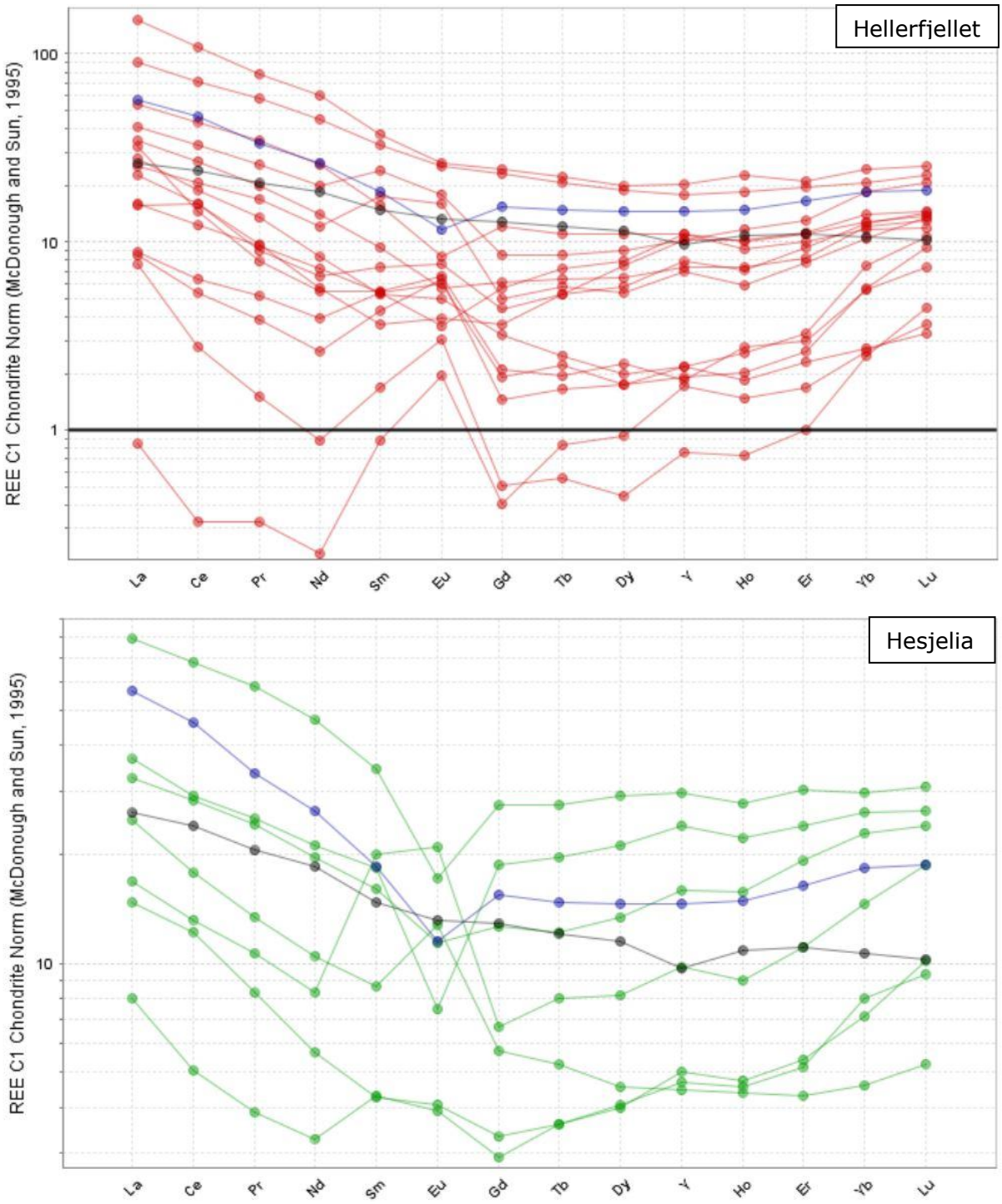

Figure 4-55 REE spider diagram normalized to chondrite (McDonough and Sun, 1995) of the muscovite gneiss and average grey gneiss and amphibolite.

Ti, Al and Zr are considered as immobile elements in hydrothermal alteration and metamorphism. In Figure 4-54 are muscovite schist plotted together with average grey gneiss and amphibolite in Ti, Al and Zr triangular diagrams.

In the upper two ternary diagrams are all the grey gneiss plotted in the left diagram and all the variations of muscovite gneiss plotted in the right. Here can we see that most of the muscovite gneiss plots in the same area as grey gneiss, while a few are closer to the amphibolite average. In the lower two ternary diagrams are the muscovite gneiss from the Hellerfjellet plotted. Most of them plots together with the grey gneiss. In the lower

ternary diagram are the samples from the Hesjelia zone, and these also plots close to the average grey gneiss.

In Figure 4-55 is the muscovite gneiss and average amphibolite and grey gneiss normalized to chondrite for the rear earth elements. Most of the muscovite gneiss in both zones plots below the grey gneiss and amphibolite in both LREE (La-Sm) and HREE (Dy-Lu), but a few samples plot above. The samples from Hellerfjellet generally displays a flat curve through the whole diagram, with slightly steeper slope for the LREE. Those samples with the least REE has a positive Eu-anomaly, these as most likely the most altered samples. Samples from the Hesjelia zone has a steeper slope for the LREE and flat for the HREE. Two of the samples has less REE than the other samples and may be of sedimentary origin since sedimentary rocks normally contain less REE than volcanic rocks.

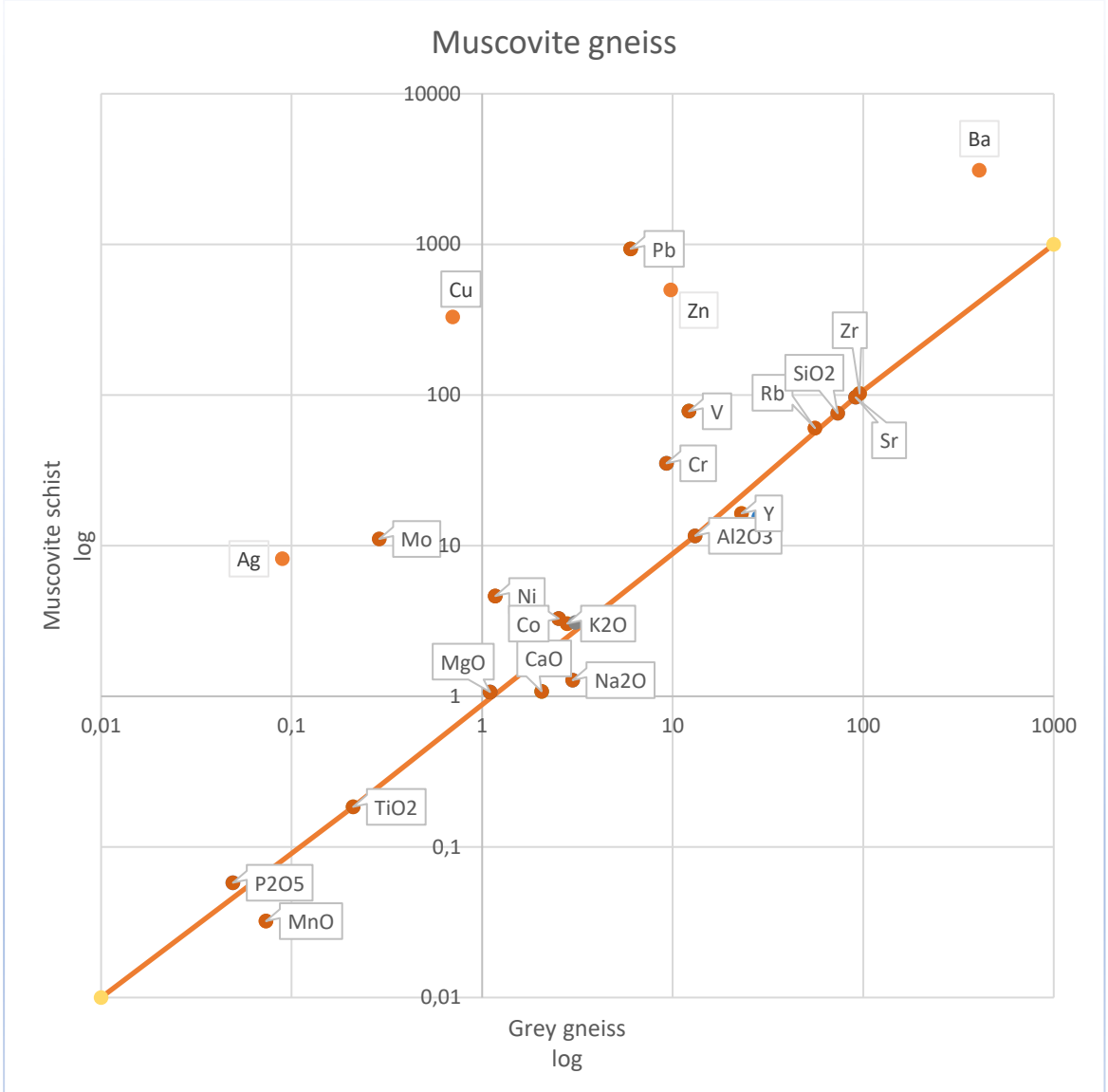

Figure 4-56 Isocon diagram for the alteration of grey gneiss to muscovite gneiss in the Hesjelia and Hammertjønna area. The line is the isocon line defined by the elements considered immobile in the alteration process (Ti, Al and Zr). The elements below are

considered as losses and those above are gained. Based on method description in Bjerkgård and Bjørlykke (1996).

During hydrothermal alteration may the mass or volume change because of the change in mineralogy and chemistry. Bjerkgård and Bjørlykke (1996); Grant (1986) presents a isocon diagram that can be used to graphically present the gains and losses during metasomatic alteration. It is the change in mass (or volume) that is exhibited in the diagram. Since this is based on the ICP results is the mass of each sample about the same. The line, called isocon, are defined by elements that are considered as immobile during the process, in this case is Ti, Al and Zr considered as immobile. The slope of the line is 1, and this equals no mass (or volume) change during the alteration. If the slope is over 1, then it has been a positive mass change, if below one, then it is a negative mass change (Grant, 1986). The elements above are considered as gained and those below are considered as losses. This is based on average results of grey gneiss and muscovite gneiss, so the amount of gains and losses may differ from sample to sample. From this diagram can we see that Mo, Ni, Co, Cr, V, Ba and Pb is gained. It is not a significant loss in this system, but Mn, Ti, Ca, Na and Y are below the line and considered as lost. There is a variation in the content of the grey gneiss, so the elements closest to the line may not actually be losses or gains.

Massive and disseminated ore

Samples from most of the prospects was collected, but not all of them are massive ore. About 8 of the prospects at Hellerfjellet and 9 in the Hesjelia zone are considered as massive ore based on the field samples. Disseminated ore are all the sample of muscovite gneiss with visible mineralisation either in bands or disseminated in the samples. These are the samples considered in this chapter.

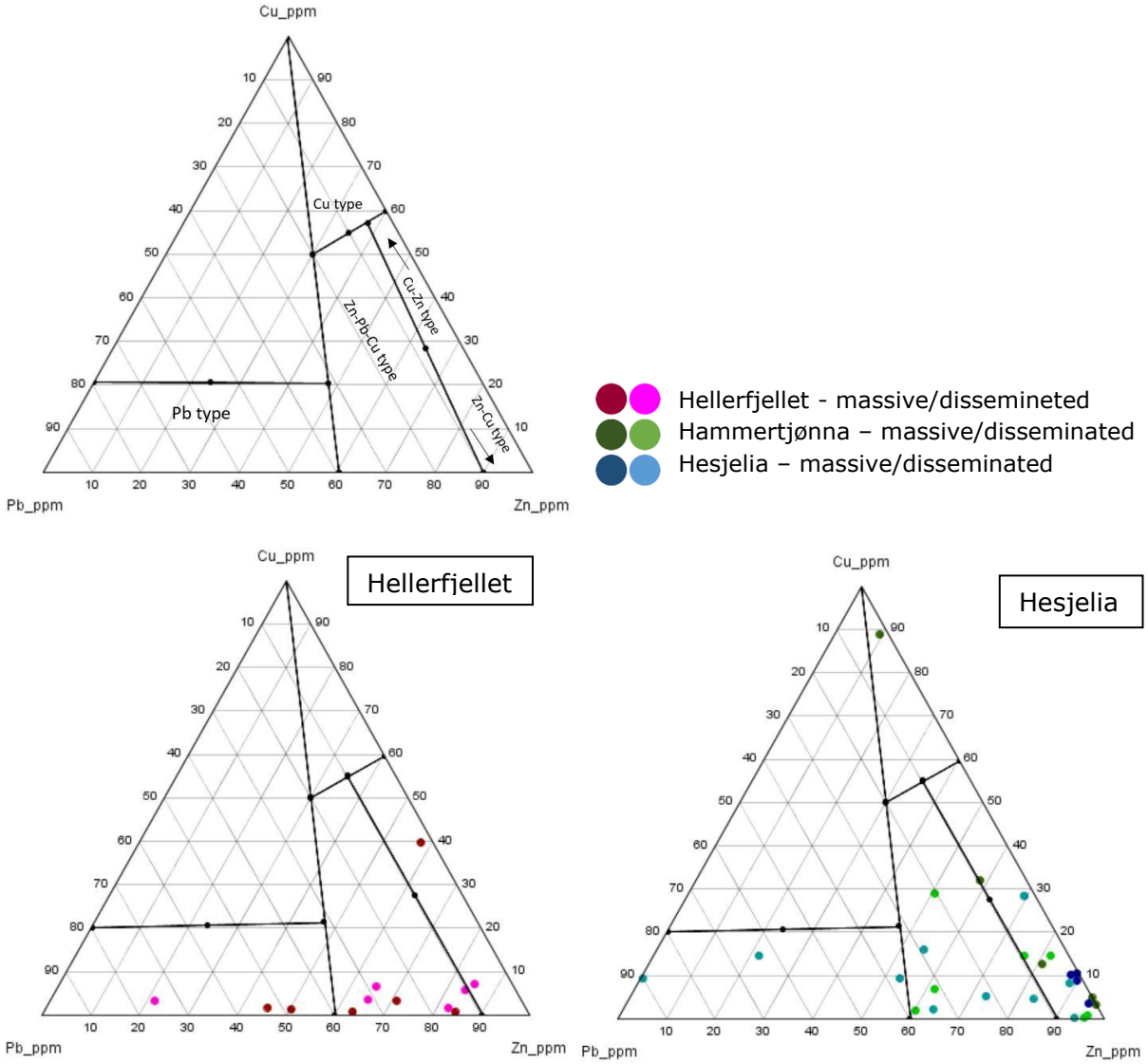

Figure 4-57 Ternary Cu, Pb and Zn diagram with the fields of classification of VMS-deposits based on metal content. The fields and the names in the upper diagram are from Large (1992); Mousivand et al. (2018). The massive ore and disseminated ore from Hellerfjellet

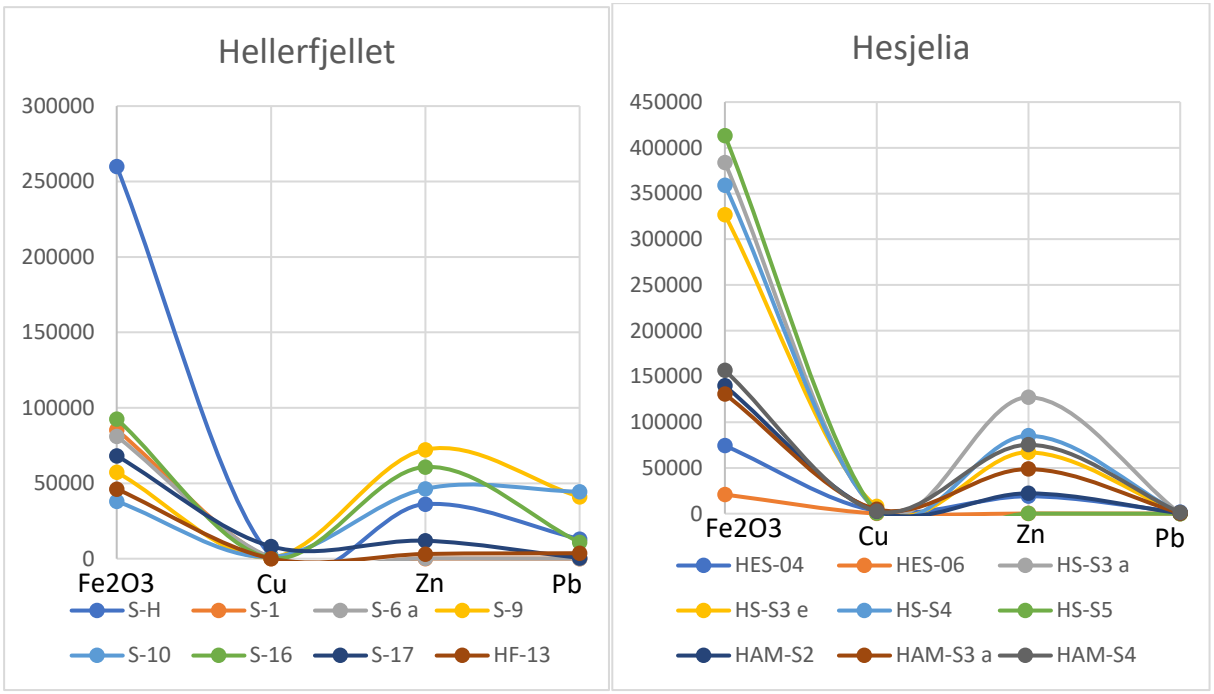

Figure 4-58 The massive ore plotted together with the Fe-, Cu-, Zn-, and Pb-content for comparison. Hellerfjellet massive ore in the left and Hesjelia in the right.

In the ternary Cu, Pb and Zn diagram in Figure 4-57 plots the massive ore samples from the Hesjelia zone more or less together in the Zn-Cu type corner, while the Hellerfjellet samples plots with a wider range in the Zn-Pb-Cu and Pb type deposits. The disseminated ore from both zones mostly plots in the Zn-Pb-Cu field. Few samples from both zones plots close and in the Cu type deposit. In the Hesjelia zone are the massive ore at Hammertjønna richer Zn while the Hesjelia deposit has more Cu. The disseminated ore from Hammertjønna are richer in Pb, while Hesjelia are richer in Zn and Cu. So here we can see a lateral zonation.

In the diagrams in Figure 4-58 are the massive ore from the zones plotted together for comparison. Here we can see that the Hellerfjellet deposit generally is a Zn-Pb deposit. Those sample with Cu has a lower content in Zn and Pb compared with the other. In the Hesjelia zone are the samples richest in Zn, and generally richer in Cu compared with Hellerfjellet. The Hesjelia zone has higher Fe-content in the massive ore than the Hellerfjellet zone.

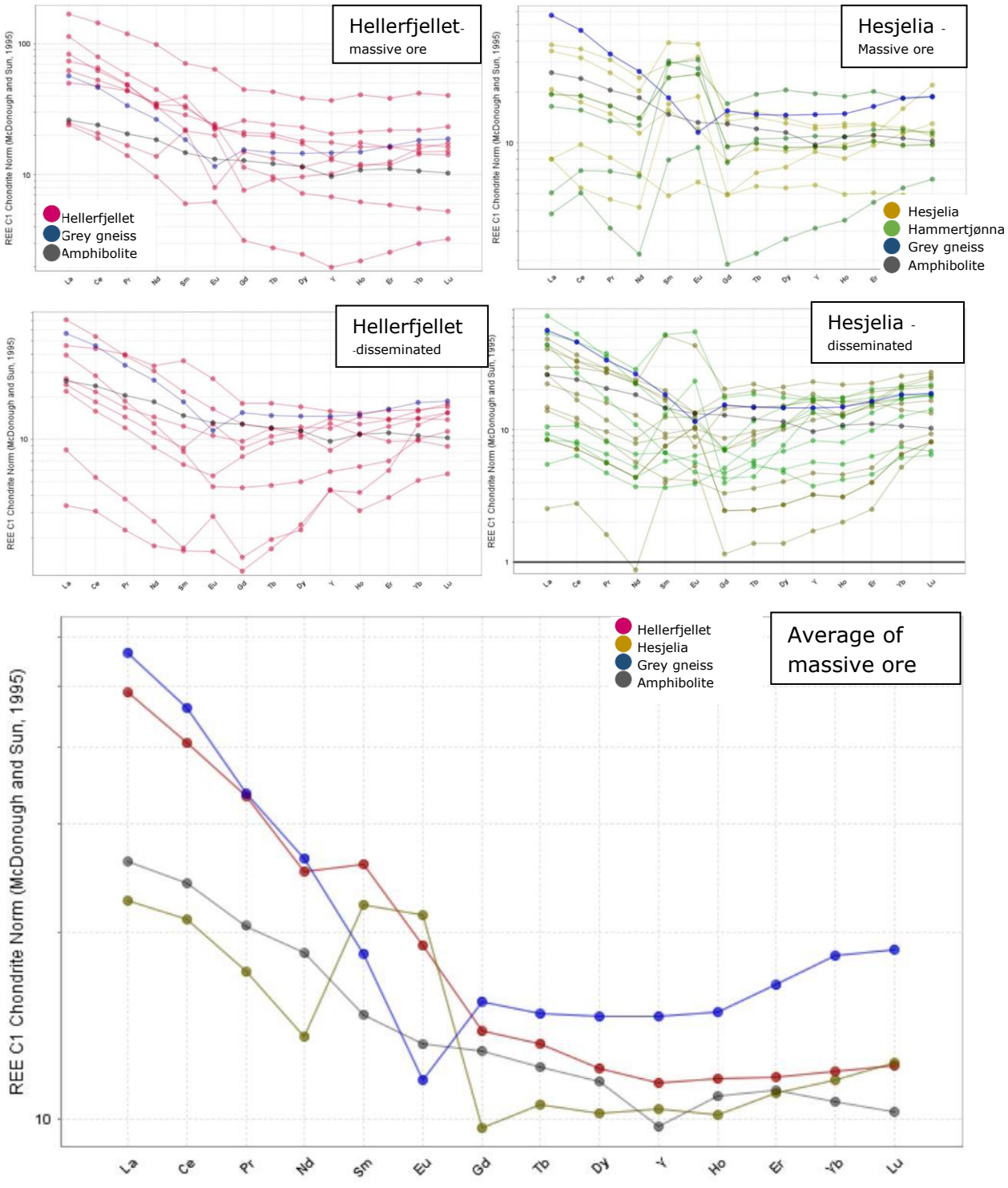
Hellerfjellet- massive ore
Hellerfjellet
Grey gneiss
Amphibolite
Hesjelia - Massive ore
Hesjelia
Hammertjønna
Grey gneiss
Amphibolite
Hellerfjellet -disseminated
Hesjelia - disseminated
REE C1 Chondrite Norm (McDonough and Sun, 1995)
La Ce Pr Nd Sm Eu Gd Tb Dy Y Ho Er Yb Lu
Hellerfjellet
Hesjelia
Grey gneiss
Amphibolite
Average of massive ore

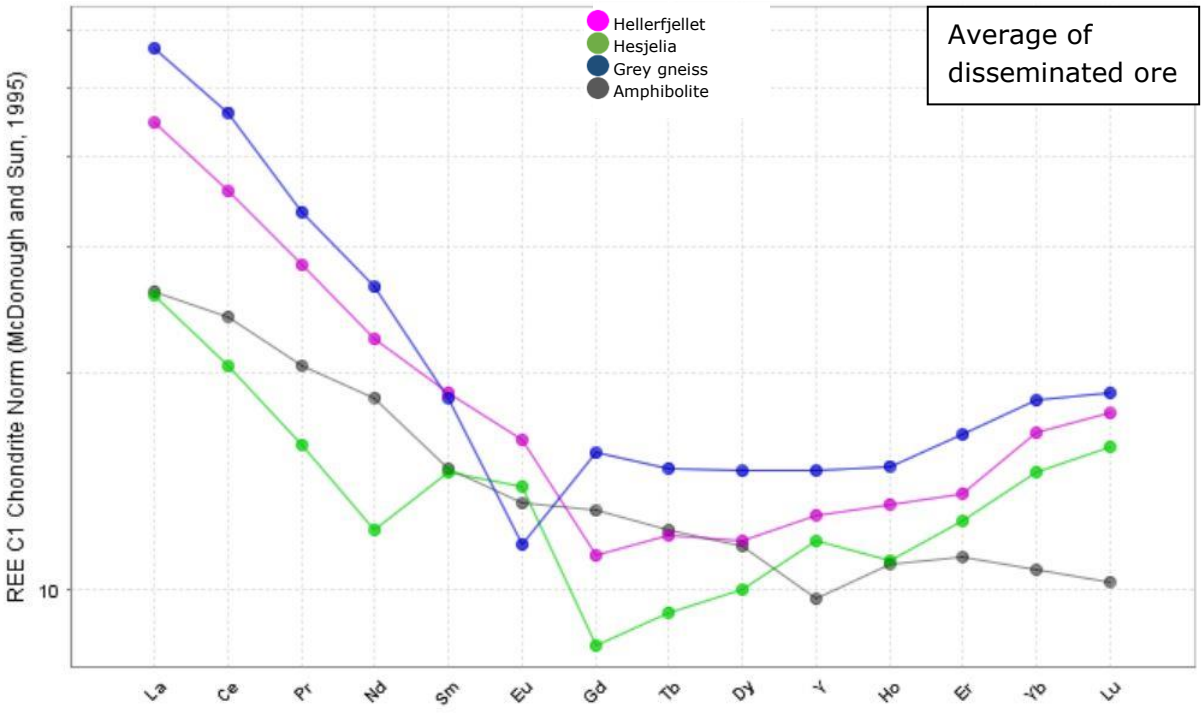

Figure 4-59 REE chondrite diagram (McDonough and Sun, 1995) of massive ore and disseminated ore from Hellerfjellet and Hesjelia.

In the REE chondrite spider diagram (McDonough and Sun, 1995) in Figure 4-59 is the massive ore from both and the average grey gneiss zones plotted. The massive ore from Hellerfjellet generally has more of the REE than grey gneiss and follow the grey gneiss gradually in a flat down curve. It is more enricher in LREE than HREE. The grey gneiss has e negative Eu-anomaly, but most of the massive ore at Hellerfjellet either has a weak anomaly, both positive or negative, or no Eu- anomaly. The massive ore from the Hesjelia zone generally has less REE than the grey gneiss and the massive ore from Hellerfjellet. It has a positive Sm- and Eu- anomaly and a negative Gd-anomaly. It is more enriched in the LREE than the HREE. According to (Bjerkgård *et al.*, 2013a) referring to (Spry *et al.*, 2000) claims that this is a typical pattern for hydrothermal reduced fluids and has probably not mixed with seawater before deposition.

Disseminated ore in the Hellerfjellet zone generally has less REE than the massive ore in Hellerfjellet (Figure 4-59). Some samples have higher HREE than LREE and some has the opposite trend. Samples with Eu-anomaly is positive, the rest does not have an anomaly. The disseminated ore in the Hesjelia zone has the same trends as the massive ore and some follow the same trend as grey gneiss, but with less amount of REE.

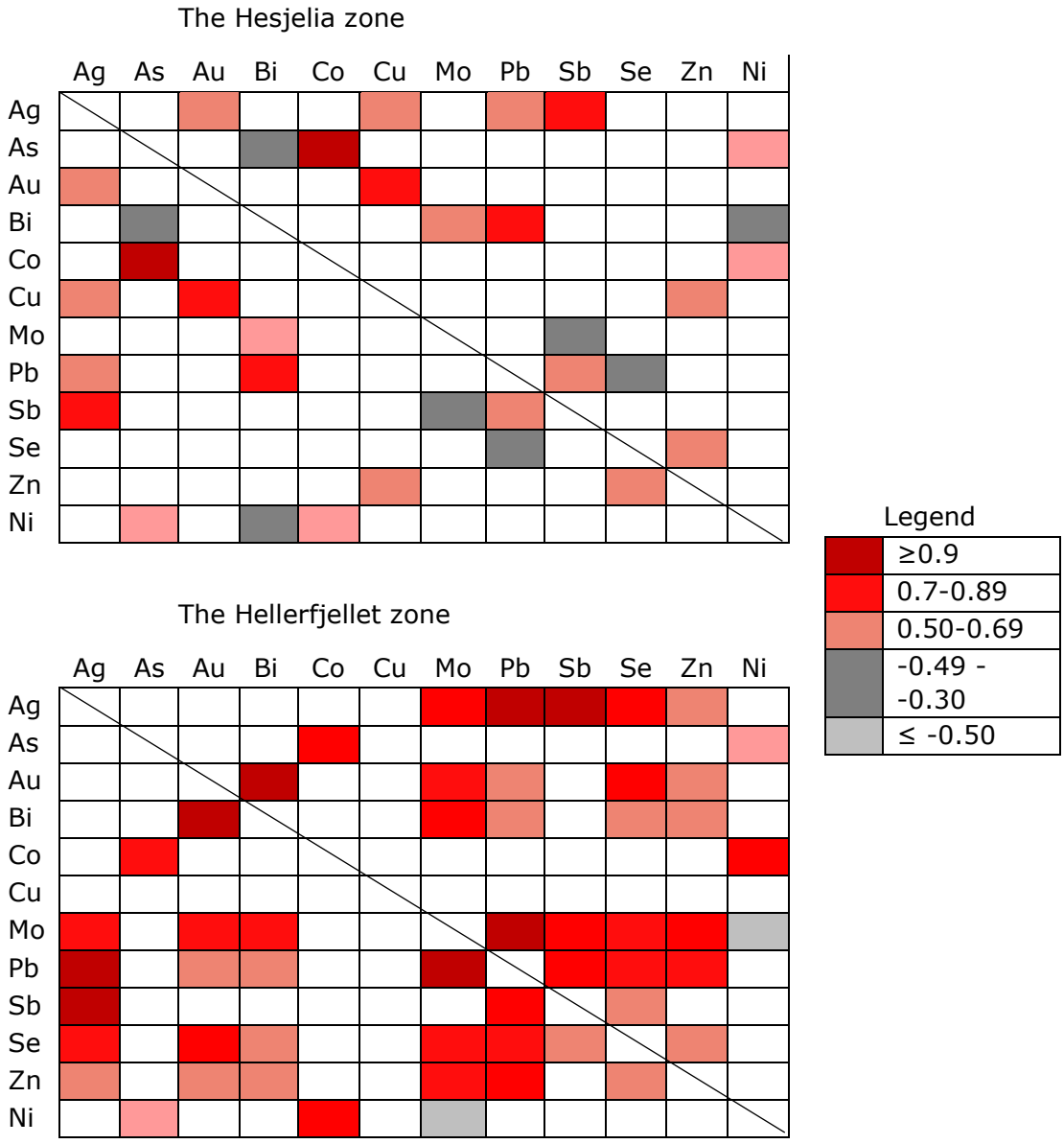

Figure 4-60 Correlation matrix of the massive ore from two zones, Hesjelia (upper) and Hellerfjellet (lower).

Correlation matrix of massive ore from the two zones are presented in Figure 4-60. The positive correlation will indicate that the metals are precipitated at the same time or it is a common mineral. Negative correlation indicates separate deposition (Bjerkgård and Bjørlykke, 1996). The correlation matrix for the two zones are not similar in all the metals, but with some. This may indicate different deposition events.

Zinc is weakly correlated with Cu and Se in the Hesjelia zone and strongly correlated with Mo and Pb in the Hellerfjellet zone. Zn and Pb are the main constitutes in sphalerite and galena, so these were probably deposited at the same time at Hellerfjellet. While in the Hesjelia zone sphalerite and chalcopyrite may have been deposited at the same time

Lead (Pb) is the main constituent in galena and correlates well with Ag, Bi, and Sb and shows a negative correlation with Se in the Hesjelia zone. In the Hellerfjellet zone it correlates well with Ag, Mo, Sb, Se, and Zn and weakly with Au and Bi. Bi is a common

impurity in galena (HudsonInstituteOfMineralogy., n.d.-b), so it may be a part of the lattice.

Copper (Cu) is the main constituent in chalcopyrite and correlates with Ag, Au, and Zn in the Hesjelia deposit and with none in the Hellerfjellet deposit. Since it does not correlate well with any elements in the Hellerfjellet zone is it probably because it is not a common element and that it did not deposit at the same time as the other ore-forming elements (Zn and Pb).

Silver (Ag) is correlating well with Au, Cu, Pb, and Sb in the Hesjelia zone. In the Hellerfjellet zone it correlates with Mo, Pb, Sb, Se, and Zn.

Molybdenum (Mo) correlates with Ag, Au, Bi, Pb, Sb, Se, and Zn in the Hellerfjellet zone. The massive ore has values from 3 to 180ppm Mo. The massive ore in the Hesjelia zone show values up to 240ppm, but it does not show the same correlation as in the Hellerfjellet zone. It may appear as illusions in sphalerite according to Bjerkgård *et al.* (2013a), so that's maybe where it is in the Hellerfjellet zone. Molybdenite is also observed in the area, so it might come from that.

Nickel (Ni) correlates well with As and Co in both zones. The maximum analysed values are 38ppm the Hellerfjellet zone and 32ppm in the Hesjelia zone. Ni are together with As and Co common impurities in pyrite and pyrrhotite HudsonInstituteOfMineralogy (n.d.); (n.d.-a), so they are probably in their lattice.

The rest of the elements are probably constituting tellurides, sulfosalts, or fahlore minerals that follows the sulphides.

4.4 Results – SEM analyses

SEM analyses was done on all together 10 samples, 4 from Hellerfjellet drill core and 6 from field samples. The main minerals to analyse was garnet, mica, and the sulphides to try to find differences in similarities between the zones. All the general mineral formulas of the minerals observed in the samples are listed in Table 10 and some of the stoichiometric formula based on the SEM-results. All the SEM-results are listed in Appendix F and the scanned thin sections with points in Appendix G.

Table 10 Formulas of the minerals found in the samples; stoichiometric formula of the sulphides based on SEM-results have been calculated.

Mineral	Mineral formula (Mommio, n.d.-a; Pracejus, 2015)	Stoichiometric formula based on SEM-results		
Ore minerals		Drill core	**Hellerfjellet** Massive /disseminated	**Hesjelia** Massive/ disseminated
Pyrite	FeS_2		/$Fe_{1.593}S_{1.507}$	$Fe_{1.930}S_{1.070}$ / $Fe_{1.509}S_{1.491}$
Pyrrhotite	$Fe_{1-x}S$	$Fe_{1.033}S_{0.967}$	$Fe_{1.008}S_{0.992}$ / $Fe_{0.999}S_{1.001}$	$Fe_{1.163}S_{0.837}$
Sphalerite	(Zn,Fe)S		$Zn_{0.958}Fe_{0.156}S_{0,886}$	$Zn_{0.955}Fe_{0.121}S_{0.924}$
Chalcopyrite	$CuFeS_2$	$Cu_{1.601}Fe_{0.889}S_{1.510}$	$Cu_{1.775}Fe_{1.033}S_{1.191}$ / $Cu_{1.588}Fe_{0.892}S_{1.520}$	$Cu_{1.623}Fe_{0.877}S_{1.499}$/ $Cu_{1.610}Fe_{0.883}S_{1.506}$
Galena	PbS		$Pb_{1.168}S_{0.832}$	$Pb_{1.154}S_{0.846}$ / $Pb_{1.142}S_{0.858}$
Illmenite	$FeTiO_3$	$Fe_{1.201}Ti_{1.251}O_{2.548}$		
Barite	$BaSO_4$			
Graphite	C			
Silicates				
Quartz	SiO_2			
Garnet	$X_3Y_2(SiO_4)_3$			
Biotite	$K(Mg,Fe^{2+})_3[AlSi_3O_{10}(OH,F)_2$			
Muscovite	$K_2Al_3[Si_6Al_2O_{20}](OH,F)_4$			
Sericite	$KAl_2(AlSi_3O_{10})(OH)_2$			
Amphibole – Hornblende	$Na_{0-1}(Ca,Na)_2(Mg,Fe^{2+},Fe^{3+},Al)_5(Si,Al)_8O_{22}(OH)_2$			
Epidote	$Ca_2(Fe,Al)_3(SiO_4)_3(OH)$			
Feldspar - plagioclase	$NaAlSi_3O_8$--$CaAl_2Si_2O_8$			
K-feldspar	$KAlSi_3O_8$			

Celcian	$BaAl_2Si_2O_8$
Kyanite	Al_2SiO_5
Other	
Freibergite	$(Ag,Cu,Fe)_{12}(Sb,As)_4S_{13}$
Chlorite	$(Mg,Fe^{2+},Fe^{3+},Mn,Al)_{12}[(Si,Al)_8O_{20}](OH)_{16}$
Calcite	$CaCO_3$
Apatite	$Ca_5(PO_4)_2$[F, OH, Cl]

4.4.1 Hellerfjellet drill core

4 samples from Hellerfjellet drill core (BH4508) were analysed with the scanning electron microscope. Two from the grey gneiss at 14.25-14.40 and 91.00-91.20 meters down the core, and two from the altered zone around to the ore zone at 102.9 and 141.5 meters down the core. The ore zone is from about 116 to 135 meters down the core.

Garnet

Garnet is present almost everywhere in the drill core with changing colour, size and shape depending on its textural setting. Garnet was analysed with SEM to determine if there are any chemical differences throughout the ore zone, the alteration zone and the unaltered host rock. Zonation patterns of the garnets was studied in profile across individual grains, this is to see if the conditions changed when the grain grew and can with that give important information of the evolution of the area. In Table 1, 2, and 3 in Appendix F all the SEM results of garnet and average result are in Table 11. Generally, we can see that the chemical composition of the garnets in the drill core is fairly constant. Iron (Fe) varies from 21wt% to 26wt% in the alteration zone. Al and Ca are fairly constant whereas Mg is lower below the ore zone, Mn is richer in the sample close to the ore zone from above (HF-102.9).

Table 11 the average results of the analyses of garnets in the drill core from Hellerfjellet.

Meters below surface	14.25-14-40	91.00-91.20	102.9	141.5
O	26.83	26.50	26.47	26.25
Fe	25.95	25.43	21.79	22.81
Si	13.60	13.30	13.63	13.48
Al	10.39	10.34	10.37	10.08
Ca	5.03	4.5	4.75	4.25
Mg	1.59	2.43	2.68	1.40
Mn	1.065	0.664	3.21	1.11

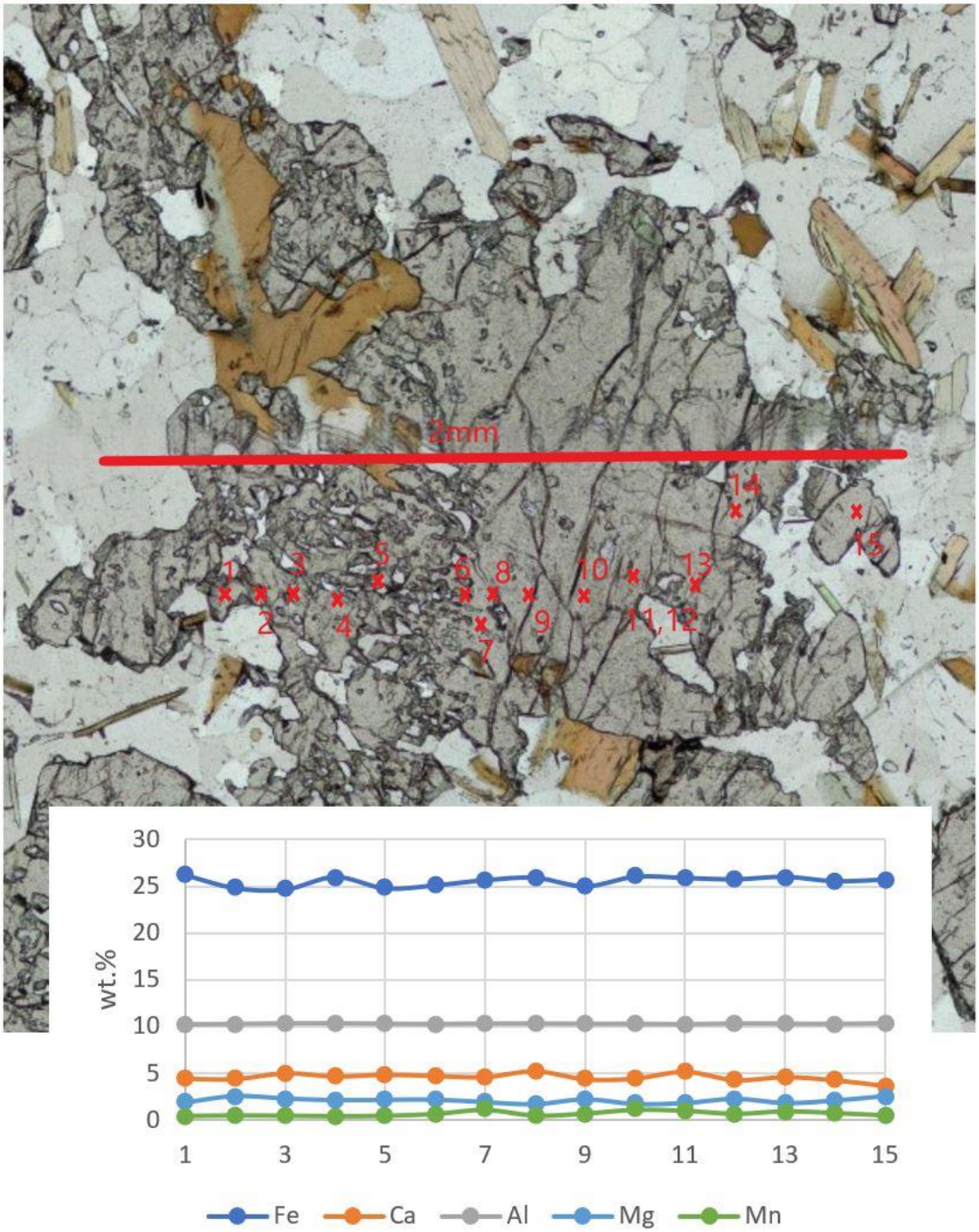

Figure 4-61 The garnet grain analysed in HF 91.00-91.20 to see if there is any zonation. The crosses represent the points analysed with the results in the graph below in wt%. The grain is about 2mm. No clear zonation was found in this garnet, and not in any other in this sample.

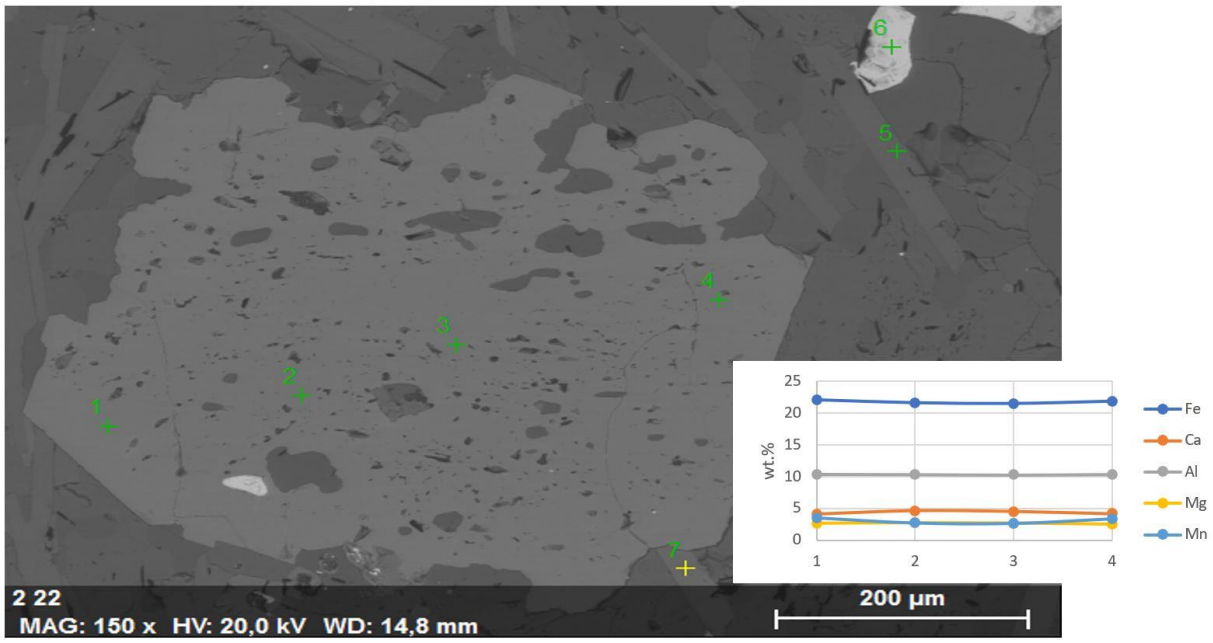

Figure 4-62 Secondary electron picture taken with SEM of the analysed garnet grain in sample HF 102.5. The results are in the graph shows the results. Mn and Ca show weak zonation while the other are the same through the whole grain.

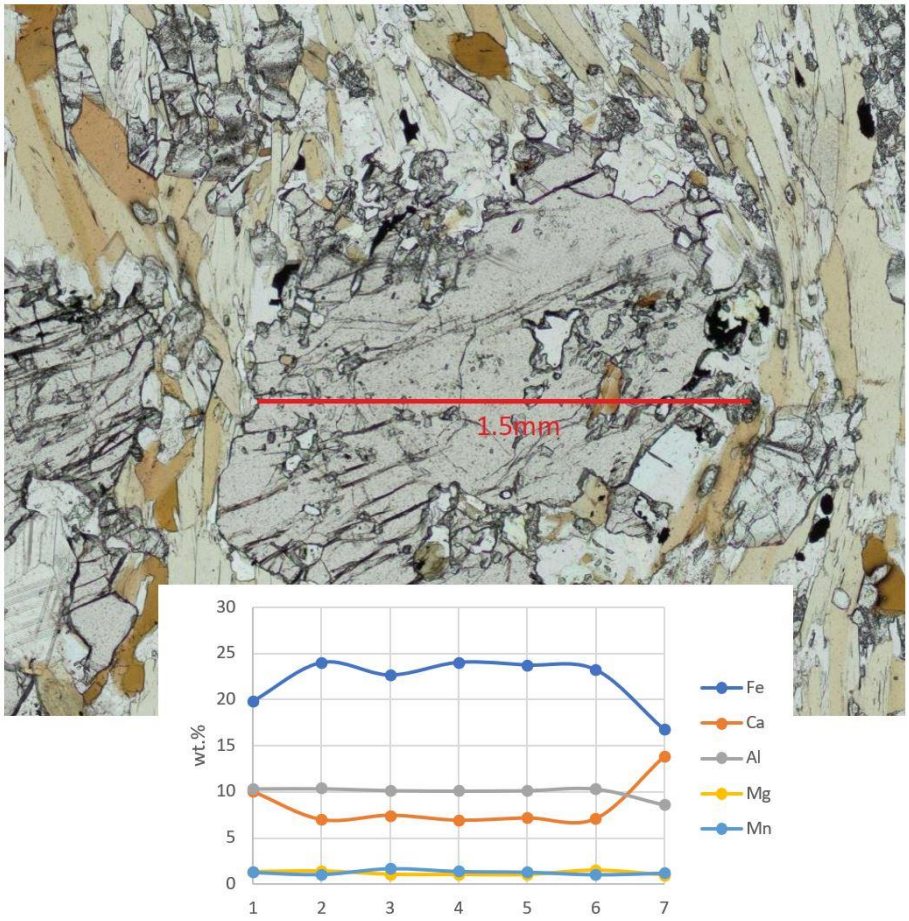

Figure 4-63 The garnet analysed with SEM in sample HF 141.5 with the results in the graph. In this grain is there a zonation with higher Ca at the rims compared with the core and the opposite for Fe.

Figure 4-61, Figure 4-62 and Figure 4-63 show garnets from HF-102, HF-91.00-91.20 and HF-141.5 that were analysed with several points throughout the whole grain to test for zonation. In Figure 4-61 is the garnet that was analysed in HF-91.00-91.20 together with a graph with the results. There is not any significant chemical zonation of this garnet grain or any other measured in this sample.

The grain of garnet tested in HF-102.9 are the points called 2-1 to 2-4 in in Table 1 in Appendix F, SEM-picture in Figure 4-62 with the points plotted and the results in a graph. The analyses show that Mn contents at the rim are slightly higher compared to the core and the opposite for Ca. The other elements are about the same throughout the whole grain.

The garnet analysed in HF-141.5 in Figure 4-63 has the numbers 4,2-1 to 4,2-7 in Table 3 in Appendix F. Here Fe and Ca are chemically zoned. The iron content is higher in the middle than at the rims. It goes from around 16wt.% in the rims and up to 24wt.% in the core. Ca is 10-13wt.% at the rims and around 6-7% in the core. The other elements are constant throughout the grain. This chemical zonation is found in only one of the analysed samples, so what this tells about the ore-forming process or the history of the area is hard to say. But if this zonation is to be found other places, then it can tell us something about the ore-forming event. These garnets are hard to see in hand specimen because of its light colour due to high Ca content and small size. The grain analysed has a zonation with lower Fe-content at the rims compared to the core and the opposite for Ca. So here has Ca and Fe has diffused in the X site to maintain the stoichiometry and this is called major element diffusion, since EPMA analyses has not been done is it unknown if there are zonation on the trace element level (Auge and Carlson, 2014). This zonation is a normal zonation with Ca-enriched borders. Normally would also Mn show the same pattern, but this is not the case here. The zonation pattern may be caused by a sudden increase in temperature and the crystal may start to grow again or it may be because of change in P and/or T conditions that causes resorption and the Ca is re-entering the garnet. This is observed in rocks where the Ca content is low (Ruiz, 1977) and references therein. The area has been through deformation after metamorphism, so this last growth episode with Ca-enrichment may have happened then.

Biotite

Biotite is present almost everywhere in the drill core, but in a lesser amount when approaching the ore-zone. In Table 4, 5 and 6 in Appendix F the results of biotite and sericite analysis are summarised. Table 12 and summarises the analytical results for biotite and sericite. The iron-content is highest in the sample farthest away from the ore zone (14.24-14.40) falling at 15wt.% and significantly lower in the sample above the ore zone with an average of 10wt.%. Only one sample of biotite was analysed below the ore-zone and having 13wt.% Fe. Mg contents are slightly higher in HF91.00-91.20 and HF-102.9 with 7-8wt.% compared 4-5wt.% elsewhere.

Sericite was analysed in the samples closest to the ore zone and here we can see that the Al and Ba content is 1wt% higher above than below the ore zone, K, Mg and Fe is higher below.

Table 12 Average results of the SEM analyses of biotite and sericite.

	Biotite				Sericite		
Mbs.	14.25-14.40	91.00-91.20	102.9	141.5	Mbs.	102.9	141..5
O	26.40	27.07	26.95	25.02	O	27.64	27.98
Fe	15.37	13.995	10.42	13.49	Si	15.9	14.49
Si	13.17	13.22	13.23	12.57	Al	16.00	15.09
Al	8.39	8.58	8.66	7.12	K	7.38	8.49
Mg	5.82	6.48	7.84	4.78	Ba	1.58	0.74
K	7.73		0.33		Mg	0.9	1.37
Ti	1.25	7,13	6.86	7.33	Fe	0.9	2.01
Mn		1.6	1.02	1.3	Na	0.61	

Other minerals

Other minerals were analysed for simple identification purposes, not study zonation purposes. Amphibole, plagioclase, chlorite, calcite, and apatite were identified. All the results are listed in Table 7, 8, 9, 10, and 11 in Appendix F. In Table 13 and Table 14 are the results summarized.

Table 13 Average results of plagioclase, chlorite and amphibole from Hellerfjellet drill core.

Plagioclase					Chlorite		Amphibole-Hornblende		
Mbs.	14.25-14.40	91.00-91.20	102..9	141.5	Mbs.	102.9	Mbs.	14.25-14.40	91.00-91.20
O	26.56	26.735	27.305	24.36	O	29.24	O	27.42	27.742
Si	21.06	20.79	20.195	19.6	Al	16.15	Si	15.07	15.224
Al	10.5	11.41	12.035	9.19	Si	13.3	Fe	15.01	13.36
Na	4.66	4.38	3.99	4.04	Mg	4.56	Ca	8.56	8.67
Ca	3.32	4.655	5.9	4.84	Fe	3.22	Al	7.74	8.044
Fe	0.485				Na	1.16	Mg	4.07	4.61
K	2.16				Ca	0.98	Na	1.3	1.17

Table 14 Average result of calcite and apatite analysed with SEM.

Calcite				Apatite	
Mbs.	14.25-14.40	91.00-91.20	141.5	Mbs.	14.25-14.40
Ca	63,24	47,68	46,76	Ca	38.31
O	15,33	28,51	32,68	O	23.47
Fe	2,4	1,46	0,84	P	13.74
Mn	0,49			F	2.9
Mg		0,39			

Sulphides

Sulphides are limited to pyrrhotite, minor ilmenite and traces of chalcopyrite, sphalerite, and galena. Several grains of pyrrhotite were analysed and are listed in Table 15 and there are no significant differences throughout the core. One example of chalcopyrite was analysed in HF 91.00-91.20. And several grains of ilmenite in 14.25-14.40. All the analysis of the sulphides is listed in Table 12, 13 and 14 in Appendix F.

Table 15 Average results of the sulphides analysed with SEM in Hellerfjellet drill core; pyrrhotite, ilmenite and chalcopyrite.

Pyrrhotite					Ilmenite		Chalcopyrite	
Mbs.	14.25-14.40	91.00-91.20	102.9	141.5	Mbs.	14.25-14.40	Mbs.	91.00-91.20
Fe	54.49	54.02	54.54	53.19	Fe	37.94	Cu	30.75
S	29.67	29.35	29.65	22.74	Ti	33.86	Fe	27.6
					O	23.06	S	96.92

4.4.2 Massive and disseminated ore

All together 3 samples of ore from the prospects, one from each locality, and 3 sample of disseminated ore from each locality were analysed with SEM.

Pyrrhotite and pyrite

In Table 16 and Table 17 is the average results of the pyrite and pyrrhotite analysed. All the results are listed in Table 15, 16, 17 and 18 in Appendix F. The pyrrhotite has a slightly higher content of iron in Hesjelia compared with Hammertjønna. Hellerfjellet has about the same as Hammertjønna. The disseminated ore from Hellerfjellet has the highest iron-content of all the measured pyrrhotites, this is probably due to more oxidation of the massive ore samples. The pyrite is about the same in all samples where pyrite is analysed.

Table 16 Average SEM-results of the pyrrhotite analysed in the massive ore and disseminated ore from the Hesjelia and Hellerfjellet zone.

Pyrrhotite				
Sample	HES-04NGU	HAM-04NGU	HF-10NGU	HF-x18
Fe	49.38	46.985	45.05	52.76
S	29.57	34.01	33.84	28.84

Table 17 Average SEM-results of the pyrite analysed in the massive ore and disseminated ore from the Hesjelia and Hellerfjellet zone

Pyrite					
Sample	HES-04NGU	HAM-04NGU	HAM-B2	HS-5	HF-x18
Fe	39.845	38.56	41.465	40.38	39.12
S	39.795	37.49	41.523	40.02	37.76

Chalcopyrite

The average results of the analysed chalcopyrite are listed in Table 18 and the complete list of results are in Table 20 and 21 in Appendix F. The Cu content is about 1-2wt.% higher in the samples from the Hesjelia one than in Hellerfjellet in both disseminated ore and in massive ore. The Fe- content is about the same in all samples.

Table 18 The results of the SEM-analyses of chalcopyrite in the massive and disseminated ore.

Sample	HAM-04NGU	HES-04NGU	HF-10NGU*	HAM-B2	HF-x18
Cu	31.57	31.08	29.78	31.65	30.92
Fe	28.1	27.17	28.03	27.49	28.08
S	31.2	26.66	18.56	26.71	27.49

*small grain

Sphalerite

Sphalerite is to be found in the massive ore from all the different localities and in two of the sample of massive ore. The summary of the results is listed in Table 19 and the complete results are in Table 22, 23 and 24 in Appendix F. The sphalerite in the Hesjelia zone (HAM and HES) has about 2wt% more Zn in the Hellerfjellet zone (HF). In the disseminated ore is it 8wt.% more Zn in the sample from Hammertjønna than in the sample from Hellerfjellet.

Table 19 The results of the SEM-analyses done on the sphalerite in the massive and disseminated ore.

Sample	HAM-4NGU	HES-04NGU	HF-10NGU	HAM-B2	HF-x18
Zn	52.66	52.84	50.02	54.455	46.79
S	24.92	25.10	22.68	24.925	25.095
Fe	5.84	22.68	6.97	6.475	6.63
Mn					2.86

Galena

In Table 20 is the average contents in galena. Galena is about the same in samples of massive ore and slightly lower in the sample of disseminated ore. All the results of the analysis of galena is listed in Table 25 in Appendix F.

Table 20 The average content of galena from the massive and disseminated ore analysed with SEM.

Sample	HAM-04NGU	HF-10NGU	HAM-B2
Fe	88.73	86.26	86.12
S	10.07	9.50	10.01

Rutile and Magnetite

Rutile and magnetite were analysed in the disseminated ore from Hellerfjellet and the results are listed in Table 21. All results are listed in Table 26 and 27 in Appendix F.

Table 21 The results of rutile and magnetite analysed with SEM in the disseminated ore from Hellerfjellet.

Rutile		Magnetite	
Sample	HF-x18	Sample	HF-x18
Ti	62.00	Fe	53.36
O	28.65	O	28.88
Nb	0.92	Al	2.04
		Si	2.02
		S	1.04

Barite and celcian

Barite and celsian was found with SEM in the sample of massive ore from Hesjelia (HES-04NGU) and in the massive ore from Hellerfjellet. The average content is listed in Table 22 where we can see that the Barium content is higher in the celsian analysed in Hellerfjellet compared with Hesjelia. All the results are listed in Table 28 and 29 in Appendix F.

Table 22 Average content of barite and celsian in the massive ore.

Barite		Celsian		
Sample	HES-04NGU	Sample	HES-04NGU	HF-10NGU
Ba	54.52	Ba	28.64	34.48
O	13.44	O	18.2	18.29
S	11.59	Si	12.52	11.1
		Al	11.72	12.47
		K	1.705	

Other minerals in disseminated ore

In the disseminated ore was several minerals analysed for identification purpose and not for zonation. These are listed in Table 23, Table 24, and Table 25 where we mostly have silicates and one phosphate. The biotite from Hellerfjellet has lower Mg-content than in Hesjelia, but the Fe- and Ti- content is higher. All the results are listed in Table 30 to 37 in Appendix F.

Table 23 Average results of the content in biotite and sericite in the disseminated ore analysed with SEM.

Biotite			Sericite		
Sample	HF-x18	HS-5	Sample	HAM-B2	HF-x18
O	26.33	27.05	O	26.65	26.53
Si	13.54	14.26	Si	15.98	16.46
Mg	6.597	10.98	Al	14.38	14.24
Al	8.197	8.81	K	7.78	8.13
K	7.76	7.08	Mg	1.615	1.14
Fe	4.39	3.16	Fe	1.445	0.66
Ti	1.19	0.55	Ba	2.455	
			Ti		0.84

Table 24 Average content of K-feldspar and plagioclase in the disseminated ore analysed with SEM.

K-feldspar		Plagioclase		
Sample	HF-x18	Sample	HF-x18	HS-5
O	24.995	O	27.98	26.095
Si	21.36	Si	15.975	21.89
K	11.145	Al	15.32	10.32
Al	8.49	Ca	12.215	2.81
Ba	1.31	Na	1.135	5.12

Table 25 Summarized content of titanite, kyanite, hyalophane and apatite in the disseminated ore analysed with SEM.

Titanite		Kyanite		Hyalophane		Apatite	
Sample	HF-x18	Sample	Sample	Sample	HAM-B2	Sample	HF-x18
O	26.215	Al	27.93	Ca	24.285	Ca	38.10
Ti	22.92	O	26.84	O	20.34	O	23.49
Ca	19.48	Si	12.38	P	9.49	P	13.85
Si	10.33			F	8.97	F	1.99
Al	1.1			Ba	5.45		

5 Discussion

5.1 Origin of host rock(s)

The origin of the host rock is important information to better understand the origin and genesis of the ore-deposits. The host rock for the main mineralisation is the muscovite gneiss/ schist, but it is thought to be a result from alteration of the grey gneiss. (Bjerkgård *et al.*, 2013a)

The grey gneiss is the dominating rock type in the Mofjell group and the two studied areas in this thesis. There are several varieties, but they are assumed to be the same rock type because of similar chemistry and lithological setting. In the field, the grey gneiss may alternate between massive and schistose at the same outcrop. At Hellerfjellet weathered pits in the grey gneiss is observed, which indicates the presence of carbonate in the rock. This may be a sign of sedimentary input.

In the earliest studies the grey gneiss is thought to be dominantly sedimentary and the deposits to be sedimentary massive sulphide deposit. But the latest studies with field evidences and litogeochemistry has revealed that it is dominantly of volcanic origin (Bjerkgård *et al.*, 2013a).

The chemical analyses of samples from earlier studies and my samples of the grey gneiss support that most of the grey gneiss is volcanic because of the negative Eu-anomaly and the consistent trend in the REE's typical of acid volcanic rocks (Figure 4-53). The REE diagram shows that the grey gneiss is more enriched in LREE than HREE and has a negative Eu-anomaly. This and Al_2O_3 <15wt% is according to Defant and Drummond (1990) a typical pattern of volcanic rocks formed by partial melting of meta-basalts in the lower crust. The REE diagrams show that the host rock has similar trends as the host rocks in the Southern Altai Metallogenic Belt in China that is formed in an island arc setting (Wan, Zhang and Xiao, 2010).

In the MORB (Figure 4-53) normalized spider diagram the volcanic samples have a pattern typical for a volcanic arc setting; enrichment in K, Rb, Ba and Th and depletion in Nb, Ti and P (Bjerkgård *et al.*, 2013a). In the Ta vs Yb (Figure 4-52) granite classification diagram the grey gneiss plots in the volcanic arc granite field. In the AFM diagram (Figure 4-52) the grey gneiss plots on the boundary between tholeiitic and calc-alkaline with a tholeiitic trend. The Zr/Y ratio shows that it is from 2 to 8 with most samples in the tholeiitic group, a few in the transition group and two in the calc-alkaline group. Lentz (1998), and references therein, claims that the footwall and hanging wall often has different affinities, so the difference here may be because there are rocks from both hanging wall and footwall. The Hokuroko district, that has a lot of similarities with the Mofjell deposit, has variable Zr/Y ratio in both footwall and hanging wall. But samples from the footwall has a higher ratio (Table 9). This may mean that sample HF-02 and HS-3 are from the foot wall while the rest is from the hanging wall.

The spider diagram with grey gneiss normalized to the primitive mantle (Figure 4-53) (Taylor and McLennan, 1985) and the Ta vs Yb granite classification diagram (Figure 4-52) (Pearce, Harris and Tindle, 1984) shows similar trends as the Kuroko district that is

formed in a rifted mature intra-oceanic island-arc (Lentz, 1998) and as the host rock of the Keketale deposit in China (Wan, Zhang and Xiao, 2010).

The grey gneiss was until the late 90s thought to be of sedimentary origin (Larsen, Bjergård and Moralev, 1995a). However, extensive lithogeochemistry carried out during fieldwork in the Mofjellet area in 2008-2009, showed that the grey gneiss mainly is of volcanic origin (Bjerkgård *et al.*, 2013a; 2013b). As discussed over; is this rock unit derived from an island-arc setting. From the bedrock maps (Mo i Rana and Storakersvatnet) in the area (Marker *et al.*, 2012; Søvegjarto *et al.*, 1988) can extensive units of amphibolite bee seen throughout the Mofjell group. These have been analysed by Bjerkgård *et al.* (2013a) and this shows that they have a thoeleiitic composition and appears to originate for an island arc setting. Since there is both felsic- and mafic-vulcanites and sediments is this area considered as bimodal-felsic. It has a lot of similarities with the host rock to the Keketale VMS Pb-Zn deposit in the Southern Altai Metallogenic Belt in China (Wan, Zhang and Xiao, 2010) and the Hokuroko deposit in Japan(Yamada and Yoshida, 2011), which also was formed in an island arc setting. According to the classification of VMS-deposits, is it up to 15% siliciclastic components in this kind of settings (Barrie and Hannington, 1999). The sedimentary part of this unit is probably greywacke sediments with micas, graphite, quartz, carbonated and phenocrysts of feldspars. The graphitic part is observed close to the prospects at Hellerfjellet, while the other rock varieties is observed other places in Hellerfjellet deposit. In the Hesjelia deposit is it mostly massive examples of grey gneiss observed.

The muscovite gneiss is the host rock of the most extensive mineralisation and is suggested to be an alteration rock from grey gneiss or/and amphibolite (Bjerkgård *et al.*, 2013a). Ti-Al-Zr ternary diagrams (Figure 4-54) were created to compare the grey gneiss, amphibolite, and muscovite gneiss since those elements are immobile in hydrothermal and metamorphic processes. These plots manifest that the muscovite gneiss plots in the same area as the grey gneiss, some are closer to the average amphibolite, but the biggest amount lies is in the grey gneiss area. The plots reveal some variations, especially in the ternary diagram with all the variations of muscovite gneiss. This may be a sign of a source rock with varying content, as also recognized in the field. These results make it possible to say that the muscovite gneiss results from hydrothermal alteration of grey gneiss, and possibly some amphibolite. The alteration type is sericitic (phyllic) alteration.

In the isocon diagram in Figure 4-56 can the lost and gained elements as a result of alteration be estimated. Since the isocon has a slope of one is the mass (or volume) constant through the metasomatism. Only the most important ore-forming elements and associated elements (Pb, Zn, Cu, Ag, Mo, Ba) are clearly gained elements. There is an indication of a loss in MnO, CaO and Na_2O, and a small gain in MgO and K_2O and Cr. Those elements with a small gain and loss is probably within the isocon area and did not change very much. The gain in K_2O and Cr may be for the formation of sericite. According to (Bjerkgård and Bjørlykke, 1996) can this be called an almost isochemical process since the rock-forming elements content is about the same in the grey gneiss and the muscovite gneiss. In the REE chondrite normalized spider diagram (Figure 4-55) we can see that it generally is less REE in the muscovite gneiss compared to the grey gneiss, this is expected since they are mobile elements in a hydrothermal process and is leached out from the rock.

The REE chondrite normalized diagrams with the muscovite gneiss can be used as a complementary source to find the source of the rock type and also to find the process responsible for the alteration. The pattern of higher content in LREE compared with HREE and positive Eu anomaly is typical for reduces fluids and has probably not been in contact with seawater before deposition according to Bjerkgård *et al.* (2013a) referring to Spry, Peter and Slack (2000).

In conclusion, the muscovite gneiss results from sericitic (phyllic) alteration of grey gneiss by an infiltrating reduced fluid. The sericite is formed by replacing the plagioclase. The resulting rock is a muscovite gneiss/schist with major, but various amounts, quartz and sericite (muscovite), with minor biotite, plagioclase, garnet, and mineralisation. The graphite at Hellerfjellet may have been emplaced by the hydrothermal fluid, and this is also a sign of reducing conditions (Rumble III *et al.*, 1986).

5.2 The mineralisations

The ore in both the Hellerfjellet zone and in the Hesjelia zone appears in lenses and layers with various ore grades. In the Hellerfjellet zone is the lenses and layers observed with a thickness of up to 1.5 meters while in the Hesjelia zone it is up to 0.5 meters. The ore grade varies from disseminated to semi massive to massive. The massive ore in Hellerfjellet consist mainly of sphalerite and pyrrhotite with minor to accessory galena and chalcopyrite. Pyrite and/or pyrrhotite is the main in Hesjelia with sphalerite as major to minor, and galena and chalcopyrite as minor to accessory. The silicates in the ore is slightly different; in the Hellerfjellet zone the gangue minerals is mainly quartz, sericite, and graphite close to the prospects. In the Hesjelia zone it is different in the two outcropping areas; in Hesjelia it is mainly quartz and sericite, whereas in Hammertjønna is chlorite a common gangue together with quartz and sericite. This indicated that the fluids circulating the area are different from the Hesjelia zone to the Hellerfjellet zone.

The chemical analyses of the ores are used to compare the two mineralisations. One major difference is the iron content, which is higher in the Hesjelia zone. In the Cu, Pb, and Zn ternary classification diagram (Figure 4-57), the massive ore in the Hesjelia zone plots as a Zn-Cu type deposit closest to the Zn-corner. In the Hesjelia deposit is the ore in Hammertjønna richer in Zn compared to Hesjelia, and the opposite with Cu, so here we see a zonation. The massive ore from Hellerfjellet plots as a Zn-Pb-Cu and Pb type deposit, and very close to the Pb-Zn line, so the Cu content is low in both zones, but Pb content is higher in the Hellerfjellet zone and Zn is highest in the Hesjelia zone. From the portable XRF result from Hellerfjellet drill core is the average contents 0.047% Cu, 0.45% Zn and 0.08% Pb, with the most massive ore having 1.23% Zn, 0.35% Cu, 0.35% Pb, and 27 g/t Ag(Bjerkgård *et al.*, 2013a). From drilling in 1959 in Hesjelia was the average content analysed to be 0.25% Cu and 3.39% Zn (Kruse, 1980). In Hammertjønna drilling was conducted in the 1980s with a massive or of 3.3% Zn, 1.1% Pb, 0.4% Cu and 9 g/t Ag (Bjerkgård *et al.*, 2013a).

The Fe2O3 content in the massive ore in the Hellerfjellet zone is mostly below 10wt.%, while the Fe-content in the massive ore from the Hesjelia zone is between 7 and 41wt.% with an average of 22wt.%. The Zn-content is high in the ore from both deposits with the highest average in the Hesjelia zone with 4.9wt% compared to 3.8wt% in the Hellerfjellet zone. The average of Cu in the Hellerfjellet zone is 0.21wt% and 0.33wt% in the Hesjelia zone. Pb is more abundant in the Hellerfjellet deposit, with an average of 1.89% compared to 0.0480% in the Hesjelia zone. Ag-content is highest in the Hellerfjellet with an average of 41 g/t, and 5 g/t in the Hesjelia zone. According to the result of the ICP

analyses of the samples from the prospects, and also the drill cores, the Hesjelia zone appears to be the richest zone. The Hellerfjellet zone is richest in Pb and Ag, but the Hesjelia zone is richest in the other metals.

In the REE chondrite normalized spider diagram (Figure 4-59) (McDonough and Sun, 1995) the massive ore from both zones show the same trend with a weak decrease for the LREE and flat HREE, except that the Hesjelia zone show a positive Sm- and Eu-anomaly. The positive Sm and Eu anomaly observed in the Hesjelia zone is not seen before and is unique for the Hesjelia zone. Hellerfjellet does not have the same trends. The positive Eu anomaly is a typical sign of interaction with hot (>200°C), reduced hydrothermal fluid (MacRae *et al.*, 1992), or with greenschist facies metamorphism (Schwinn and Markl, 2005). Literature of other VMS deposits with positive Sm anomaly has not been found. But Bossart and Milnes (2017) reports positive Sm anomaly in a gouge infilling in a fault and claim that this has not been reported in pure minerals before. They claim that a positive Sm-anomaly cannot form in a closed chemical system and suggests that it may be from fluids that have interacted with organic matter. This may also be the case here, i.e. that the hydrothermal fluids interacted with organic matter in the sediments before or during deposition of the metals. Since we do not see this trend in the Hellerfjellet zone is it a strong indication of two different ore-forming fluids in the two zones, and by that we have two different systems.

The source of the metals could be the grey gneiss because it contains an elevated concentration of economic elements. One method to check this is by comparing the ratio between the metals in the grey gneiss and in the ore. The similar ratio between the metals (Cu, Pb, Zn, REE) in the ore and the grey gneiss indicates that most of the metals in the ore are derived from the grey gneiss, at least in the Hellerfjellet zone. Pb in the Hesjelia zone has another ratio than the others and may be of another source than the grey gneiss. The amphibolite may be the source for the metals not found in the Grey gneiss. According to Large (1992) may the magma chamber causing the heat and volcanism in the area be a source of volatile elements and fluid together with the other fluid circulating the area. Some metals may come directly from the magma chamber by fractionation.

The most important ore-forming metals, Zn, Pb, Cu, Ag, and Fe, is occurring mainly in the sphalerite (Zn), galena (Pb), chalcopyrite (Cu) and pyrite/ pyrrhotite (Fe). Correlation of the metals in the massive ore are presented in (Figure 4-60). Important minor element in the sulphide minerals were supposed to be analysed with EPMA, but because of COVID-19 analysis had to be cancelled.

Zink (Zn) is the dominating economic metal in both deposits. In the Hesjelia zone the massive ore has 1.9-12wt% and 0.3-7wt% in the Hellerfjellet zone. Zinc follows Cu and Se in the Hesjelia zone, and Ag, Au, Bi, Mo, Pb, and Se in the Hellerfjellet zone. Zn and Pb are the main constituents in sphalerite and galena, so they were probably deposited at the same time at Hellerfjellet. Whereas, in the Hesjelia zone sphalerite and chalcopyrite may have been deposited at the same time. In Figure 5-1 below is the Cu-, Zn- and Se-content from the massive ore in the prospects in the Hesjelia zone plotted together. Here we can see that they actually do correlate. According to Huston *et al.* (1995) is copper often present in the sphalerites lattice in VMS deposits, so the correlation may be because of that. Also, some chalcopyrite may be an exsolution from sphalerite happening during the metamorphism. Chalcopyrite is often occurring as inclusion in the sphalerite. The remaining elements probably constitutes tellurides,

sulfosalts, and/or fahlore minerals that have been reported from the area by Bjerkgård *et al.* (2009). Freibergite is an important silver bearing phase.

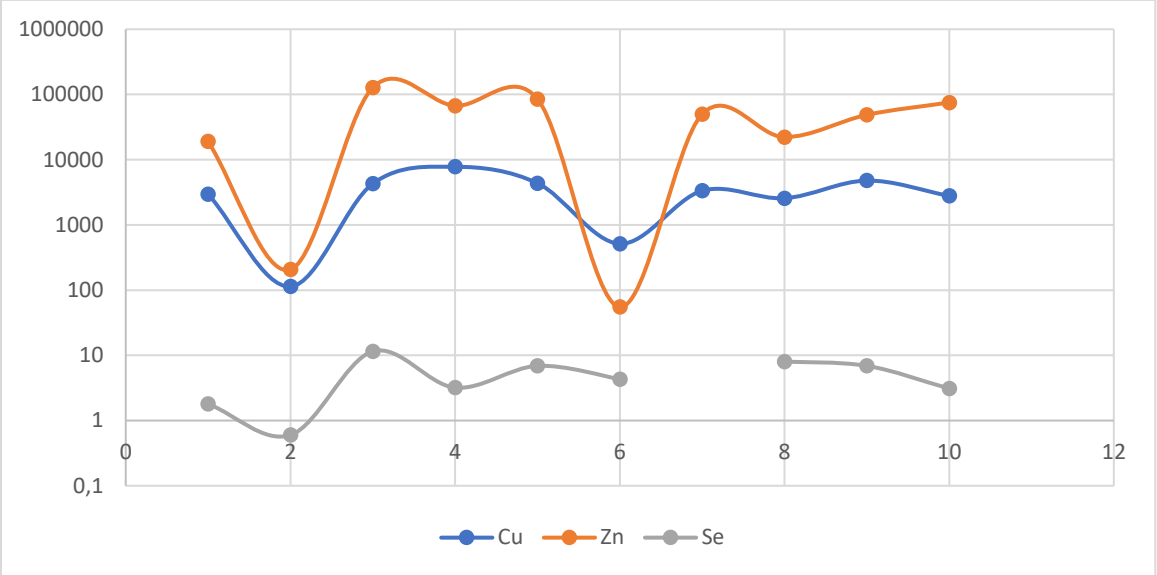

Figure 5-1 The Cu-, Zn- and Se- content in the massive ore from the prospects in the Hesjelia zone. Can see that they actually correlate.

Lead (Pb) is the main constituent in galena and correlates well with Ag, Bi, and Sb and a has a negative correlation with Se in the Hesjelia zone. In the Hellerfjellet zone it correlates with Ag, Au, Bi, Mo, Ab, Se, and Zn. Bi is a common impurity in galena (HudsonInstituteOfMineralogy., n.d.-b), so it may be a part of the atomic lattice structure. The rest of the elements are probably constituting tellurides, sulfosalts, or fahlore minerals. Sb is negatively correlated with Pb, so this is probably deposited at a different time in the ore-forming process. Pb in the Hellerfjellet zone has an average of 1947ppm with the highest value of 4.4wt%. In the Hesjelia zone the average is 1462ppm and the maximum value is 2wt%.

Silver (Ag) is well correlated with Au, Cu, Pb, and Sb in the Hesjelia zone. In the Hellerfjellet zone it correlates with Mo, Pb, Sb, Se, and Zn. Freibergite was analysed with SEM, and it appeared that this important Ag-host lies as inclusions in galena. The deposits have many similarities with the Bleikvassli deposit and there it was estimated that about 40% of the Ag in the ore is present in the Galena's lattice whereas Freibergite in galena formed during regional metamorphism in the early stage of the Caledonian orogeny(Cook *et al.*, 1998). According to Bjerkgård *et al.* (2013a) it is common for Ag to be lattice-bound in the main sulphides, especially galena, but it may also be present in pyrite, pyrrhotite, chalcopyrite and sphalerite in minor amounts.

Barium (Ba) contents are very high in both the alteration and mineralized zones and is thought to be an element deposited during hydrothermal alteration. Barite and celcian feldspar is observed and analysed with SEM, hyalophane is observed in the Hesjelia zone by Bjerkgård *et al.* (2013a). Values up to 8wt% Ba is present in samples from Hellerfjellet and up to 4wt% in the Hesjelia zone. Barite is according to Lydon (1984) a common gangue mineral that may co-precipitate with the sulphides.

N*ickel (Ni)* is according to the isocon diagram an element that has been gained from grey gneiss to the muscovite gneiss and is found both in the muscovite gneiss/ schist and in the ore zone. It is a common constituent in both pyrrhotite and pyrite

(HudsonInstituteOfMineralogy, n.d.; HudsonInstituteOfMineralogy., n.d.-a). The maximum analysed values are 118ppm the Hellerfjellet zone and 32ppm in the Hesjelia zone. Breithaupite (NiSb) was found in samples from Hellerfjellet by Bjerkgård *et al.* (2013a).

From this we can see that the most important ore-forming elements follow each other and are most likely deposited at the same time and in the same process together with sulphosalts, tellurides and fahlore minerals. Those may have been exsolutions from the other minerals during metamorphism, but this has not been studied very much in this thesis.

Similar deposits

As already discussed, the deposits have several similarities with the *Keketale deposit* in China. The host rock to the *Keketale Pb-Zn deposit* is meta-sedimentary rocks alternating with volcanic rocks. The REE chondrite normalized spider diagram, and the MORB normalized spider diagram from the unaltered volcanic host rock in the Keketale has about the same trend as for the grey gneiss in the Mofjell group (see Figure 5-2). They also plot in the same field in the Ta vs Yb granite classification diagram (Wan, Zhang and Xiao, 2010). The Keketale deposit seems to have more sedimentary rocks than the Mofjell group. As in the Hesjelia zone, the pyrite occurs as idiomorphic grain and hypidiomorphic granular aggregates, somewhere together with pyrrhotite. Sphalerite and pyrrhotite occurs as xenomorphic aggregates and appear as a matrix for pyrite. Cu is rare in the Keketale deposit as it also is in the Mofjell deposits. The host rock in Keketale has the same signature as in Mofjell, and the ore is very similar.

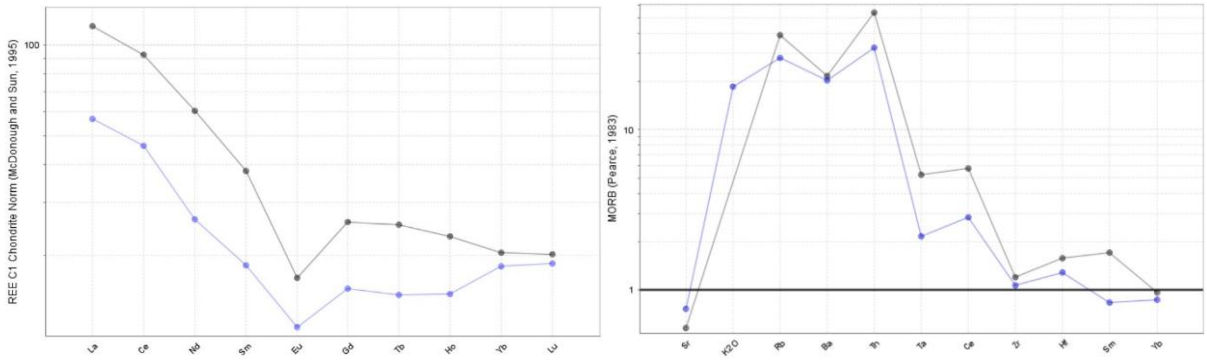

Figure 5-2 REE chondrite normalized and MORB normalized diagrams (McDonough and Sun, 1995; Pearce, 1983) with the average meta-sedimentary and meta-volcanic rocks from the Keketale (black) deposit and average grey gneiss in the Mofjell group (blue).

Several large VMS deposits, including the world-class *Brunswick No. 12* are deposited in the Middle Ordovician bimodal volcanic and sedimentary sequence in the northern Appalachians of New Brunswick, Canada. The No.12 deposit is emplaced within an intra-continental back-arc basin. The sedimentary rocks are continentally derived comprising, among others, quartzite, siltstone, and black shale. This is probably what the sedimentary part of the grey gneiss in the Mofjell group constitutes, and the graphite at Hellerfjellet may be derived from organic-rich black shales. Brunswick is a part of the Appalachian Mountains that has been a part of the same Palaeozoic belt as the Caledonian mountains. Brunswick occur in the Appalachian Mountain chain that essentially is the southern continuation of the Caledonian orogeny. The deposits and the host rock in the Mofjell Group apparently formed at the same conditions and was deposited during the same time range during closure of the Iapetus ocean. The average

content of the ore forming metals is not very different from what we see in the massive ore in Mofjellet; Brunswick have 10,4% Zn, 4.2% Pb, 0,34% Cu, and 115 g/t Ag, the highest found in the Hesjelia and Hellerfjellet deposit is 12.73% Zn, 4.44% Pb, 0.78 Cu and 60 ppm Ag.

The two zones have many similarities with the *Bleikvassli* Zn-Pb-Cu deposit that lies 50 km south of Mo i Rana, and that also in the Rödningfjëll nappe complex. It is now defined as a VMS-deposit, but it was a long time defined as a sediment hosted exhalative massive sulphide deposit. The description of the host rocks has many similarities with those in the Hesjelia and Hammertjønna zone. The ore lies in a quartz-muscovite schist in lenses with a total length of at least 1500 meters and two outcropping lenses 400 meters apart along the strike. The ore consists dominantly of pyrite and pyrrhotite in layers, with a variable amount of galena, sphalerite and chalcopyrite (Skauli, 1993). The host rock is mostly meta-vulcanites and meta-sediments, as in the Hesjelia and Hellerfjellet zones (Bjerkgård, Larsen and Marker, 1997). Since the mineralogy is very similar, the host rock may be from the same regime.

In conclusion, the Hellerfjellet and Hesjelia deposits are formed in the same type of regime as Keketale, Brunswick and Bleikvassli, but not at the exact same lithological setting. Keketale and Brunswick and probably also Bleikvassli, are deposited in a back-arc basin, whereas the Mofjell Group is deposited in an island arc. The Hellerfjellet deposit appears to have more meta-sedimentary rocks compared to the Hesjelia zone, so it is might deposited in the back-arc basin as well.

5.3 Zonation pattern

Another goal was to unravel mineralogical or chemical zonation pattern associated with the mineralising process. Zonation has been searched for with SEM in different minerals, portable XRF in the drill core and in the whole rock litogeochemical results.

In the Hesjelia zone, the metal content in the massive and disseminated ore differs from Hesjelia to Hammertjønna. According to the ternary Cu, Pb and Zn triangular plot in Figure 4-57 is the Hesjelia deposit is richer in Zn and Cu. The Hammertjønna deposit is also rich in Zn, but it contains more Pb compared to Hesjelia. This is a lateral zonation. The disseminated ore from both areas plots in the Zn-Cu field and in the Zn-Pb-Cu field, so the disseminated ore appears to be richer in both Cu and Pb compared with the massive ore. This zonation may indicate that we are in different parts of the same VMS stockwork since the chemistry is the same in other elements but the ore forming metals. Hammertjønna with chlorite in the matrix may be further down in the stockwork if we think of a classic VMS deposit while Hesjelia is further up.

Barium is an abundant element in both zones and is an element that is associated with hydrothermal deposits. Often it is high close to and in the mineralized zones, so it might be an element to use to find the ore. The drill core from Hellerfjellet was analysed with the portable XRF, a few meters above and below the ore zone was analysed to see if any zonation could be reviled. No clear zonation was recorded close to the ore, only the barium content seems to increase with some ppm's when approaching the ore zone and the Fe content decrease slightly. If a pattern was to be found, then it would a been a good indicator to use to find the ore. Change in Ca and K toward the ore zone has not to be seen, but in the ore zone it generally is lower than outside. If analyses were done a few meters more from the ore zone, then it might would have reviled a clearer zonation pattern. From the chemical results is high barium-content found in both the mineralized

zones (0.4-1.6% Ba) and the muscovite gneiss (0.02-1.8% Ba). The grey gneiss has 0.01-0.03% Ba.

In the Hesjelia zone is it a more obvious difference between the mineralized zones and the not mineralized zones. From the chemical results is barium content analysed to be 0.7 to 3.1% in the mineralized zone, 0.03 to 4.4% in the disseminated ore, 0.01 to 1.4% in the muscovite gneiss, and 0.04 to 0.8% in the grey gneiss is from 0.04 to 0.08%. In earlier studies by Bjerkgård *et al.* (2013a) was the area analysed with a portable XRF in the field, from this they found a barium halo up to 0.5 meters in the main mineralisation zone with values of 0.1-0.3% Ba at Hammertjønna. In the drill core drilled in 2008 in between Hesjelia and Hammertjønna was a barium halo found beneath the richest zone of mineralisation.

The Barium content can probably be uses as an element that leads us to the ore, at least in the Hesjelia zone. A halo of barium has been identified around the ore zone in both the drill core and in the field, and it appears to be highest below the mineralized zone according to the analyses from the drill core. This may vary if the area is folded and deformed. In the Hellerfjellet zone is the Barium content high in both the mineralized zone and in the muscovite gneiss, so it may be difficult to use it as a guide for where the ore is.

SEM analyses was conducted on the minerals to try find chemical differences between the two zones and in the drill core at Hellerfjellet. In Hellerfjellet drill core was mainly garnet and biotite analysed to see if there are any differences when we come closer to the ore zone. The *Biotite* results are listed in Table 12 and from these results can we see that the Fe content is less in the altered rock close to the ore zone. K content is highest (7.73wt% vs 0.33%) far away from the ore and Ti is high (6.86-7.33wt%) near the ore and low (1.25wt%) in the grey gneiss furthest away. This is probably because of leaching and infiltration from the fluid that circulated the area. Some elements are lost to make other minerals, i.e. garnet and muscovite, while some are gained from the metal rich fluid, i.e. Ti.

Garnet is the most important mineral analysed for zonation in this thesis, and it is a result of metamorphism. It can be used to find age, duration and rates of the processes or conditions at which the garnet was made. The garnet can be formed in a wide range of pressure, temperature and composition conditions and the thermodynamics controlling it is well understood. It can be used to record the metamorphic condition whether prograde or retrograde. The age and chemical zonation patterns spanning millions of years may be preserved in the garnet, so it is a very useful mineral to record the geological history of a lithology. (Baxter and Scherer, 2014)

In this thesis, the chemical zonation and textures of the garnets were studied. The SEM results showed that almandine garnets dominate. The colour changes from light red to a strong red colour to a very light red colour closer to the ore zone. This may result from changes in the Fe, Mg and Ca contents, where Fe-rich are dark red, Mg-rich are red and Ca-rich are paler and has a yellowish colour. From the SEM-analyses, the iron content is about 3-4wt% lower in the samples closest to the ore in the muscovite gneiss compared to the samples further away in the grey gneiss. The Ca content decrease closer to the ore and is 3wt% higher below the ore, Mn contents increase, and the Al content is about the same. So, from these results it seems likely that the Fe, Ca, and Mn content is the most important factor controlling the colour.

Chemical zonation through a garnet grain was only found in one sample from Hellerfjellet drill core, the other analysed samples did not show any zonation. Since only

one sample was found is there no point in discussing what this means since it is hard to know if it affected a bigger area or only this minor part of the area.

From the SEM analyses of biotite and garnet in the drill core is it a trend with more Fe-rich far away from the ore zone in the grey gneiss and less Fe when we come closer to the ore zone and into the alteration zone. This may be because the metals have been used to make the sulphides, so this might be a clue to a mineralization close by.

Barium is probably the most obvious element that has a zonation towards the ore, at least in the Hesjelia zone where there is found a 0.5 meters halo of barium around the massive ore. In Hellerfjellet may biotite and garnet be used as a clue for approaching the ore, but this needs more proof and moor investigation with different methods and on more samples.

5.4 Metamorphism

Regional metamorphism includes regional burial and regional dynamothermal metamorphism caused by later intrusions. Massive sulphides are often associated with large orogenic belts and by that it is common that it has been through regional metamorphism in some extent. Regional metamorphism may be responsible for changes in mineralogy and fabric, mobilization and concentration of minerals and elements and this can be an important factor in development of an economical interesting ore deposit (Vokes, 1969).

The area has been through regional metamorphism during the Caledonian orogenesis. The regional metamorphism of the RNC occurred at 464 ± 22 Ma by Cook (1993) is the early stages of the Caledonian orogenesis. The Bleikvassli area experienced peak-metamorphic conditions at 560-580°C and 7-9kbar (Cook, 1993). The metamorphic conditions of the Mofjell deposit has been analysed to have a peak of ~550°C and ~7kbar(Barrie *et al.*, 2010). Hellerfjellet and Hesjelia deposit are parts of the same nappe complex as Bleikvassli and Mofjell deposits and contains an amphibolite facies mineral assemblage and probably formed at comparable conditions. The metamorphic condition based on the temperature and pressure is (garnet-)amphibolite facies metamorphism following the Barrovian sequence (Figure 5-3). This, together with deformation, has modified the mineralogy to the host rock, ore, and alteration zone.

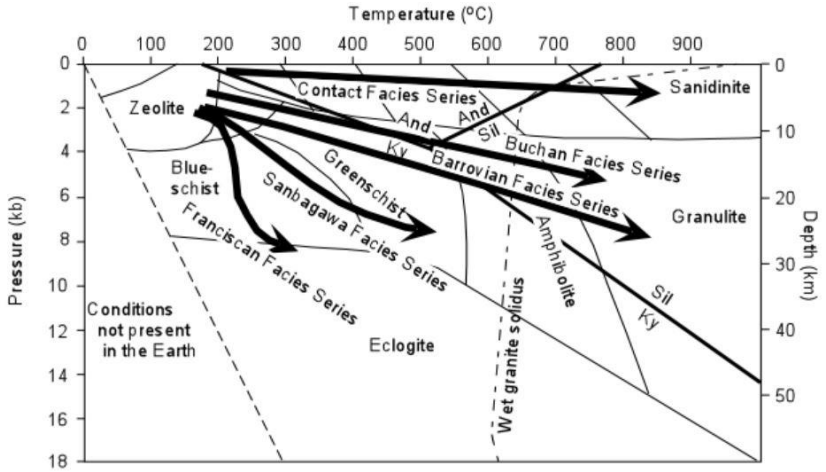

Figure 5-3 Metamorphic facies with temperature and pressure estimates. The regional metamorphism often follows the Barrovian facies series which is based on the regional metamorphism in the Appalachian Mountains. Figure from Nelson (2012).

The gangue minerals have a clearer metamorphic overprint with triple junctions, lepidoblastic micas, gneisses, graphite, garnet, kyanite and staurolite.

Graphite observed in Hellerfjellet formed during metamorphism of Carbon-rich sediments infiltrated by hydrothermal fluids (TheEditorOfEncyclopaediaBritannica, 1998). The graphite is observed as veins in the muscovite gneiss near the mineralisations at Hellerfjellet.

Garnet is a typical mineral that forms because of metamorphism, also in this case. It forms from stealing elements from the pre-existing minerals. The presence of garnets indicates a metamorphism up to amphibolite facies. Most examples of garnets have a sub- to euhedral (Figure 5-4) shape and has several inclusions. They are porphyroblasts and some are poikiloblasts. This is a mineral that is expected to form in Al-rich sites, but it may be difficult to complete the lattice if the Al-poor minerals are dominant and ends up as inclusions, this is called skelelat garnet (Mommio, n.d.-c). The inclusion is mostly quartz and some amphibole, staurolite has also been observed. The amphibole and staurolite as inclusions in garnets is probably a metamorphic phase. Zonation of the garnet has been observed in one sample from the drill core at Hellerfjellet. This zonation indicates that either the pressure or temperature increased after the first metamorphic top. The area has been through deformation after metamorphism, so it might result from this. Since different textures is observed it may indicate several growing phases, either several metamorphic events or prograde and retrograde metamorphism. Since some grains are following the foliation and some are not it is most likely two different metamorphic events forming the garnets. One before the deformation and making of the gneissic texture, and one post or syn deformation.

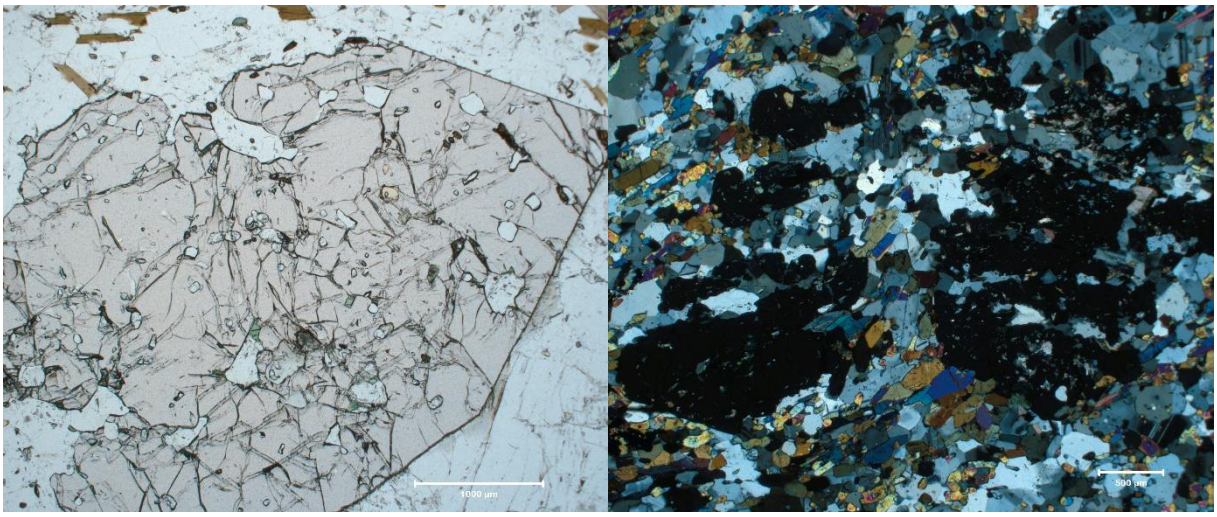

Figure 5-4 Garnets in the Hellerfjellet drill core, one example of a grain with a poikiloblastic structure and 4 perfect crystal phases (left, HF 55.40-55.55). The right picture is an example of a poikiloblast of garnet with no perfect crystal phases (HF 80.7-80.9) that follows the foliation in the sample.

Kyanite and staurolite are minerals that often occur together in the area and are thought to have formed during regional metamorphism. Staurolite is occurring in intermediate to high grade metamorphism while kyanite in medium to high pressure and low-to-moderate temperature based on the Barrovian type metamorphic sequence (Mommio, n.d.-d).

Triple junctions and cobble creep in the quartz (Figure 5-5) is observed in both the grey gneiss and the muscovite gneiss in both zones. It has experienced what is called slow grain boundary migration, and this is seen on the uneven boundaries between the grain and it looks like it is "eating" the other grain. This may be formed in lower amphibolite-facies conditions (Liebl *et al.*, 2007).

The gangue mineral assemblage and textures made by metamorphism fits with the temperature and pressure earlier estimated for this area. That is in the (garnet)-amphibolite facies with the peak metamorphism on 560-580°C and 7-9 kbar. The metamorphism was followed by extensive deformation as a part of the Caledonian orogeny.

Vokes (1963) has described the mineralogy and textures of the sulphides in the Bleikvassli deposit, and it has many of the same textures as in the Hellerfjellet and the Hesjelia deposit. In *the Hellerfjellet deposit* it is no euhedral grains of sulphides in the massive ore, it appears more as a matrix (Figure 5-5), also called xenomorphic or polymineralogic masses (Vokes, 1969). Only pyrrhotite may appear as subhedral grains with sphalerite as a matrix. Galena appears as infill between other minerals, both sulphides and gangue. Chalcopyrite appears in small amounts randomly throughout the ore and are probably remobilized and concentrated during metamorphism. It often occurs together with pyrrhotite and sphalerite. In the disseminated ore, euhedral grains of pyrite (Figure 5-6) are observed and the grains are aligned in the same direction as the foliation which is a result of the deformation.

Freibergite is observed in small amounts in the massive ore at Hellerfjellet (Figure 5-6) as inclusions in galena. Freibergite is also found in the Bleikvassli deposits associated with Galena, and galena is an Ag-carrier in the Bleikvassli deposit and it has been estimated that about 40% of the Ag is bound in the galena lattice (Cook, Spry and Vokes, 1998). Bjerkgård *et al.* (2013a) has reported the same in the Hellerfjellet deposit. Freibergite is a sulphosalt and formed during metamorphic recrystallization of galena (Cook, Spry and Vokes, 1998).

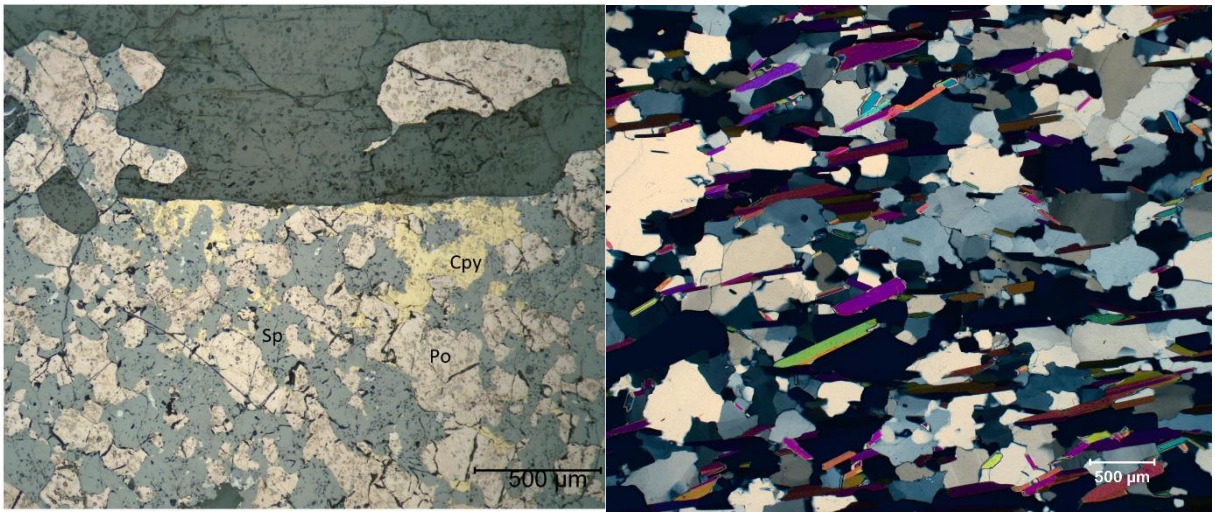

Figure 5-5 Sample of massive ore in Hellerfjellet (left, HF-7NGU) and muscovite gneiss from the Hesjelia zone (right, HAM-B7). In the massive ore can we see embayment and recrystallization of especially pyrrhotite. Pyrrhotite is showing crystal phases. In the

muscovite gneiss can recrystallization of quartz be observed because of the uneven boundaries and the weak undulose extinction.

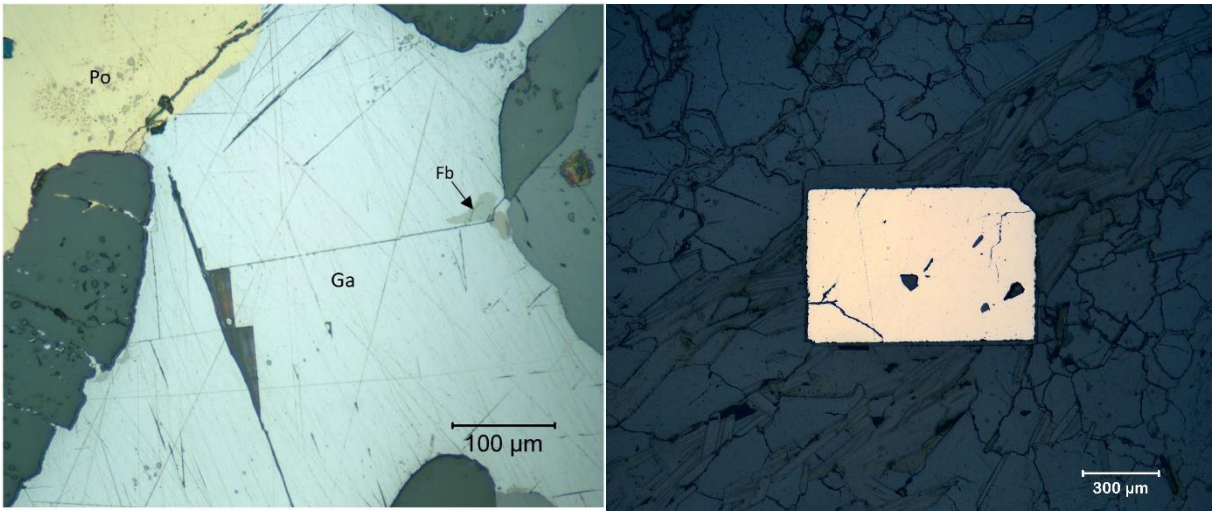

Figure 5-6 Example from massive ore (left, HF-7NGU) and disseminated ore (right, HF-x25) at Hellerfjellet. Galena with inclusion of freibergite. These two grains of galena and pyrrhotite is recrystallized since there are no inclusions in them. In the disseminated or is it a metablastic grain of pyrite that has recrystallized because of metamorphism and accomplished an almost perfect euhedral shape.

In the *Hesjelia deposit* we observe the same mineral assemblage in the massive ore, but here we also have pyrite. Pyrite is often observed as more euhedral and is bigger than the other minerals, this is probably because of metamorphism, and the pyrite is what is called idiomorph (Figure 5-7). The pyrite is metablastically recrystallized or form as exsolution from pyrrhotite. Exsolution from pyrrhotite to pyrite is according to Craig, Vaughan and Hagni (1981) a result of mixing of pyrite in pyrrhotite at ~400°C or higher T's. Subsequently, the pyrite exsolves during cooling below 400°C. It may also be annealing/ recrystallization that usually results in an increase in grain size and recrystallization to euhedral grains for high energy minerals, like pyrite. It is normal that high energy minerals, as pyrite, recrystallizes to get a higher contrast to the low energy matrix; galena, chalcopyrite, sphalerite and pyrrhotite. The resulting porphyroblasts of pyrite often have inclusions of sphalerite and gangue minerals (mostly quartz and sericite). The other sulphides do not have the same idomorphic tendencies as pyrite (Craig, Vaughan and Hagni, 1981; Vokes, 1969). Few pyrite grains have accomplished a perfect cubic crystal shape, but most are more subhedral with a few crystal phases others being anhedral. Pyrite often have the euhedral contact towards pyrrhotite and sub- anhedral contact towards the matrix. Inclusions in pyrite are probably trapped when the pyrite was recrystallizing. The presence of inclusions also supports crystal growth that leads to closing of embayment.

The disseminated ore in the Hesjelia zone mainly consists of pyrite (Figure 5-7). They have sub- to euhedral shape probably caused by recrystallization during metamorphism. The elongation of the crystals results from plastic deformation during the regional metamorphism where the pyrite has elongated in one direction.

To conclude, the massive and disseminated ore has been affected and modernised by the regional metamorphism in some degree. The pyrite is the most obvious sign of metamorphism in the massive ore and the size of pyrite is increasing with increasing

metamorphic grade. The softer matrix sulphides appear to have behaved ductile when the pyrite recrystallised and was remobilized and deformed at lower temperatures. The pyrrhotite has behaved less ductile than the sphalerite.

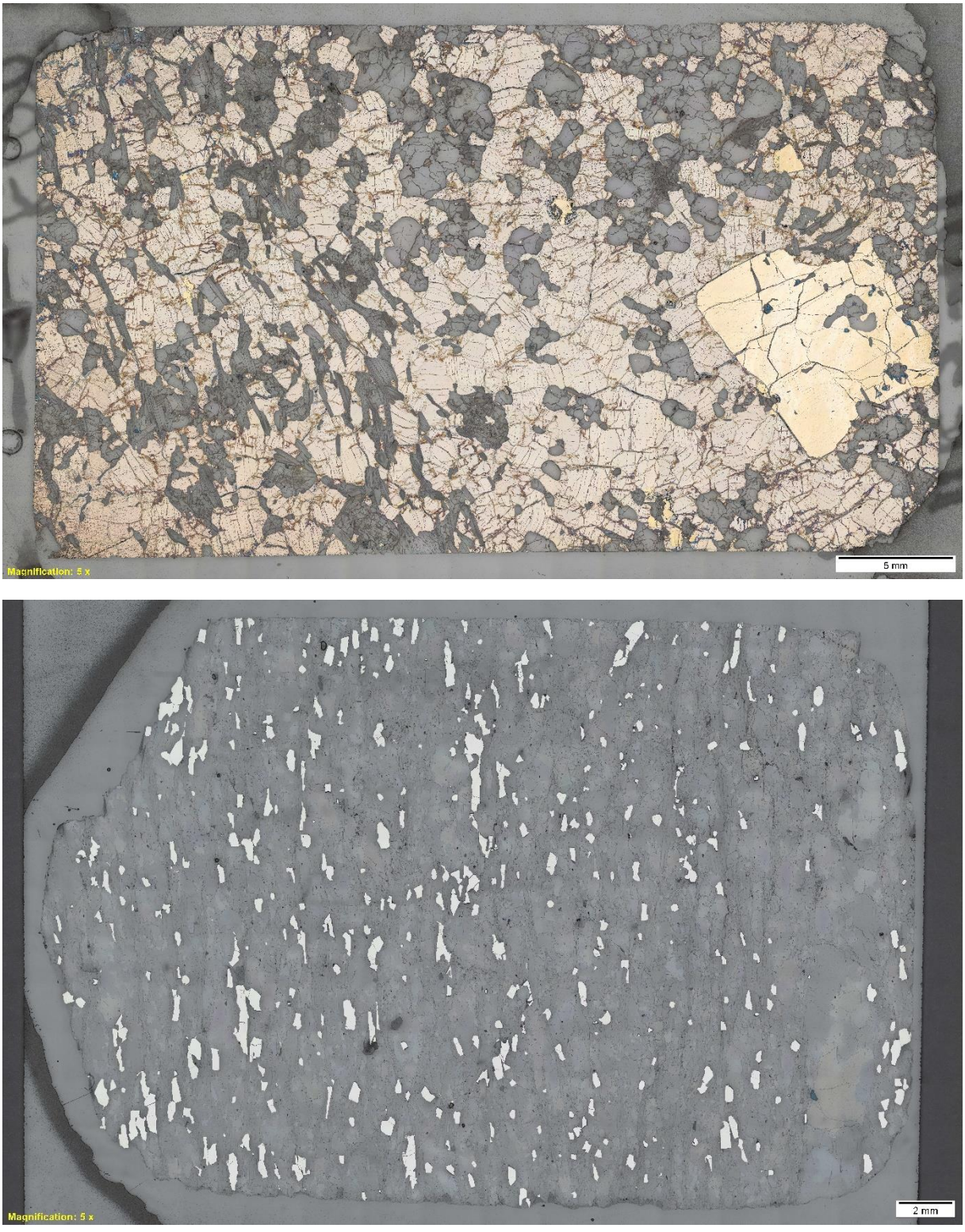

Figure 5-7 Sample of massive ore (upper, HES-01NGU) and disseminated ore (lower, HAM-B1) in the Hesjelia zone. Pyrite has formed metablasts because of metamorphism in a matrix of pyrrhotite. In the disseminated ore is the pyrite grains has lepidoblastic texture.

5.5 Connected or not

The Hellerfjellet and Hesjelia zone may or may not be connected, and one goal with this thesis is to unravel this possibility. This includes to assess if they are at the same structural/stratigraphic level and define the similarities and the differences between the two.

The *grey gneiss* in both zones has the same distribution in all the diagrams showing the chemistry. One sample from Hesjelia has another trend, and this is probably of sedimentary origin. The proportion of sedimentary rocks appears to be bigger in the Hellerfjellet zone in the field since graphite, carbonates and a meta-conglomerate has been observed in the grey gneiss unit. The grey gneiss in the Hesjelia zone is coarser grained compared to the Hellerfjellet zone and appears more massive, probably because of higher quartz contents or less mica. Since the chemical compositions compares well, it is possible that the grey gneiss unit in the Hellerfjellet zone and the Hesjelia zone has the same origin. I.e. an island-arc setting close to the continent characterized by bimodal-felsic volcanism and minor contributions of sedimentary siliciclastic rocks. They may be from different parts of the same unit but are most likely formed in the same volcanic system with a sedimentary influx from various sources.

The *muscovite gneiss* has been proved to result from the alteration of the grey gneiss by hydrothermal ore-forming solutions. The muscovite gneiss is generally coarser grained and more massive in the Hesjelia zone compared to the Hellerfjellet zone. The REE chondrite normalized spider diagrams in Figure 4-55 from both zones does not have all the same trends. The Hellerfjellet zone is flatter but has a weak enrichment in LREE compared to HREE, there is a weak decrease of the LREE while the HREE is rather flat. Some samples have a weak positive Eu-anomaly. The muscovite gneiss in the Hesjelia zone has a larger contrast between the LREE and HREE compared to the Hellerfjellet zone and has a stronger decrease of the LREE and a flat HREE pattern. It has both positive and negative Eu-anomalies, and this may be because those with negative anomalies are less altered. If the amount of the elements is considered, then the Hellerfjellet zone generally is richer in the REE and other ore-forming elements in the muscovite gneiss. Given these features, it appears that the two zones have been through slightly different alteration processes.

Type of alteration around the massive ore seems to be slightly different between the two deposits. In the Hellerfjellet deposit is appears to be sericitic (phyllic) alteration where sericite has replaced feldspars. In the Hesjelia zone, chlorite also occur in the alteration zone and in the matrix of the massive ore in the prospects at Hammertjønna. Chlorite is typically a part of the alteration mineral assemblage below the massive ore in a VMS body. While sericitic alteration is enveloping the chlorite alteration zone. This might mean that we have different chemistry of the fluids circulating the two areas, both are reduced, but with different content. Hesjelia and Hammertjønna are probably the same zone, but since chlorite only is observed at Hammertjønna are we probably in different part of the same VMS-deposit. If we consider the typical construction of a bimodal-felsic VMS-deposit in Figure 5-8are Hammertjønna in the lower lens closest to the chlorite alteration, while Hesjelia is further up in another lens.

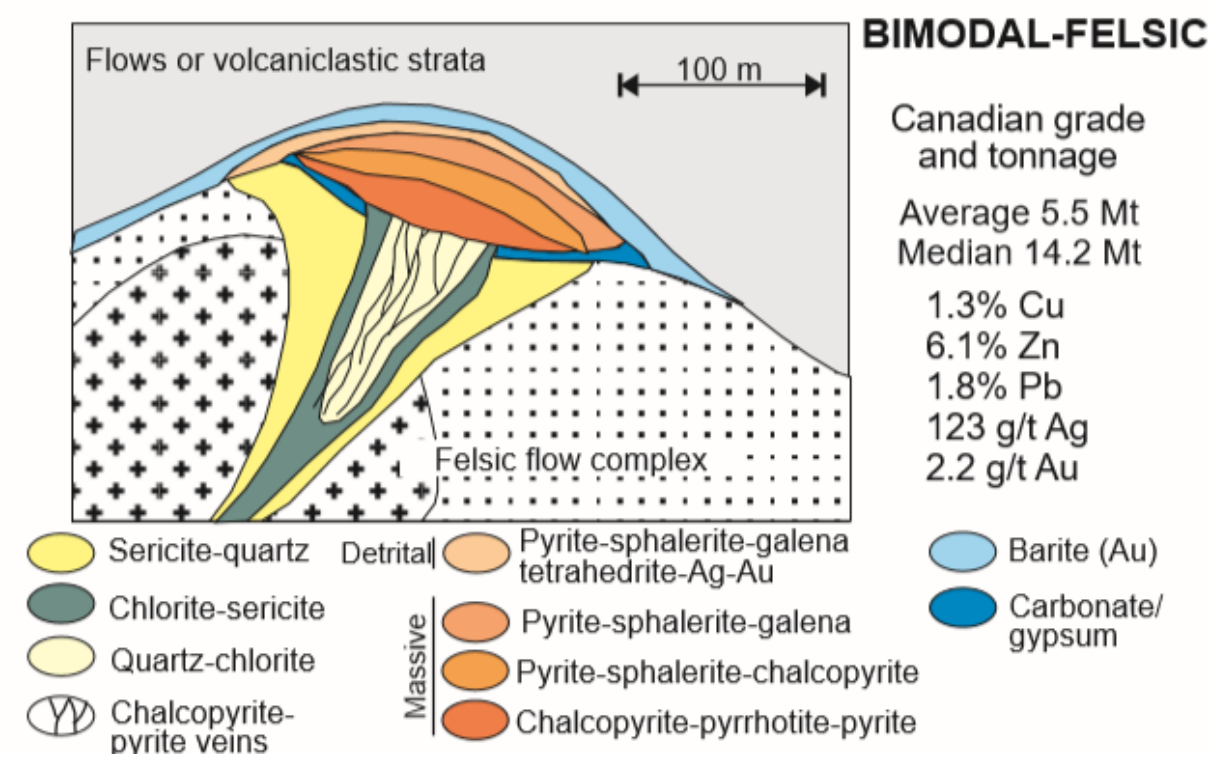

Figure 5-8 Figure 4 from Galley, Hannington and Jonasson (2007). The most important characteristics of a bimodal-felsic volcanic massive sulphide deposit with its average content in Canadian deposits.

The *massive and disseminated ore* in the two zones has differences and similarities both in the field and on the chemical results. The ore appears in lenses and in layers of different size and ore grade in both zones. The maximum thickness of the massive ore seen in the prospects is about 50 cm's in the Hesjelia zone and in the Hellerfjellet zone maximum 1.5m thick lens of massive ore is observed. In prospects at Hammertjønna chlorite is a part of the matrix, but this is not the case at Hellerfjellet. At Hellerfjellet there is muscovite schist with and without graphite, graphite is not observed in the Hesjelia zone. Pyrite is not observed in the massive ore at Hellerfjellet, pyrrhotite, and sphalerite is the main minerals. In the Hesjelia zone pyrite and/or pyrrhotite are the major minerals, sphalerite is major to minor. Galena and chalcopyrite are minor to accessory in both.

In the Cu, Pb and Zn ternary diagrams (Figure 4-57), Hellerfjellet, and Hesjelia follows different trends. The massive ore in Hellerfjellet plots in the Zn-Pb-Cu and Pb fields, while the massive ore from Hesjelia plots in the Zn-Cu field. The disseminated ore at Hellerfjellet plots mostly in the Zn-Pb-Cu field, while the Hesjelia zone plots in the Zn-Cu and the Zn-Pb-Cu field. In the diagrams in Figure 4-58 the most important metals are plotted for the massive ore samples. Here we can see that both zones contain high values of Fe and Zn, Hellerfjellet has higher contents of Pb compared to Hesjelia. From these graphs we can see that the Hesjelia zone has higher contents in both Zn and Fe and is probably a richer zone, but the Hellerfjellet zone seems to be a larger deposit from what is observed in the field. From the SEM-analyses of the sulphides in Chapter 4.4 are the amount of elements in the sulphides similar between the two zones. Since EPMA analyses were cancelled due to the COVID-19 pandemic, trace element data for the sulphide minerals could not be determined. These data could have provided in depth

knowledge of similarities and differences. However, the current confirms important similarities as well as differences between the two systems.

Why we generally see more pyrrhotite than pyrite and why we do not see pyrrhotite in the massive ore at Hellerfjellet is an interesting thing. This may be due to different fluid properties. The stability field of sulphides depends on temperature (T), salinity, oxygen fugacity ($f O_2$), pH and total sulphur content ($\sum S$) of the fluid. Often is the contact with seawater an important factor to change the fluids conditions and cause precipitation, but as pointed out earlier it is evidences that the fluid was not in contact with seawater. According to Large (1977) and references therein, the water has to be from at least 500m deep to prevent boiling on its way to the sea floor. Further, he proposes different conditions where copper, zinc, and lead can be carried as chlorite complexes in ore-forming solutions that also affect pyrite and pyrrhotite. He proposes two different environments; one with high temperature fluids (>270°C), low pH and H_2S is the dominant sulphur species–reducing conditions. The other is at high to low temperatures, acid to alkaline pH and SO_4, KSO_4 or HSO_4 are the dominant sulphur species. In the first environment may increase in pH and decrease in T cause precipitation of sphalerite and galena, while an increase in pH and change in $f O_2$ will cause precipitation of chalcopyrite. In number two will an increase in temperature make galena and sphalerite precipitate and increase in T, decrease in $f O_2$ and pH will make chalcopyrite precipitate. The deposits considered in this thesis will most likely correspond to environment one, since we know we have reducing conditions from the start. Chalcopyrite is a rare constitute in both deposits, so that may mean that the $f O_2$ did not change much before the ore was precipitated. Which means there was a change in temperature and pH that caused the ore to precipitate. Since the massive ore at Hellerfjellet does not have any pyrite, it may mean that the temperature and pH did not reach the right conditions for pyrite to form before precipitation. Since chalcopyrite is rare at Hellerfjellet, it may indicate that the $f O_2$ did not change enough for it to be a main mineral. For pyrrhotite and sphalerite to deposit and not pyrite and chalcopyrite, the $f O_2$ needs to be 10^{-44} or lower and temperatures above 230°C according to the diagram in Figure 5-9(Large, 1977). From thermodynamic studies done on Australian VMS deposits has the commo fluid temperature on Zn-Pb-rich deposits and Cu-poor deposits ranged from 175° to 235°C (Large (1992) and references therein), but this is with pyrite as a common mineral, but in the Mofjell deposit is the pyrrhotite dominant. So, the fluid temperature in the Mofjell deposits is most likely higher, at least in the Hellerfjellet deposit.

In the Hesjelia deposit we have pyrite in the massive ore, and we have more chalcopyrite. This indicates a fluid with slightly different properties, since both zones most likely was deposited by a reducing fluid is it other factors that plays a bigger role. Since we have pyrite and pyrrhotite together, the fluid had to be on the stability field of both pyrrhotite and pyrite, but since sphalerite and galena is a big constitute also here, it must have had the right conditions for them to precipitate as well. So, the properties of the ore-forming fluid in the Hesjelia zone may have been similar as those from the Australian VMS-deposits. Temperature ranging from 175°C to 235°C where we may have precipitation of pyrrhotite, pyrite, chalcopyrite, sphalerite and galena according to the stability diagram of iron-sulphides (Figure 5-9).

From the SEM-analyses of the massive and disseminated ore from each location is there not any significant differences in the sulphides. The pyrrhotite and pyrite composition is about the same, also between Hesjelia and Hammertjønna. The sphalerite shows 2 to 6wt% higher Zn in the Hesjelia zone compared to the Hellerfjellet zone, the same in

Hesjelia and Hammertjønna. The biotite in the Hellerfjellet zone has 4wt% less Mg than the Hesjelia zone. Plagioclase has higher content of Al and Ca in the Hellerfjellet zone, while Na is higher in the Hesjelia zone. The differences in the gangue indicates that there has been different fluid with slightly different properties infiltrating the areas.

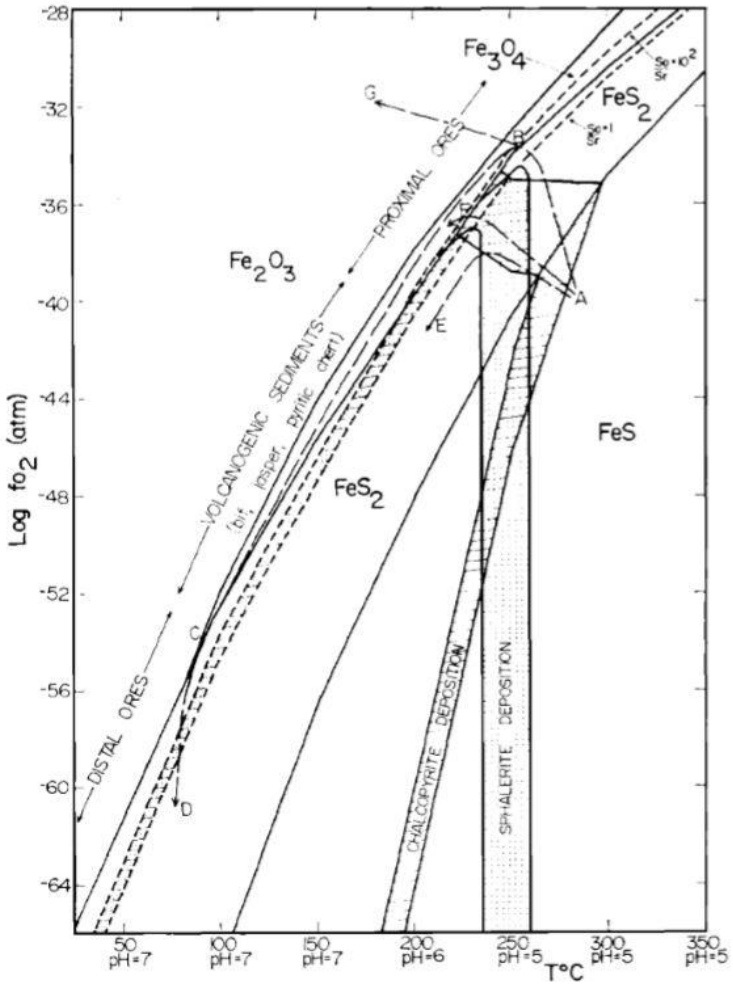

44

Figure 5-9 Stability of iron sulphides and oxides in the fO_2, temperature and pH range. From Large (1977).

Given the geographical separation of 15 kilometres in beeline they probably formed in two separate lenses with each their ore-forming stockwork. The outcropping mineralisations are most likely from different parts of the typical bimodal-felsic VMS deposit as seen in Figure 5-8. The figure is from Galley, Hannington and Jonasson (2007) and describes an idealized deposit and its associated stockwork zone. One suggestion is that the Hesjelia zone is from the chalcopyrite-pyrrhotite-pyrite part of the massive ore, since Hesjelia is richer in Cu and has pyrite in the massive ore compared with Hellerfjellet. Also, the alteration zone with chlorite is directly below that zone, and chlorite is only observed in the Hammertjønna zone. Lydon (1984) holds that the Cu content decrease and the Zn content increases when going from the proximal to the more distal parts of the stockwork. Accordingly, the prospects in the Hellerfjellet zone is the upper part of the massive sulphide lens with dominantly sphalerite, galena, and pyrite in this model. More studies are required to unravel this issue. Most likely,

Hellerfjellet and the Hesjelia zone are from two different VMS-lenses deposited in different parts of the same island arc system.

If the two zones are at the same structural level in unlikely. The grey gneiss appears to be of the same origin but does not have the same local properties. Generally, can we see that the Hellerfjellet zone has more sedimentary signature as observed in the field; carbonates, meta-conglomerates, graphite rich zones and more schistose. The Hesjelia zone has more massive appearance in the field with a few places that is more schistose. The Hesjelia zone is generally coarser grained and has less mica content. One explanation for this may be that the Hesjelia zone is deposited in the arc, whereas the Hellerfjellet zone is closer the back-arc basin.

5.6 Tectonic setting of the ore-forming process

VMS deposits are mostly formed in an extensional regime. As discussed further up, the deposits in the Hellerfjellet and Hesjelia zone are VMS-deposit that were emplaced in a bimodal volcanic and sedimentary rock assemblage. The host rocks has a volcanic arc signature and appears to have formed in an extensional back-arc regime associated with both felsic and mafic magma (Bjerkgård *et al.*, 2013a). The signature of the host rock is typical for volcanic rocks made by partial melting of metabasalts in the lower crust(Defant and Drummond, 1990).

According to the classification of VMS deposit based on lithology and tectonic setting, this is a bimodal-felsic type deposit made at the continental margin in an island arc and related back-arc or rifted volcanic arc setting. Several stratabound sulphide bodies are deposited in the Scandinavian Caledonides, both sedimentary hosted, volcanic hosted and mixed. All these were deposited during continental rifting or ocean floor spreading and in the beginning of plate convergence and ocean closure. There has been documented VMS deposits in four different paleotectonic environments in the Caledonides; ophiolites, immature arcs, mature arcs and mixed sedimentary-volcanic sequences (Grenne, Ihlen and Vokes, 1999).

The deposits in the Mofjell group are probably deposited in an immature arc in ocean-continent margin arcs and/or continental back-arc rifting system. This type of VMS deposits is related to tholeiitic and felsic volcanic rocks. The Stevenjokk deposit in the Køli nappe complex below the Rødningsfjell nappe complex is deposited in the same type of system. Stevenjokk is suggested to be from the Baltic margin. If we were to put it into the Caledonian orogeny, then it would fit well with beginning of plate convergence and ocean closure in the Ordovician period (Swinden *et al.*, 1990).

The Hellerfjellet zone appears to have more sedimentary rock assemblage than the Hesjelia zone, and this is interpreted to be because they are deposited in a different part of the system. The Hesjelia zone with its more massive signature, less mica and sedimentary input may be deposited in the volcanic arc. Whereas Hellerfjellet with its more sedimentary assemblage of meta-conglomerate, carbonate bearing grey gneiss and graphite-rich muscovite gneiss is deposited in the basin. Keketale and Brunswick deposits have the same host lithologies as Hesjelia and Hellerfjellet zone, and they were emplaced in a back-arc basins. They appear to have more sedimentary rocks, so the deposits in the Mofjell group might be deposited close to or in the volcanic arc.

Bleikvassli has many similarities with the deposits in the Mofjell group and is probably deposited in the same regime. According to Bjerkgård, Larsen and Marker (1997)the

amphibolites in the Mofjell group has an island-arc signature while amphibolites in the Bleikvassli area is closer to MORB composition, so this might mean that the Bleikvassli deposit is formed in the basin while the Mofjell group is closer to and in the island arc. A possible paleotectonic setting for the Hellerfjellet and Hesjelia together with Bleikvassli deposit is in Figure 5-10. Here is the Hesjelia deposit placed in the volcanic arc, but close to the basin since it has some sedimentary input. The Hellerfjellet deposit is placed in the bac-arc basin, but close to the volcanic arc since there is a lot of vulcanites and the amphibolite has an island-arc signature. Bleikvassli is placed on the other side of the basin because it is far away from the other two deposits and the amphibolite has a MORBs signature, and it has some sedimentary input. This is probably deposited on the Laurentian margin since this is placed in the uppermost allochthon.

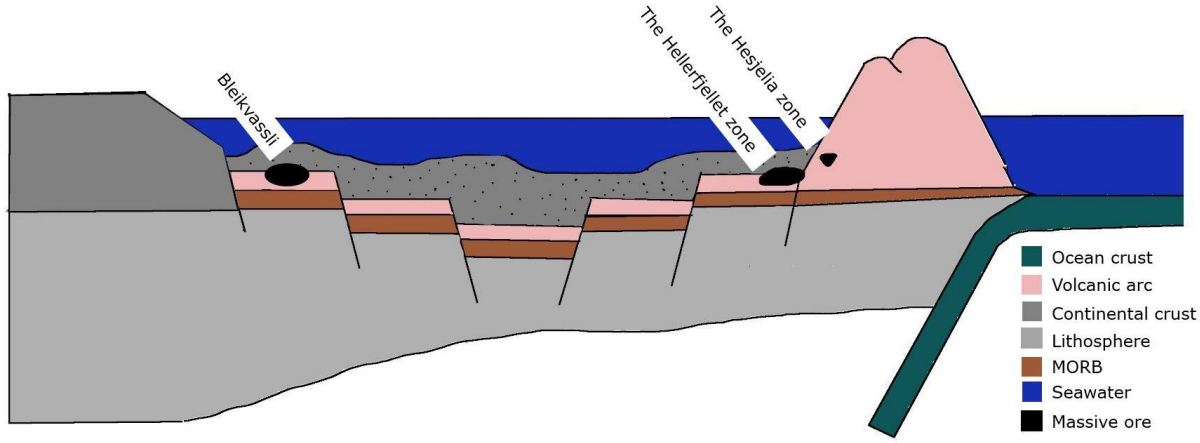

Figure 5-10 Paleotectonic model of how the Hellerfjellet and the Hesjelia zone togheter with the Bleikvassli deposit might be deposited. The Hesjelia zone has more sedimentary rock and may be formed in or close to the basin. The Hesjelia zone is appears to have less sedimentary rock and may be formed in the volcanic arc. The Bleikvassli deposit is in another group and far away from the other two deposits, that is why it is placed on the other side of the basin. The model is made with inspiration from Bjerkgård *et al.* (2013a); Grenne, Ihlen and Vokes (1999); Wan, Zhang and Xiao (2010)

6 Conclusion

The grey gneiss and the amphibolite in the Mofjell group appears to have a volcanic arc signature formed by partial melting of meta basalts in the lower crust. The rock assemblage is defined as bimodal-felsic host rock, and according to the VMS-classification (Galley, Hannington and Jonasson, 2007) it may have up to 15% sedimentary input.

The muscovite gneiss/ schist, which is the host rock to the mineralisation, is assumed to be an altered rock from mainly grey gneiss and probably also some amphibolite. This is based on field evidences and chemical analyses where elements that are considered as immobile in this process has about the same content in the grey gneiss and the muscovite gneiss.

It is not found any clear zonation patterns from the portable XRF-analyses of the drill core from the Hellerfjellet zone. The Ba-content increase with some 100's ppm closer to the ore, but if few more meters from the ore was analysed, it might have been a clearer zonation. From the SEM-analyses of biotite and garnet in four different samples from different parts of the core it was established that the Fe-content in biotite decrease closer to the ore zone, K-content is higher in the grey gneiss far away and Ti-content is highest close to the ore-zone while it is very low far away. The composition of biotite might be used as a trace for the ore, but this needs to be more investigated. The Fe-content in garnet is 3-4% less in the muscovite gneiss close to the ore compared with the grey gneiss further away.

Many "tests" was done to figure out if the Hellerfjellet zone and the Hesjelia zone are connected or not. The grey gneiss and amphibolite have the same signature in both zones and appears to be made in an island arc setting on the continental margin. In the Hellerfjellet zone there is more sedimentary input with presence of carbonates, graphite, and meta-conglomerates. The muscovite gneiss/ schist from the two zones does not show the same trends in the classification diagrams. Neither does the ore; Hellerfjellet is a Zn-Pb-Cu-type deposit and Hesjelia zone is Zn-Cu-type and they have slightly different mineral assemblage.

The massive ore at Hellerfjellet contains an average of 2.9% Zn, 1.4% Pb, 0.17% Cu, 41 g/t Ag. Whereas the Hesjelia zone contain 5.5% Zn, 0.05% Pb, 0.4% Cu and 5 g/t Ag. So, the Hellerfjellet zone is richest in Pb and Ag, while the Hesjelia zone is richest in Zn and Cu, and also has higher values of Fe. Pyrite is not present in the massive ore in the Hellerfjellet zone, whereas in the Hesjelia it occurs as a major constitute in some prospects.

Based on these analyses are the Hellerfjellet and Hesjelia zone most likely two different deposits that is not connected. They are made in the same regimen, but from different ore-forming fluids and in different parts of the volcanic arc system. The Hesjelia zone is thought to be formed in the volcanic arc, while the Hellerfjellet deposits is deposited in the back-arc basin close to the arc. See Figure 5-10 for a suggestion for the paleotectonic model of the ore forming setting.

7 Application to exploration and further work

The Hellerfjellet and the Hesjelia zone are two very interesting areas regarding Zn- and Pb- rich deposits that also has some Ag and Au. Cu is found in smaller amounts. The two deposits are assumed to be made from two different ore-forming fluids in different parts of the same island arc system.

The Hellerfjellet deposit is rich in Zn (2.9%) and Pb (1.4%) with a subordinate amount of Cu (0.17%) and Ag (41g/t), it is richer in Ag and Pb compared with Hesjelia. It seems like the Hesjelia deposit generally is richer in metals, but the Hellerfjellet zone appears more extensive and it might contain more ore in total compared to Hesjelia. The drill core (BH4508) intersected the ore zone at 116 to 134 meters below surface with massive and semi-massive ore. This may indicate that here are several lenses in this zone. Several places in the muscovite schist far away from the prospects there are lenses with semi-massive ore, and these may be connected with the ore in the prospects. If any connection is to be found between the prospects, drill core and the semi-massive ore other places may make it easier to predict how the ore continues below the surface.

The Hesjelia zone is outcropping in two areas, 2.9 km apart, connected with a recumbent fold. The ore is rich in Zn (5.5%), with subordinate Pb (0.05%), Cu (0.4%) and Ag (5 g/t). Massive ore in Hesjelia and Hammertjønna has similar geochemistry and appears to be a part of the same zone, and this is probably confirmed by the drilling done in between in 2008. The ore was found at 110 m below the surface. If the folding continues in depth, it may be a big and rich zone with great mining potential of Zn, Pb, Cu and Fe. Follow up work here will be to obtain more structural mapping that makes it easier to find the appropriate place for drilling to figure out how the ore continues below the surface.

More samples of the *grey gneiss* should be collected, at least of the variations in the Hellerfjellet zone, to figure out even more about the origin of the sedimentary part. Isotopic data on the grey gneiss would be interesting to obtain to find more about the origin of the volcanic rock and where the melt came from.

More analyses of zonation pattern should be done to see if it may be used as a clue for the proximity to the ore. Some interesting patterns were found in the biotite and garnet, and also the barium content that increase when approaching the ore.

References

Abramowitz, M. and Davidson, M. W. (n.d.) *Reflected Light Microscopy - Introduction to Reflected Light Microscopy*. Available at: https://www.olympus-lifescience.com/en/microscope-resource/primer/anatomy/reflected/ (Accessed: 09.03. 2020).

Allen, R. L., Weihed, P., The Global VMS Research project team and (2002) Global comparisons of volcanic-associated massive sulphide districts, in Blundell, D. J., Neubauer, F. and Von Quadt, A. (ed.) *The Timing and Location of Major Ore Deposits in an Evolving Orogen. .* London: Geological Society, Special publication, 204, pp. 13-37.

Auge, J. J. and Carlson, W. D. (2014) Metamorphism as Garnet Sees it: The kineticks of Nucleation and Growth, Equilibration, and diffusional relaxation in Baxter, E., Caddick, M. J. and Ague, J. J. (ed.) *Elements - an international magazine of mineralogy, geochemistry, and petrology, vol.9.* USA.

Barrett, T. J. and MacLean, W. H. (1999) Volcanic sequences, lithogeochemistry, and hydrothermal alteration in some bimodal volcanic-associated massive sulfide systems, *Reviews in Economic Geology*, 8, pp. 101-131.

Barrie, C. D., Boyle, A. P., Cook, N. J. and Prior, D. J. (2010) Pyrite deformation textures in the massive sulfide ore deposits of the Norwegian Caledonides, *Tectonophysics*, 483(3-4), pp. 269-286.

Barrie, C. T., Cathles, L. M., Erendi, A., Schwaiger, H. and Murray, C. (1999) Heat and fluid flow in Volcanic-associated Massive Sulfide-forming Hydrothermal Systems, in Barrie, C. T. and Hannington, M. D. (ed.) *Volcanic-associated massive sulfide deposits: processes and examples in modern and ancient settings* Society of Economic Geologists, pp. 201-219.

Barrie, C. T. and Hannington, M. D. (1999) Classification of volcanic-associated massive sulfide deposits based on host-rock composition, *Reviews in Economic Geology*, 8, pp. 1-11.

Baxter, E. and Scherer, E. E. (2014) Garnet Geochronology: timekeeper of Tectonometamorphic processes, in Baxter, E. F., Caddick, M. J. and Ague, J. J. (ed.) *Elements - an international magazine of Mineralogy, Geochemistry, and Petrology, vol.*

Bjerkgård, T., Larsen, R. B. and Marker, M. (1995) Regional Geology of the Okstinden Area, the Rödningsfjäll Nappe Complex, Nordland, Norway, (95.153), pp. 87.

Bjerkgård, T. and Bjørlykke, A. (1996) Sulfide Deposits in Folldal, Southern Trondheim Region Caledonides, Norway: Source of Metals and Wall-Rock Alteration Related to Host Rocks *Economic Geology*, vol. 91, pp. 676-696.

Bjerkgård, T., Larsen, R. B. and Marker, M. (1997) Regional setting of the Bleikvassli Zn-Pb deposit in Nordland, Norway, *NGU-Bull*, 433.

Bjerkgård, T., Marker, M., Slagstad, T. and Solli, A. (2008) *Mofjell-prosjektet: statusrapport 2008*. Report 2008.088: Norges Geologiske Undersøkelse

Bjerkgård, T., Slagstad, T., Solli, A. and Marker, M. (2009) *Mofjell-prosjektet: staturapport pr. juni 2009*. Rapport 2009.038: Norges Geologiske undersøkelse.

Bjerkgård, T., Boyd, R., Ihlen, P., Korneliussen, A., Nilsson, L. P., Often, M., Sandstad, J. S., Eilu, P. and Hallberg, A. (2012) Metallogenic areas in Norway, *Special Paper of the Geological Survey of Finland*, 2012(53), pp. 35-138.

Bjerkgård, T. and Hallberg, A. (2012) NO28 Rana-Hemnes Zn-Pb-Cu, in Eilu, P. (ed.) *Mineral deposits and metallogeny of Fennoscandia, Special Paper 53.* Espoo: Geological Survey of Finland pp. 100-102.

Bjerkgård, T., Marker, M., Slagstad, T. and Solli, A. (2013a) *The Mofjell Project: Summary and conclusions* Report 2013.048: Geological Survey of Norway.

Bjerkgård, T., Marker, M., Slagstad, T. and Solli, A. (2013b) Geology and massive sulfide deposits in the Mofjell Group in the Rödningsfjället Nappe Complex, Norland, Norway.
BNN (1953) *Kartlegging Mofjell Vest. Høsten 1953.* Nordland: Bergverkselskapet Nord-Norge A/S.
Bossart, P. and Milnes, A. G. (2017) *Mont Terri Rock Laboratory, 20 Years: Two Decades of Research and Experimentation on Claystones for Geological Disposal of Radioactive Waste*. Birkhäuser.
Chin, E. J., Shimizu, K., Bybee, G. M. and Erdman, M. E. (2018) On the development of the calc-alkaline and tholeiitic magma series: A deep crustal cumulate perspective, *Earth and planetary science letters*, 482, pp. 277-287.
Cook, N., Spry, P. and Vokes, F. (1998) Mineralogy and textural relationships among sulphosalts and related minerals in the Bleikvassli Zn-Pb-(Cu) deposit, Nordland, Norway, *Mineralium Deposita*, 34(1), pp. 35-56.
Cook, N. J. (1993) Conditions of metamorphism estimated from alteration lithologies and ore at the Bleikvassli Zn-Pb-(Cu) deposit, Nordland, Norway, *Norsk Geologisk Tidsskrift*, 73(4), pp. 226-233.
Cox, D. P. and Singer, D. A. (1986) *Mineral deposit models*. US Government Printing Office Bulletin.
Craig, J. R., Vaughan, D. J. and Hagni, R. D. (1981) *Ore microscopy and ore petrography*. Wiley New York.
Defant, M. J. and Drummond, M. S. (1990) Derivation of some modern arc magmas by melting of young subducted lithosphere, *nature*, 347(6294), pp. 662-665.
DirektoratetForMineralforvaltning (n.d.) Bergrettigheter. Available at: https://minit.dirmin.no/kart/.
Franklin, J. M., Gibson, H. L., Jonasson, I. R. and Galley, A. G. (2005) Volcanogenic massive sulfide deposits, in Hedenquist, J. W., Thompson, J. F. H., Goldfarb, R. J. and Richards, J. P. (ed.) *Economic Geology 100th Anniversary Volume.* The Economic Geology Puplishing Company, pp. 523-560.
Galley, A. G., Hannington, M. D. and Jonasson, I. (2007) Volcanogenic massive sulphide deposits, *Mineral deposits of Canada: A synthesis of major deposit-types, district metallogeny, the evolution of geological provinces, and exploration methods: Geological Association of Canada, Mineral Deposits Division, Special Publication*, 5, pp. 141-161.
Geological Survey of Norway (n.d.) Map-database: Mineralressurser *Norges Geologiske Undersøkelser*. http://geo.ngu.no/kart/mineralressurser_mobil/.
GeologicalSurveyofNorway (n.d.) Berggrunn - Nasjonal bergrunnsdatabase. Available at: http://geo.ngu.no/kart/berggrunn_mobil/.
Goldstein, J. I., Newbury, D. E., Michael, J. R., Ritchie, N. W. M., Scott, J. H. J. and Joy, D. C. (2018) *Scanning Electron Microscopy and X-Ray Microanalysis*. Springer New York : Imprint: Springer.
Goodge, J. (2016) *Back-scattered Electron Detector (BSE)*. Available at: https://serc.carleton.edu/research_education/geochemsheets/bse.html (Accessed: 04.03. 2020).
Goodge, J. (2017) *Energy-Dispersive X-Ray Spectroscopy (EDS)*. Available at: https://serc.carleton.edu/research_education/geochemsheets/eds.html (Accessed: 04.03. 2020).
Grant, J. A. (1986) The isocon diagram; a simple solution to Gresens' equation for metasomatic alteration, *Economic Geology*, 81(8), pp. 1976-1982.
Grenne, T., Ihlen, P. M. and Vokes, F. M. (1999) Scandinavian Caledonide Metallogeny in a plate tectonic perspective, *International Journal of Geology, Mineralogy and Geochemistry of Mineral Deposits*, 34(5-6), pp. 422-471. doi: 10.1007/s001260050215.
Gundersen, S. F. (2020 in prep.) *Structural controls on selected ore deposits in Mofjellet, Nordland.* , Norwegian University of Science and Technology

Gustavson, M. (1978) Caledonides of north-central Norway, in Tozer, E. T. and Schenk, P. E. (ed.) *IGCP Project 27, Caledonian-Appalachian Orogen of the North Atlantic Region.* Geological Survey of Canada, Paper 78-13, pp. 25-30.
HudsonInstituteOfMineralogy (n.d.) *Pyrrhotite*. Available at: https://www.mindat.org/min-3328.html (Accessed: 05.05. 2020).
HudsonInstituteOfMineralogy. (n.d.-a) *Pyrite*. Available at: https://www.mindat.org/min-3314.html (Accessed: 05.05. 2020).
HudsonInstituteOfMineralogy. (n.d.-b) *Galena*. Available at: https://www.mindat.org/min-1641.html (Accessed: 28.04. 2020).
Huges, L. (2016) *An introduction to Electron Microscopy for Biologists*. Available at: https://bitesizebio.com/29197/introduction-electron-microscopy-biologists/ (Accessed: 3.3 2020).
Huston, D. L., Sie, S. H., Suter, G. F., Cooke, D. R. and Both, R. A. (1995) Trace elements in sulfide minerals from eastern Australian volcanic-hosted massive sulfide deposits; Part I, Proton microprobe analyses of pyrite, chalcopyrite, and sphalerite, and Part II, Selenium levels in pyrite; comparison with delta 34 S values and implications for the source of sulfur in volcanogenic hydrothermal systems, *Economic Geology*, 90(5), pp. 1167-1196.
Irvine, T. and Baragar, W. (1971) A guide to the chemical classification of the common volcanic rocks, *Canadian journal of earth sciences*, 8(5), pp. 523-548.
Kartverket (n.d.). Norgeskart.no. Available at: https://www.norgeskart.no/#!?project=norgeskart&layers=1004&zoom=9&lat=7349518.84&lon=463446.39&markerLat=7355037.108998331&markerLon=461572.06083965866&panel=searchOptionsPanel&sok=Mo.
Kleine-Hering, R. and Schulze, D. (1969) Bericht zu den geologischen untersuchungen in der umgebung des Akersvatn. Intern rapport Bleikvassli Gruber A/S.
Koski, R. A. (2012) Hypogene Ore Characteristics, in Shanks, W. C. and Thurston, R. (ed.) *Volcanogenic Massive Sulfide Occurrence Model, . Scientific Invesigations Report 2010-5070-C..* U.S. Geological Survey, pp. 137-143.
Kruse, A. (1964) Oversikt over malmfelt og malmletingsarbeider i Ranen. Rapport Bergverksselskaper Nord-Norge.
Kruse, A. (1980) *Undersøkelser av Hesejlia* Mo i Rana: Bergverkselskapet Nord-Norge A/S.
Kuno, H. (1969) Andesite in time and space, *Bulletin of the Oregon Department of Geoloyg and Mineral Industry*, 65, pp. 13-20.
Large, R. R. (1977) Chemical evolution and zonation of massive sulfide deposits in volcanic terrains, *Economic Geology*, 72(4), pp. 549-572.
Large, R. R. (1992) Australian volcanic-hosted massive sulfide deposits; features, styles, and genetic models, *Economic Geology and the Bulletin of the Society of Economic Geologists*, 87(3), pp. 471-510. doi: 10.2113/gsecongeo.87.3.471.
Larsen, R. B., Bjergård, T. and Moralev, G. V. (1995a) *Distribution of ore-forming elements in sediment-hosted massive sulphide mineralisation in the Rana region, Norway*. Trondheim: Geological survey of Norway.
Larsen, R. B., Walker, N., Birkeland, A. and Bjerkgård, T. (1995b) *Flourine-rick biotites and alkali-metasomatism as guides to massive sulphide deposits: an example from the Bleikvassli Zn-Pb-Ag-(Cu) deposit, Norway*. Report nr.: 95.152: Geological Survey of Norway.
Le Maitre, R. *et al.* (1989) A classification of igneous rocks and glossary of terms. Recommendations of the IUGS Subcommission on the Systematics of Igneous rocks, *London: Blackwell Scientific Publications*.
Lentz, D. R. (1998) Petrogenetic evolution of felsic volcanic sequences associated with Phanerozoic volcanic-hosted massive sulphide systems: the role of extensional geodynamics *Ore Geology Reviews*, vol. 12, pp. 289-327.
Liebl, C., Kuntcheva, B., Kruhl, J. r. H. and Kunze, K. (2007) Crystallographic orientations of quartz grain-boundary segments formed during dynamic

recrystallization and subsequent annealing, *European Journal of Mineralogy*, 19(5), pp. 735-744.
Lydon, J. W. (1984) Ore deposit models-8. Volcanogenic massive sulphide deposits Part I: A descriptive model, *Geoscience Canada*, 11(4).
MacRae, N., Nesbitt, H. and Kronberg, B. (1992) Development of a positive Eu anomaly during diagenesis, *Earth and planetary science letters*, 109(3-4), pp. 585-591.
Marker, M. (1983) *Caledonian and pre-caleconian geology of the Mofjell area, Nordland, Norway*, Københavns Universitet.
Marker, M., Bjergård, T., Slagstad, T. and Solli, A. (2012) Bergrunnskart STORAKERSVATNET 2027 III, M 1:50 000: Norges Geologiske Undersøkelser.
McClenaghan, S. H., Lentz, D. R., Martin, J. and Diegor, W. G. (2009) Gold in the Brunswick No. 12 volcanogenic massive sulfide deposit, Bathurst Mining Camp, Canada: Evidence from bulk ore analysis and laser ablation ICP— MS data on sulfide phases, *Mineralium Deposita*, 44(5), pp. 523-557.
McDonough, W. F. and Sun, S.-S. (1995) The composition of the Earth, *Chemical geology*, 120(3-4), pp. 223-253.
Mommio, A. D. (n.d.-a) *Plutonic Rocks* Available at: http://www.alexstrekeisen.it/english/pluto/index.php (Accessed: 27.1. 2020).
Mommio, A. D. (n.d.-b) *Porphyroblastic Texture*. Available at: https://www.alexstrekeisen.it/english/meta/porphyroblastic.php (Accessed: 07.04. 2020).
Mommio, A. D. (n.d.-c) *Skeletal garnet*. Available at: http://www.alexstrekeisen.it/english/meta/skeletalgarnet.php (Accessed: 01.05. 2020).
Mommio, A. D. (n.d.-d) *Metamorphic rock*. Available at: https://www.alexstrekeisen.it/english/meta/index.php (Accessed: 01.05. 2020).
Morgan, L. A. and Schulz, K. J. (2012) Physical volcanology of volcanogenic massive sulfide deposits, in Shanks III, W. C. P. and Thurston, R. (ed.) *volcanogenic massive sulfide occurence model, Scientific Investigations Report 2010-5070-C.* U.S. Geological Survey, pp. 61-95.
MSAnalytical (2017a) Multi-element determination of mineralogical samples using a lithium borate fusion and ICP-OES finish *MSA-QUA-PO42.002*.
MSAnalytical (2017b) Multi-element determination of minaralogical samples using a four acid digestion and ICP-AES/MS finish, *MSA-QUA-PO28.001*.
MSAnalytical (2017c) Multi-element determination of mineralogical samples using a lithium borate fusion and ICP-MS finish, *MSA-QUA-PO30.002*.
MSAnalytical (2017d) Multi-element determination of mienralogical samples using a two acid digestion and ICP-AES/MS finish *MSA-QUA-PO25.002*.
Pearce, J. A. (1983) Role of the sub-continental lithosphere in magma genesis at active continental margins.
Pearce, J. A., Harris, N. B. and Tindle, A. G. (1984) Trace element discrimination diagrams for the tectonic interpretation of granitic rocks, *Journal of petrology*, 25(4), pp. 956-983.
Pracejus, B. (2015) *The ore minerals under the microscope: an optical guide*. Elsevier.
Robb, L. (2005) Hydrothermal ore-froming processes, in Robb, L. (ed.) *Introduction to Ore-Forming Processes.* Malden, Mass: Blackwell, pp. 129-219.
Roberts, D. and Gee, D. G. (1985) An introduction to the structure of the Scandinavian Caledonides, in Gee, D. G. and Sturt, B. A. (ed.) *The Caledonide orogen : Scandinavia and related areas : 1.* Chichester: Wiley, pp. 55-68.
Ruiz, J. L. (1977) The zoning of garnets as an indicator of the PT history of their host-rocks, *Annales de la Société géologique de Belgique*.
Rumble III, D., Duke, E. F. and Hoering, T. L. (1986) Hydrothermal graphite in New Hampshire: Evidence of carbon mobility during regional metamorphism, *Geology*, 14(6), pp. 452-455.
Saager, R. (1966) Erzgeologische Untersuchungen an Kaledonischen Blei, Zink und Kupfer fürenden Kieslagerstätten im Nord-Rana Distrikt, Nord-Norwegen. Doktoravhandling ETH, Zürich.

Schwinn, G. and Markl, G. (2005) REE systematics in hydrothermal fluorite, *Chemical geology*, 216(3-4), pp. 225-248.
SGS (2019) *Multi-Acid (4-acid) digestions*. Available at: https://www.sgs.com/en/mining/analytical-services/geochemistry/digestion-and-fusion/multi-acid-4acid-digestions (Accessed: 9.10. 2019).
Shanks III, W. C. P. (2012) Hydrothermal Alteration, in Shanks III, W. C. P. and Thurston, R. (ed.) *Volcanogenic Massice Sulfide Occurence Model. Scientific Invesigations Report 2010-5070-C.* U.S geological Survey, pp. 165-179.
Shanks III, W. C. P. and Koski, R. A. (2012) Introduction in volanogenic massice sulfide occurence model, in Shanks III, W. C. P. and Thurston, R. (ed.) *Volcanogenic Massice Sulfide Occurence Model, Scientific Invesigations Report 2010-5070-C.* U.S. Geological Survey pp. 4.
Skauli, H. (1993) A metamorphosed, potassic alteration zone associated with the Bleikvassli Zn · Pb · Cu orebody, Northern Norway, *Lithos*, 31(1-2), pp. 1-15.
Slack, J. F. (2012) Hypogene Gangue Chaaracteristics, in Shanks III, W. C. P. and Thurston, R. (ed.) *Volcanogenic massive sulfide occurence mode, Scientific Investigations Report 2010-5070-C.* U.S. Geological Survey, pp. 149-153.
Spross, E. (1956) Berichy über die Untersuchungsarbeiten im Sommer 1956. Upubl. rapp.
Spry, P. G., Peter, J. M. and Slack, J. F. (2000) Meta-exhalites as exploration guides to ore., in Spry, P. G., Marshall, B. and Vokes, F. M. (ed.) *Metamorposed and metamorphigenic ore deposits.* Reviews in Economic Geology, pp. 163-201.
Stephens, M. B., Gustavson, M., Ramberg, I. B. and Zachrisson, E. (1985) The Caledonides of central-north Scandinavia - a tectonostratigraphic overview, in Gee, D. G. and Sturt, B. A. (ed.) *The Caledonide orogen : Scandinavia and related areas : 2.* Chichester: Wiley, pp. 134-162.
Swinden, H., Evans, D. and Kean, B. (1990) *Geological Survey of Canada, Open File 2156*. Natural Resources Canada.
Søvegjarto, U., Marker, M., Graversen, O. and Gjelle, S. (1988) Bergrunnskart MO I RANA 1927 I-M. 1: 50 000: Norges Geologiske undersøkelser.
Taylor, S. R. and McLennan, S. M. (1985) The continental crust: its composition and evolution.
TheEditorOfEncyclopaediaBritannica (1998) Graphite, *Britannica*. Available at: https://www.britannica.com/science/graphite-carbon.
TheEditorOfEncyclopaediaBritannica (n.d.) *Appalachian orogenic belt*. Available at: https://www.britannica.com/place/North-America/Transportation (Accessed: 29.04. 2020).
Vernon-Parry, K. D. (2000) Scanning electron microscopy: an introduction, *III-Vs Review*, 13(4), pp. 40-44. doi: 10.1016/S0961-1290(00)80006-X.
Vogt, J. H. L. (1890) *Praktisk-geologiske Undersøgelser af Nordlands Amt : 1 : Salten og Ranen : med særligt Hensyn til de vigtigste Jernmalm- og Svovelkis-kobberkis-forekomster samt Marmorlag*. Christiania: Brøgger.
Vokes, F. (1969) A review of the metamorphism of sulphide deposits, *Earth-Science Reviews*, 5(2), pp. 99-143.
Vokes, F. (1976) Caledonian massive sulphide deposits in Scandinavia: a comparative review, in Wolf, K. H. (ed.) *Handbook of stratabound and stratiform ore deposits 6.* Elsevier, Amsterdam, pp. 79-128.
Vokes, F. M. (1963) *Geological studies on the Caledonian pyritic zinc-lead orebody at Bleikvassli, Norland, Norway*. Universitetsforlaget.
Wan, B., Zhang, L. and Xiao, W. (2010) Geological and geochemical characteristics and ore genesis of the Keketale VMS Pb-Zn deposit, Southern Altai Metallogenic Belt, NW China, *Ore Geology Reviews*, vol.37, pp. 114-126.
Winchester, J. A. and Floyd, P. A. (1977) Geochemical discrimination of different magma series and their differentiation products using immobile elements, *Chemical geology*, 20, pp. 325-343.

Yamada, R. and Yoshida, T. (2011) Relationships between Kuroko volcanogenic massive sulfide (VMS) deposits, felsic volcanism, and island arc development in the northeast Honshu arc, Japan, *Mineralium Deposita*, 46(5-6), pp. 431-448.

Berit Berbusmel

Ore-forming processes in volcano-sedimentary hosted massive sulphide deposits in the Mofjell group

NTNU
Norwegian University of
Science and Technology

SOTKAMO SILVER